ARR No. 3H23

NATIONAL ADVISORY COMMITTEE FOR AERONAUTICS

WARTIME REPORT

ORIGINALLY ISSUED

August 1943 as
Advance Restricted Report 3H23

WIND-TUNNEL INVESTIGATION OF A FULL-SPAN RETRACTABLE FLAP IN COMBINATION WITH FULL-SPAN PLAIN AND INTERNALLY BALANCED AILERONS ON A TAPERED WING

By F. M. Rogallo, John G. Lowry, and Jack Fischel

Langley Memorial Aeronautical Laboratory
Langley Field, Va.

NACA

WASHINGTON

NATIONAL ADVISORY COMMITTEE FOR AERONAUTICS

ADVANCE RESTRICTED REPORT

WIND-TUNNEL INVESTIGATION OF A FULL-SPAN RETRACTABLE FLAP IN COMBINATION WITH FULL-SPAN PLAIN AND INTERNALLY BALANCED AILERONS ON A TAPERED WING

By F. M. Rogallo, John G. Lowry, and Jack Fischel

SUMMARY

An investigation was made in the LMAL 7- by 10-foot tunnel of a 20-percent-chord full-span retractable flap in combination with 8-percent-chord full-span plain and internally balanced ailerons on a semispan model of the tapered wing of a typical fighter airplane. The full-span flap fits into a cut-out ahead of the aileron to conform to the original wing contour when in the retracted position and moves down and back to its extended position. Increments of maximum lift coefficient of approximately 1.3 and 1.5 were obtained from the full-span flap at deflections of 30° and 50°, respectively. The aileron effectiveness for a deflection range of ±15° is thought to be adequate in the flap-retracted condition. With the flap fully extended, the aileron effectiveness was about 50 percent greater than with the flap retracted. A reduction of aileron effectiveness of approximately 40 percent relative to the aileron effectiveness with the flap retracted appeared unavoidable at certain intermediate flap positions. The internal balance reduced the estimated aileron stick forces to acceptable values for all flap positions and deflections along a selected path.

INTRODUCTION

One of the problems arising from the increased speed and wing loading of modern airplanes is the difficulty of obtaining high lifts for landing and take-off without impairing lateral control. In order to obtain solutions to this problem, the NACA is investigating, on a semispan model of the tapered wing of a modern fighter airplane, lateral-control devices that appear promising from previous wind-tunnel tests.

The present tests of an 8-percent-chord full-span aileron on a tapered wing with a full-span retractable flap may be considered an extension of the work reported in references 1 and 2. The object of the wind-tunnel tests was to determine the lift characteristics and the aileron-control characteristics for various positions and deflections of the flap. Most of the tests were made with a sealed internally balanced aileron with small overhang in order to obtain data over a large aileron deflection range; with the flap retracted, comparative tests were made of the aileron with the seal removed. The results indicated that an aileron deflection of $\pm 15^{\circ}$ would provide adequate rate of roll if the aileron were sealed; the sealed internal balance was therefore increased to the maximum overhang permissible with an aileron deflection of $\pm 15^{\circ}$. With the large internal balance, tests were made to determine the hinge-moment characteristics of the aileron with the flap retracted. Some additional tests were made with the flap extended, primarily to obtain lift and rolling-moment data at angles of attack or flap positions not investigated with the small overhang.

The stick forces and the rates of roll were estimated for an airplane with $\pm 15^{\circ}$ aileron linkage for several flap positions along a selected flap path. With the flap fully extended, two arrangements of the flap and aileron were investigated; one of these arrangements retained the $\pm 15^{\circ}$ aileron linkage, but the other required a differential linkage.

APPARATUS AND METHODS

A semispan wing model was mounted in the LMAL 7- by 10-foot tunnel (reference 3) as shown schematically in figure 1. The root chord of the model was adjacent to one of the vertical walls of the tunnel, the vertical wall thereby serving as a reflection plane. The flow over a semispan in this setup is essentially the same as it would be over a complete wing in a 7- by 20-foot tunnel. Although a very small clearance was maintained between the root chord of the model and the tunnel wall, no part of the model was fastened to or in contact with the tunnel wall. The model was supported entirely by the balance frame, as shown in figure 1, in such a way that the magnitude of all the forces and moments acting on it could be determined. Provisions were made for changing the angle of attack while the tunnel was in operation.

The aileron deflections and hinge moments were determined by means of a calibrated torque rod and linkage system developed especially for this type of setup (fig. 2). The aileron was deflected by turning the hinge-moment dial which, through the torque rod, drove the aileron-deflection drive tube and the link to the aileron horn. When the desired aileron deflection had been attained, the torque rod was clamped in position in order that all wing forces and moments could be determined without any interference from the operator of the hinge-moment unit. The aileron deflection was determined by the reading of the aileron-deflection dial with respect to the pointer attached to the angle-of-attack drive tube. The aileron hinge moments were determined from the twist of the torque rod as indicated by the reading of the hinge-moment dial with respect to the pointer mentioned. The torque rod was calibrated after it was installed in the test setup.

The tapered wing model used in these tests was built to the plan form shown in figure 3 and represents the cross-hatched portion of the airplane shown in figure 4. The basic airfoil sections were of the NACA 230 series tapering in thickness from approximately 15½ percent at the root to 8¼ percent at the tip. The basic chord $\bar{o}_1$ of the wing model was increased 0.3 inch to reduce the trailing edge thickness and the last few stations were refaired to give a smooth contour. The airfoil ordinates are given in table I.

The full-span retractable flap was built to the ordinates of table II and had a chord of about 20.7 percent of the wing chord. The flap could be pivoted about its nose at the positions shown by the grid in figure 5. The positions shown in this figure will be indicated hereinafter by a letter and a number, as follows: A-1, B-3, and so forth, where the letter shows the chordwise flap position and the number, the vertical gap in percentage wing chord. The retracted flap was assumed to be at zero deflection. The 8-percent-chord aileron had provisions for sealing and changing the balance. A balance plate, which was tapered along the span of the aileron to give the maximum overhang with the required deflection, was attached to the aileron nose. The balance chord is defined as the distance from the aileron hinge axis to the midpoint of the seal. The trailing edge of the curtain was moved rearward for the large-balance condition to improve the balance effectiveness. This effect is discussed in reference 4.

Series of tests in which the angle-of-attack and aileron deflection were varied over the useful ranges were made for many flap positions and deflections. These flap positions were taken on both sides of a path that appeared promising from the results of reference 5.

All tests with the flap retracted were made at a dynamic pressure of 16.37 pounds per square foot, which corresponds to a velocity of about 80 miles per hour and to a test Reynolds number of about 2,050,000, based on the mean aerodynamic chord of 33.66 inches. The tests with the flap deflected were run at a dynamic pressure of 9.21 pounds per square foot, which corresponds to a velocity of about 60 miles per hour and to a test Reynolds number of about 1,540,000. The tests were made at low values of Mach and Reynolds numbers and at high turbulence relative to flight conditions (turbulence factor = 1.6). The effects of these variables were not determined or estimated.

RESULTS AND DISCUSSION

Symbols

The symbols used in the presentation of results are:

C_L	lift coefficient (L/qS)
C_D	uncorrected drag coefficient (D/qS)
C_m	pitching-moment coefficient (M/qSc')
$C_{l'}$	rolling-moment coefficient (L'/qbS)
$C_{l'_u}$	uncorrected rolling-moment coefficient
$C_{n'}$	yawing-moment coefficient (N'/qbS)
C_h	aileron hinge-moment coefficient $(H_a/qb_a\bar{c}_a^2)$
ΔC_h	C_h of up aileron minus C_h of down aileron
c	actual wing chord at any spanwise location with flaps retracted
c_l	chord of basic airfoil section at any spanwise location
c'	mean aerodynamic chord

c_a aileron chord measured along airfoil-chord line from hinge axis of aileron to trailing edge of airfoil

c_b aileron balance chord measured from aileron hinge axis to the midpoint of the seal

$\overline{c}_a$ root-mean-square chord of the aileron

$\overline{c}_b$ root-mean-square chord of aileron balance

$\frac{\overline{c}_b}{\overline{c}_a}$ balance ratio

b twice span of semispan model

b_a aileron span

S twice area of semispan model

L twice lift on semispan model

D twice drag on semispan model

M twice pitching moment of semispan model about support axis (0.24c)

L' rolling moment, due to aileron deflection, about wind axis in plane of symmetry

N' yawing moment, due to aileron deflection, about wind axis in plane of symmetry

H_a aileron moment about hinge axis

q dynamic pressure of air stream $\left(\frac{1}{2}\rho V^2\right)$ uncorrected for blocking

V free-stream velocity

V_i true airspeed at zero altitude, miles per hour

C_{h_α} $(\partial C_h/\partial \alpha)_{\delta_a}$

$C_{h_{\delta_a}}$ $(\partial C_h/\partial \delta_a)_\alpha$

α angle of attack

δ_a aileron deflection relative to wing, positive when trailing edge is down (the notation $\pm$ with δ_a indicates that both ailerons are simultaneously deflected, one up and the other down)

δ_f flap deflection relative to flap-retracted position, positive when trailing edge is down

$C_{l'_p}$ rate of change of rolling-moment coefficient $C_{l'}$ with helix angle $pb/2V$

p rate of roll

F_s stick force

θ_s control-stick deflection

A positive value of L' or $C_{l'}$ corresponds to a decrease in lift of the model, and a positive value of N' or $C_{n'}$ corresponds to an increase in drag of the model. Twice the actual lift, drag, pitching moment, area, and span of the model were used in the computation of the results because the model represented half of a complete wing. The angle of attack, the drag coefficient, the rolling-moment coefficient, and the yawing-moment coefficient have been corrected for the effect of the tunnel walls in accordance with the theory of trailing vortex images. No corrections have been applied to the hinge-moment coefficients, and no corrections have been applied to any of the results for the effects of the support strut, the blocking effect of the wing, the small gap between the wing and the wall, the leakage through the wall around the support tube, or the boundary layer at the wall. The drag values are believed to be comparative and not directly applicable to performance estimations.

The over-all corrections applied (by addition) to the angle of attack (in deg), to the drag coefficient, and to the rolling- and yawing-moment coefficients were:

$$\Delta\alpha = 1.3\ C_L$$
$$\Delta C_D = 0.023\ C_L^2$$
$$\Delta C_{l'} = -0.26\ C_{l'_u}$$
$$\Delta C_{n'} = -0.061\ C_{l'_u}\ C_L$$

Lift, Drag, and Pitching-Moment Coefficients

The results indicate that at all flap positions investigated, even at negative flap deflections, the maximum lift coefficient was approximately as high or higher than that obtained with the flap retracted (figs. 6 to 12). A progressive increase of the lift, the drag, and the negative pitching-moment coefficients was obtained as the flap was deflected positively or moved rearward. The effect of the vertical position of the fully extended flap on the maximum lift coefficient is shown in figure 12(a). For any given flap deflection, with aileron neutral, $C_{L_{max}}$ increased as the gap decreased within the test range. With the flap deflected 30° at position L-3 and the aileron neutral, an increment of $C_{L_{max}}$ due to flap deflection of approximately 1.3 was obtained (fig. 12(a)). An additional increase in $C_{L_{max}}$ was obtained by drooping the aileron; with the flap deflected 50° and the aileron drooped 5°, an increment of approximately 1.5 in $C_{L_{max}}$ was obtained (fig. 12(b)). These values of $\Delta C_{L_{max}}$ are slightly higher than those reported in reference 1 for somewhat similar arrangements in two-dimensional flow and may be attributed, in the present investigation, to the increased thickness and camber of the flap.

Some disagreement will be noted between results of the original and the check tests for the various characteristics with 30° flap deflection at L-3 (fig. 12(a)). The check test was made several weeks after the original test and small discrepancies may have existed in the aileron or flap setting for the two tests.

A comparison of the results of tests of various arrangements of high-lift and lateral-control devices on the same basic wing model (fig. 13) indicates that the $\Delta C_{L_{max}}$ of the present arrangement is about 0.5 higher than that of the duplex flap (reference 5) and about 0.4 higher than that of the full-span slotted flap (reference 6) and that the drag coefficient of the present arrangement is, in general, lower at any given lift coefficient.

The variation of maximum pitching-moment coefficient with maximum lift coefficient for several flap arrangements is presented in figure 14. The variation is almost independent of flap arrangement and the full-span flap

reported herein has higher values of $C_{m_{max}}$ than the other arrangements only in the range of higher $C_{L_{max}}$. The loss of airplane lift coefficient required to trim the wing pitching-moment coefficient is given by the expression

$$\text{Loss of } C_L = \frac{C_m}{\text{tail length}}$$

Curves of loss of C_L for tail lengths of 2.5 and 5 wing-chord lengths are presented in figure 14. The net gain in airplane $C_{L_{max}}$ resulting from use of the retractable flap is over 80 percent of the gain in $C_{L_{max}}$ of the wing alone for a tail length of 2.5 c'. The percentage gain would, of course, increase with the tail length.

As the Reynolds number is increased to full scale, the values of $C_{L_{max}}$ will be expected to increase and the increments of $C_{L_{max}}$ due to the flaps may change because of a change in the progression and position of the stall. The effects of the tunnel boundaries and of scale upon the stall of the wing were not investigated.

Rolling-, Yawing-, and Hinge-Moment Coefficients.

Flap retracted.- The results of the aileron investigation with the flap retracted are presented in figure 15. The variation of rolling-, yawing-, and hinge-moment coefficients with aileron deflection appears approximately linear for the range of $\delta_a = \pm 15^\circ$. A comparison of figure 15(a) with figure 15(b) indicates that sealing the aileron gap increased the rolling-moment coefficient approximately 20 percent for aileron deflections of $\pm 15^\circ$ and approximately 5 percent for aileron deflections of $\pm 30^\circ$. For the $0.30\bar{c}_a$ balance, gap sealed, the aileron effectiveness was adequate for $\delta_a = \pm 15^\circ$ (estimated to give a value of $pb/2V$ of 0.09, as will be discussed subsequently). In order, however, to reduce the values of the hinge-moment coefficient, the balance was increased to $0.56\bar{c}_a$ (fig. 15(c)). A deflection range of $\pm 15^\circ$ was obtained with this aileron balance before testing but, because of the distortion of the aileron under aerodynamic loads, the lead-

ing edge of the balance plate came in contact with the retracted flap when the aileron was deflected about -11°. The hinge-moment coefficients for negative aileron deflections beyond -10° were therefore not used and extrapolation of the hinge-moment curves to -15° was required for computation of the estimated stick forces. The addition of balance to the sealed aileron appeared to have little or no effect on the rolling-moment coefficient.

Sealing the gap decreased the hinge-moment coefficient in addition to increasing the rolling-moment coefficient available. For $\delta_a = \pm 15^{\circ}$ and $\pm 30^{\circ}$, the reduction in the hinge-moment coefficient was approximately 21 percent and 11 percent, respectively. The addition of balance to the sealed aileron caused a further reduction of approximately 50 percent in hinge-moment coefficient for $\delta_a = \pm 15^{\circ}$ near zero angle of attack. This effect of balance on hinge-moment coefficient is indicated in figure 16, where the values of C_{h_α} and $C_{h_{\delta_a}}$ are compared for the three amounts of aileron balance used. Values of C_{h_α} were estimated for the α ranges of approximately -4° to 4° and 9° to 17° with aileron neutral. Values of $C_{h_{\delta_a}}$ were estimated for the aileron range of approximately 5° to -5° at angles of attack of 0.1° and 13.3°. The effective balance of the unsealed aileron was assumed to be one-half the thickness of the airfoil at the hinge axis (as was done in reference 7), and was found to be $0.153\bar{c}_a$. As anticipated, both the sealing of the gap and the addition of balance decreased the negative values of $C_{h_{\delta_a}}$ and C_{h_α} in both the high-lift and the high-speed range. The values of both parameters were greater negatively in the high-lift range than in the high-speed range. The hinge-moment data obtained in the present investigation were only incidental to the high-lift and rolling-moment data sought and the leakage past the seals was not experimentally checked; the results, however, indicate approximately the variation of hinge-moment slopes with balance ratio expected for the arrangement tested.

Flap extended.- The values of the rolling-moment coefficient available with sealed aileron deflections of $\pm 15^{\circ}$, at the various flap positions investigated, are presented in figure 17. The range $\pm 15^{\circ}$ was chosen because it was thought that sufficient rolling effectiveness could be ob-

tained in this range. Where similar results were available, as for the $0.30\bar{c}_a$ and $0.56\bar{c}_a$ balance, average values are given. Rolling-, yawing-, and hinge-moment data for all the positions investigated are available but are not presented herein. Figure 17 indicates that the chordwise position of the flap nose, the flap-nose gap, and the deflection of the flap influence the values of the rolling-moment coefficient. When the flap attained a positive deflection of 30° or greater near the fully extended position, the aileron effectiveness increased and was considerably higher than when the flap was retracted. A reduction in the available rolling-moment coefficient appeared unavoidable for some intermediate positions. This effect is, in general, similar to that encountered with the duplex flap arrangement (reference 5). The results indicated that the flap should be extended over most of its path at negative deflections; whereas, the flap of the duplex arrangement of reference 5 was extended at positive deflections. In the present arrangement, the flap-extended position was at the wing trailing edge, whereas the flap-extended position of the duplex arrangement was several percent ahead of the wing trailing edge.

L-504

Fairly complete aileron data are presented (figs. 18 to 48) and show that the rolling- and hinge-moment coefficients are generally nonlinear with aileron deflection and vary with angle of attack. As previously indicated, a reduction of available rolling-moment coefficient was obtained at some intermediate flap positions, and this reduction appeared greatest at flap deflections near 0°. With the flap in position L-3, $\delta_f = 30°$, and an aileron deflection of ±15°, a value of C_l' of 0.070 at $\alpha = 13.8°$ was obtained (figs. 45 and 48), which was approximately 60 percent greater than was available with the flap retracted. With the flap in position L-2, $\delta_f = 50°$, the maximum lift was obtained with the aileron drooped 5° (fig. 12(b)). A reduction of rolling moment coefficient, obtained when the aileron was deflected more than 10° (fig. 46), indicated that the best lateral control for this flap position would be obtained by only a small positive and a large negative aileron deflection from the neutral position, $\delta_a = 5°$. Thus, the aileron and stick-force characteristics were estimated for an airplane with the flap in the two following extended positions: L-3, $\delta_f = 30°$ with an equal up-and-down control system that would allow an aileron deflection of ±15°; and L-2, $\delta_f = 50°$, $\delta_a = 5°$

with two differential control systems that would allow only a 5° positive aileron deflection.

With the flap in the fully extended position (L), the aileron characteristics of the present arrangement are similar to those of the slot-lip arrangement with the flap extended (references 8 and 9) and show the same increases in effectiveness with flap deflection as were shown by the slot-lip aileron.

In general, with the flap in positions back of the aileron hinge axis, there was an increase in rolling-moment coefficient available and a noticeable increase in the slope of the hinge-moment-coefficient curve as the flap deflection increased. Also, as the flap was moved rearward the aileron floating angle became increasingly negative. As previously discussed for the flap-retracted condition, the addition of balance reduced the sealed aileron hinge-moment slope with flap extended. (See figs. 35 and 37 or 45 and 48.) It is indicated in figures 45 and 48 that the addition of balance to the sealed aileron reduced the hinge-moment coefficient for $\delta_a = \pm 15^\circ$ approximately 13 percent for flap position L-3, $\delta_f = 30^\circ$. However, the reduction in hinge-moment coefficient was greater with the flap retracted than with the flap fully extended, possibly because the flap, when retracted, acted as a curtain over the aileron balance and, when extended, completely exposed the aileron balance.

Estimated Airplane Characteristics

From the data presented in the curves, a flap path was selected (fig. 49) and some of the characteristics of the airplane shown in figure 4 were estimated. These airplane characteristics are presented in figures 50 to 59 and indicate the results that may be expected with the flap in various positions on the selected flap path.

The rates of roll were estimated by means of the relationship

$$\frac{pb}{2V} = \frac{C_l'}{C_{l'_p}} \qquad (1)$$

where the coefficient of damping in roll $C_{l'_p}$ was taken as 0.46 from the data of reference 10. Wing twist has been

neglected and it was assumed that yawing moment would be counteracted by the rudder.

The stick forces were estimated from the relationship

$$F_s = 45.8 \frac{\Delta C_h}{C_L} \qquad (2)$$

for the equal up-and-down aileron deflection and $\delta_{a_{max}} = \pm 15^\circ$; and from the relationship

$$F_s = \frac{64.1}{C_L} \left[C_{h_{up}} \left(\frac{d\delta_a}{d\theta_s} \right)_{up} - C_{h_{down}} \left(\frac{d\delta_a}{d\theta_s} \right)_{down} \right] \qquad (3)$$

for the differential control systems of 3:1 and 2:1, as presented for the flap-extended position L-2, $\delta_f = 50^\circ$, $\delta_a = 5^\circ$. These relationships may be derived from the aileron dimensions and the following airplane characteristics:

Wing area, square feet	260
Span, feet	38
Taper ratio	1.67:1
Airfoil section	NACA 230 series
Mean aerodynamic chord, inches	84.14
Weight, pounds	7063
Wing loading, pounds per square foot	27.2
Stick length, feet	2
Maximum stick deflection, degrees	±21
Maximum aileron deflection, degrees	
$0.15\bar{c}_a$ balance	±15
$0.30\bar{c}_a$ balance	±15
$0.56\bar{c}_a$ balance	±15
3:1 differential control (from an initial 5° droop)	5,-15
2:1 differential control (from an initial 5° droop)	5,-10

The values of the constants in equations (2) and (3) are dependent upon the wing loading, the size of the ailerons, and the stick length; the constant in equation (2) depends, in addition, on the deflection of the ailerons relative to the stick. A factor of 0.805, moreover,

is included in the constants to correct for that part of the wing and aileron that is included in the fuselage and which, therefore, provides neither lateral control nor stick force. The loss in aileron effectiveness from this area is negligible (reference 11). Incidentally, in a twin-engine airplane, the aileron would not be installed inboard of the nacelles. The values of $C_{l'}$ and C_h used in equations (1), (2), and (3) are the values thought to exist during steady rolling; the difference in angle of attack of the two ailerons due to rolling has been taken into account.

The estimated lateral-control characteristics and the corresponding stick forces for the airplane, with the flap following a selected path to its extended position, are presented in figure 50 for the $0.30\overline{c}_a$ sealed aileron at several velocities and attitudes. A value of $pb/2V$ less than 0.07, the minimum required (reference 10), is indicated at several flap positions. A reduction of aileron effectiveness, as compared to that for the flap-retracted condition, is observed as the flap is extended and a considerable increase in effectiveness is obtained with the flap near or at its fully extended position. From figure 50, it is apparent that the reduction of aileron effectiveness is approximately 34 percent at position B-4, $\delta_f = -10^\circ$; but the maximum reduction occurs at or near position I-6 when the flap passes through 0°, as mentioned previously, and results in a loss of effectiveness amounting to approximately 40 percent with $pb/2V = 0.054$. The reduction varies with velocity, flap deflection, and flap path. Because the flap would normally be in these intermediate positions for a relatively short period of flight, that is, during retraction or extension, a relatively low aileron effectiveness may be acceptable. At the fully extended flap position, the aileron effectiveness improves considerably, as is shown in figure 50, with very little increase in stick force.

The relatively linear variation of stick force with aileron effectiveness $pb/2V$ for the flap-retracted condition with the three amounts of aileron balance tested is indicated by figure 51 at several velocities. Sealing the gap increased the maximum value of $pb/2V$ by approximately 20 percent and reduced the stick force approximately 33 percent for full stick deflection. Adding the balance had no effect on $pb/2V$ of the sealed aileron but reduced the stick force approximately 50 percent for full stick deflection at high speed. With the ailerons sealed,

the available $pb/2V$ for $\delta_a = \pm 15^\circ$ was greater than the minimum required; whereas, with the unsealed ailerons this effectiveness was not provided at all velocities. The aileron characteristics for the airplane with the $0.56\overline{c}_a$ balanced aileron and the flap in several extended positions are presented in figure 52 and show the effect of this balance as compared with the $0.30\overline{c}_a$ balance on stick forces and aileron effectiveness. The aileron effectiveness for flap position I-6, $\delta_f = -10^\circ$ represents the most unsatisfactory condition investigated near the selected path and indicates a $pb/2V$ of 0.05 at $V_i = 101$ miles per hour. This low value may be increased somewhat by using a different flap deflection at this position.

In the flap-extended position, the necessity of a differential control for the aileron is indicated with flap at L-2, $\delta_f = 50^\circ$, $\delta_a = 5^\circ$, because of a change in slope of rolling-moment coefficients at deflections beyond $\delta_a = 10^\circ$. Two differential systems were therefore devised as follows: a 3:1 differential that gave aileron deflections (from the initial 5° droop) of 5° down, 15° up; and a 2:1 differential that gave aileron deflections of 5° down, 10° up. The mechanical characteristics of these differentials are given in figures 53 to 57. Because the aerodynamic stick forces (figs. 58 and 59) obtained for both differential systems were negative, springs were required to provide positive forces. The aileron effectiveness appeared to be adequate for both proposed systems and, in all attitudes, was greater than that obtained in the flap-retracted condition.

Several aileron and flap arrangements have been tested on the wing model of the present investigation (references 5 and 6). The lift, drag, and pitching-moment characteristics of the several arrangements are compared in figures 13 and 14. Estimated rates of roll for the several arrangements (arrangements 1 to 10) are compared in figure 60(a), in which it may be seen that the present arrangement and the plug aileron gave much higher rates of roll with flap deflected than with flap neutral. In both conditions the plug aileron had a much lower available rate of roll than the present arrangement, but this deficiency of the plug aileron could be remedied by increasing its size. (See reference 6.) With regard to rolling effectiveness and stick forces, it appears that all the arrangements considered could be made satisfactory.

The variation of $C_{n'}/C_{l'}$ with C_L of the several arrangements was essentially the same (fig. 60(b)), but the $C_{n'}/C_{l'}$ at any given value of C_L differed widely among the several arrangements. The plug aileron gave the lowest values of adverse $C_{n'}/C_{l'}$ and, with all the arrangements, the adverse $C_{n'}/C_{l'}$ was much lower with flaps down than with flaps neutral at any particular lift coefficient. If drooped ailerons are used, however, high adverse $C_{n'}/C_{l'}$ may be expected, as is indicated by the single point obtained from arrangement 4. The effect of yawing moment on aileron control is treated analytically in reference 12. High yawing-moment ratios of either sign should be avoided if possible, and flight tests may indicate the desirability of modifying all the arrangements except the plug aileron to reduce the adverse $C_{n'}/C_{l'}$ at high C_L.

CONCLUSIONS

1. The results of this investigation of a full-span retractable flap in combination with a full-span aileron indicate that an increment of maximum lift coefficient of 1.3 may be attained by deflecting the full-span flap 30° with the flap nose about 3 percent below the trailing edge of the wing. This increment was increased to 1.5 by increasing the flap deflection and drooping the aileron. The pitching-moment coefficient obtained at any given lift coefficient with the flap extended was approximately the same as that of other partial and full-span flap arrangements tested in the same wing.

2. The estimated aileron effectiveness was adequate in the flap-retracted condition and was increased by about 50 percent when the flap was extended. A reduction of aileron effectiveness of approximately 40 percent relative to the flap-retracted condition appears unavoidable at some intermediate flap positions. An internal balance reduced the estimated stick forces to acceptable values for all flap positions and deflections along a selected path.

3. It is indicated by the estimated rates of roll and the stick forces that the wing arrangement tested would provide satisfactory lateral control on the assumed fighter airplane.

Langley Memorial Aeronautical Laboratory,
National Advisory Committee for Aeronautics,
Langley Field, Va.

REFERENCES

1. Rogallo, F. M., and Lowry, John G.: Wind-Tunnel Investigation of an NACA Full-Span High-Lift Lateral-Control Combination. I - Section Characteristics, NACA 23012 Airfoil. NACA A.R.R., July 1942.

2. Platt, Robert C., and Shortal, Joseph A.: Wind-Tunnel Investigation of Wings with Ordinary Ailerons and Full-Span External-Airfoil Flaps. Rep. No. 603, NACA, 1937.

3. Wenzinger, Carl J., and Harris, Thomas A.: Wind-Tunnel Investigation of an N.A.C.A. 23012 Airfoil with Various Arrangements of Slotted Flaps. Rep. No. 664, NACA, 1939.

4. Rogallo, F. M., and Lowry, John G.: Résumé of Data for Internally Balanced Ailerons. NACA R.B., March 1943.

5. Rogallo, F. M., and Lowry, John G.: Wind-Tunnel Investigation of a Plain Aileron and a Balanced Aileron on a Tapered Wing with Full-Span Duplex Flaps. NACA A.R.R., July 1942.

6. Lowry, John G., and Liddell, Robert B.: Wind-Tunnel Investigation of a Tapered Wing with a Plug-Type Spoiler-Slot Aileron and Full-Span Slotted Flaps. NACA A.R.R., July 1942.

7. Rogallo, F. M., and Lowry, John G.: Wind-Tunnel Development of Ailerons for the Curtiss XP-60 Airplane. NACA A.C.R., Sept. 1942.

8. Rogallo, Francis M., and Spano, Bartholomew S.: Wind-Tunnel Investigation of a Plain and a Slot-Lip Aileron on a Wing with a Full-Span Slotted Flap. NACA A.C.R., April 1941.

9. Rogallo, F. M., and Schuldenfrei, Marvin: Wind-Tunnel Investigation of a Plain and a Slot-Lip Aileron on a Wing with a Full-Span Flap Consisting of an Inboard Fowler and an Outboard Slotted Flap. NACA A.R.R., June 1941.

10. Gilruth, R. R., and Turner, W. N.: Lateral Control Required for Satisfactory Flying Qualities Based on Flight Tests of Numerous Airplanes. Rep. No. 715, NACA, 1941.

11. Weick, Fred E., and Jones, Robert T.: Résumé and Analysis of N.A.C.A. Lateral Control Research. Rep. No. 605, NACA, 1937.

12. Fehlner, Leo F.: A Study of the Effect of Adverse Yawing Moment on Lateral Maneuverability at a High Lift Coefficient. NACA A.R.R., Sept. 1942.

TABLE I

ORDINATES FOR AIRFOIL

[Spanwise stations in inches from root section. Chord stations and ordinates in percent of basic wing chord, c_1]

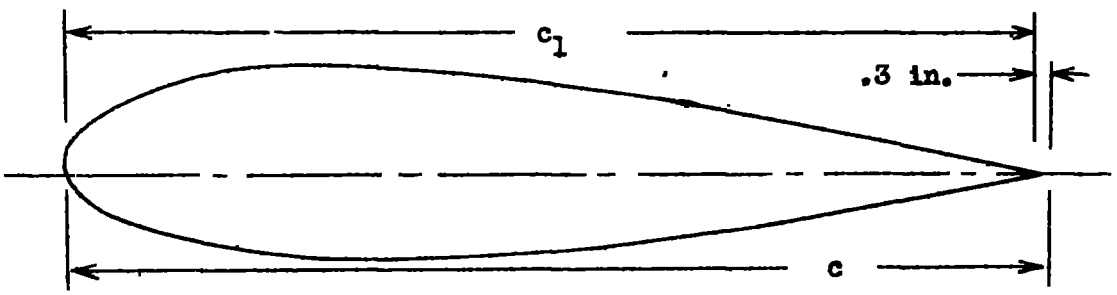

Model wing station 0		
Station	Upper surface	Lower surface
0	0	0
1.25	3.48	-1.60
2.5	4.61	-2.36
5	6.10	-3.21
7.5	7.14	-3.82
10	7.89	-4.33
15	8.80	-5.12
20	9.22	-5.71
25	9.40	-6.10
30	9.37	-6.28
40	8.90	-6.23
50	8.02	-5.78
60	6.85	-5.05
70	5.44	-4.10
80	3.87	-2.97
90	2.12	-1.67
95	1.16	-.94
100	.18	-.16
100.73	.03	-.03
L.E. radius: 2.65. Slope of radius through end of chord: 0.305		

Model wing station 88.8		
Station	Upper surface	Lower surface
0	0	0
1.25	1.89	-.84
2.5	2.65	-1.07
5	3.70	-1.26
7.5	4.45	-1.40
10	4.98	-1.52
15	5.54	-1.86
20	5.73	-2.22
25	5.77	-2.46
30	5.71	-2.62
40	5.36	-2.70
50	4.78	-2.56
60	4.06	-2.27
70	3.21	-1.87
80	2.26	-1.36
90	1.22	-.78
95	.70	-.46
100	.18	-.14
101.2	.05	-.05
L.E. radius: 0.70. Slope of radius through end of chord: 0.305		

TABLE II

ORDINATES FOR FULL-SPAN FLAPS

[Spanwise stations in inches from root section. Chord stations and ordinates in percent of basic wing chord, c_1]

Flap stations

Model wing station 0		
Station	Upper surface	Lower surface
0	-1.29	-1.29
.52	-.08	-2.30
1.04	.48	-2.50
2.07	1.29	-2.60
4.15	2.17	-2.44
6.22	2.53	-2.18
8.29	2.40	-1.91
12.44	1.65	-1.32
16.58	.85	-.69
20.72	.03	-.03
L.E. radius: 1.19		

Model wing station 88.8		
Station	Upper surface	Lower surface
0	-0.76	-0.76
.53	.01	-1.16
1.06	.36	-1.23
2.12	.80	-1.22
4.24	1.30	-1.10
6.36	1.42	-.99
8.48	1.35	-.87
12.72	.93	-.62
16.96	.51	-.32
21.20	.05	-.05
L.E. radius: 0.32		

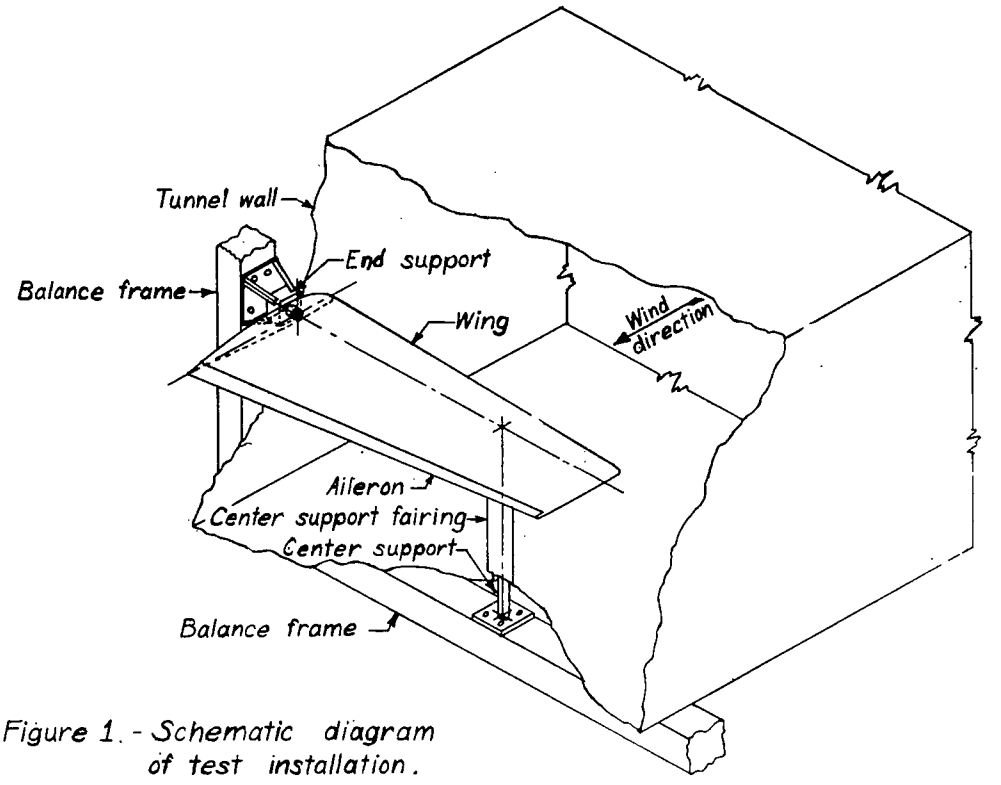

Figure 1. - Schematic diagram of test installation.

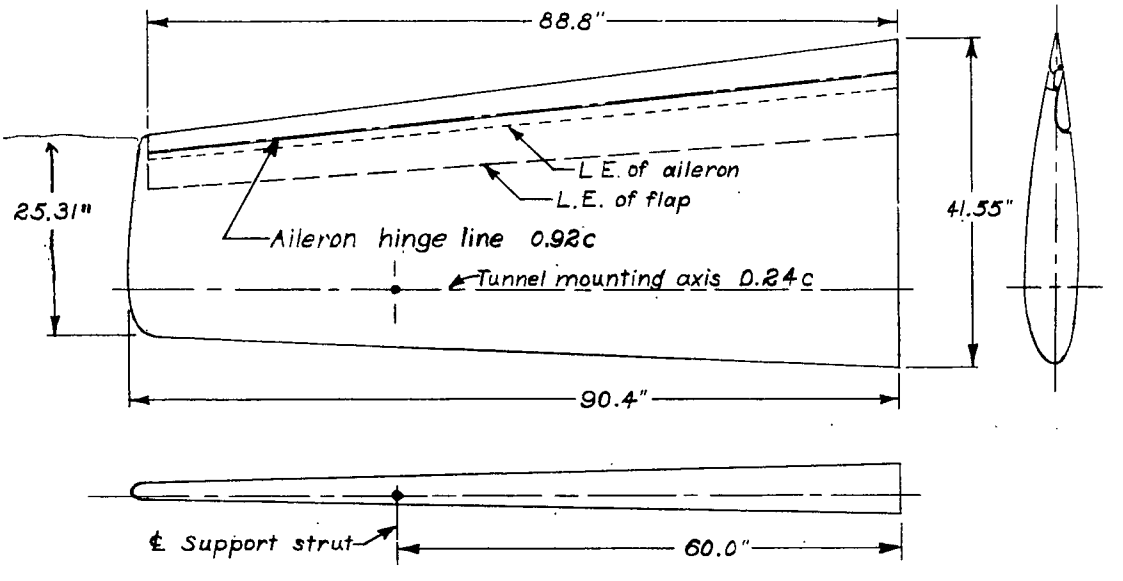

Figure 3 - Semispan model of tapered wing

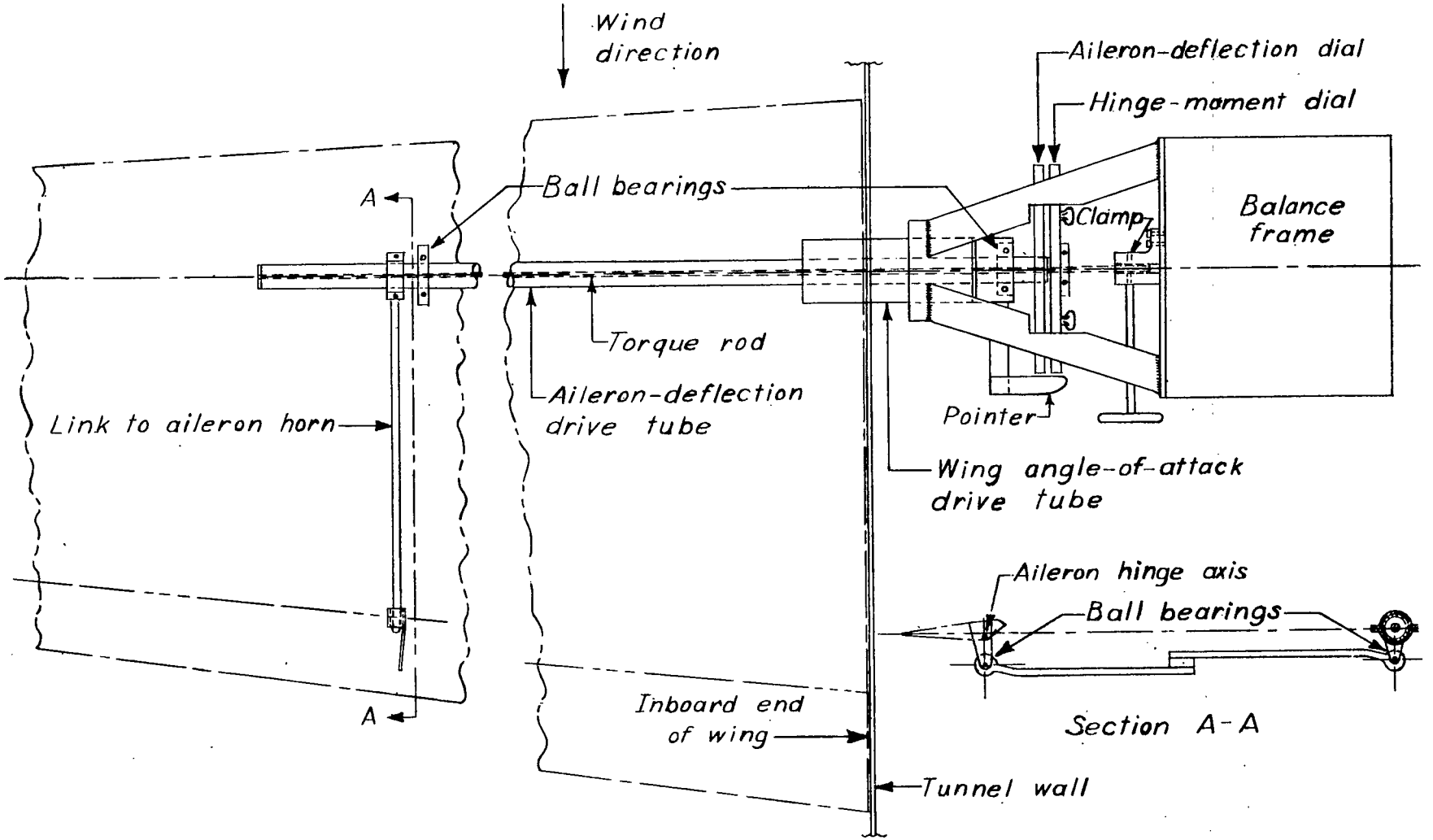

Figure 2. - Schematic diagram of the torque-rod assembly for measuring aileron hinge moments.

Fig. 2

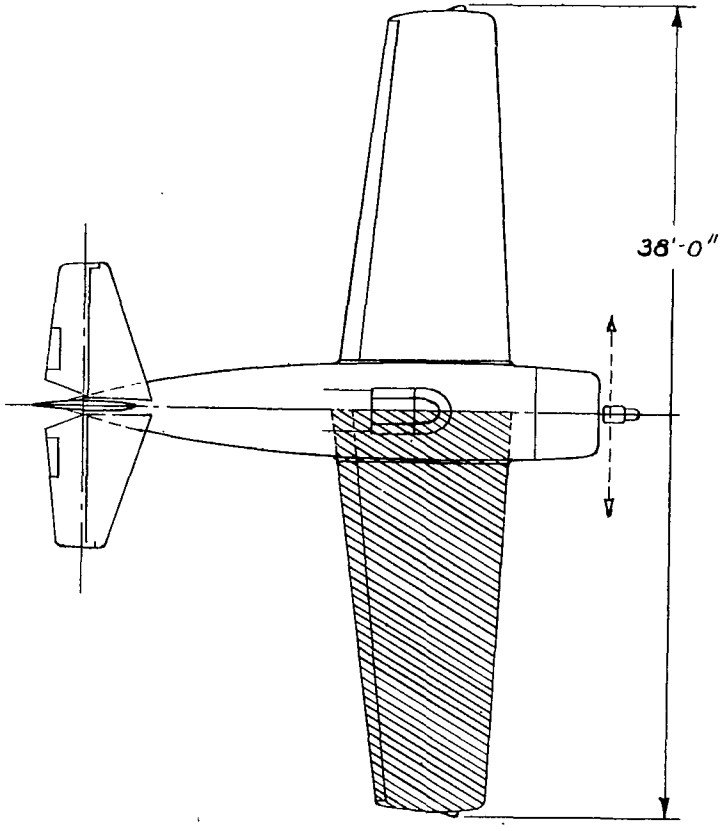

Figure 4. - Portion of airplane simulated by model.

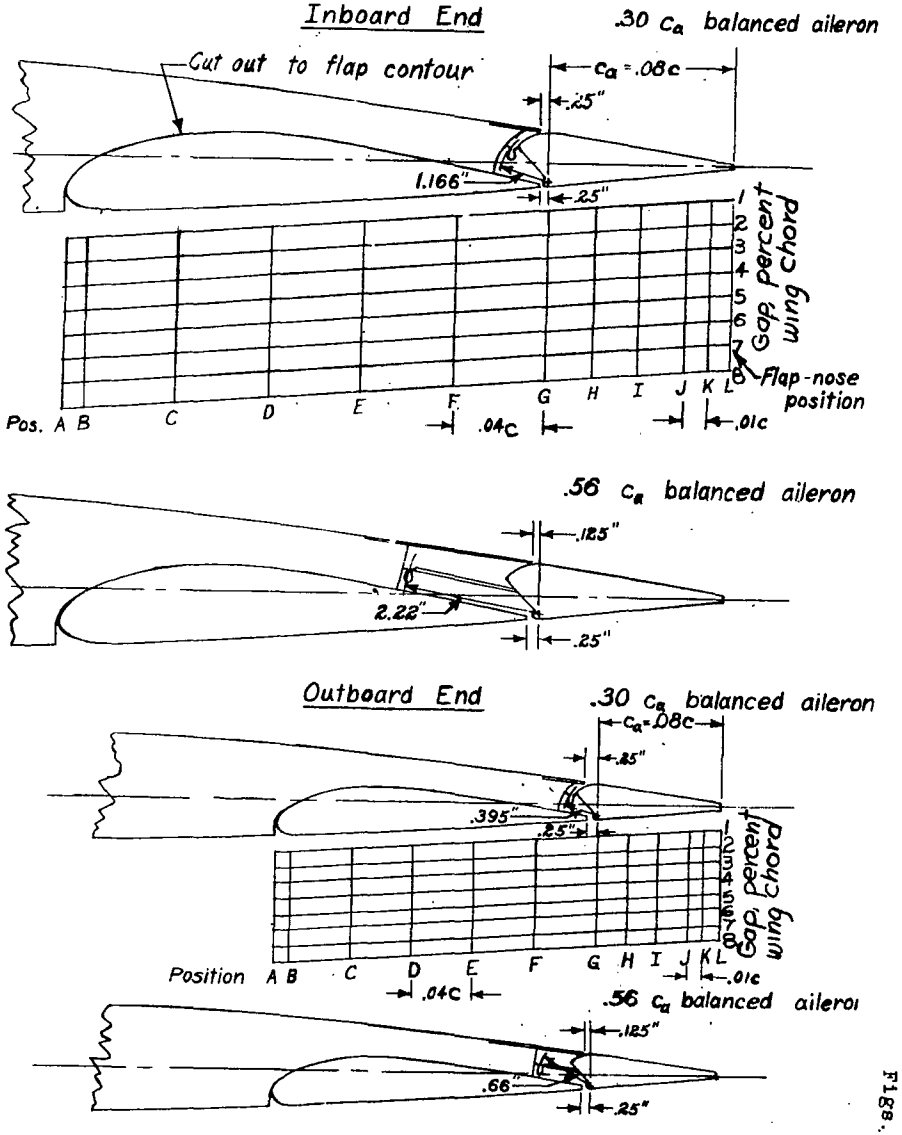

Figure 5. - Aileron details of model.

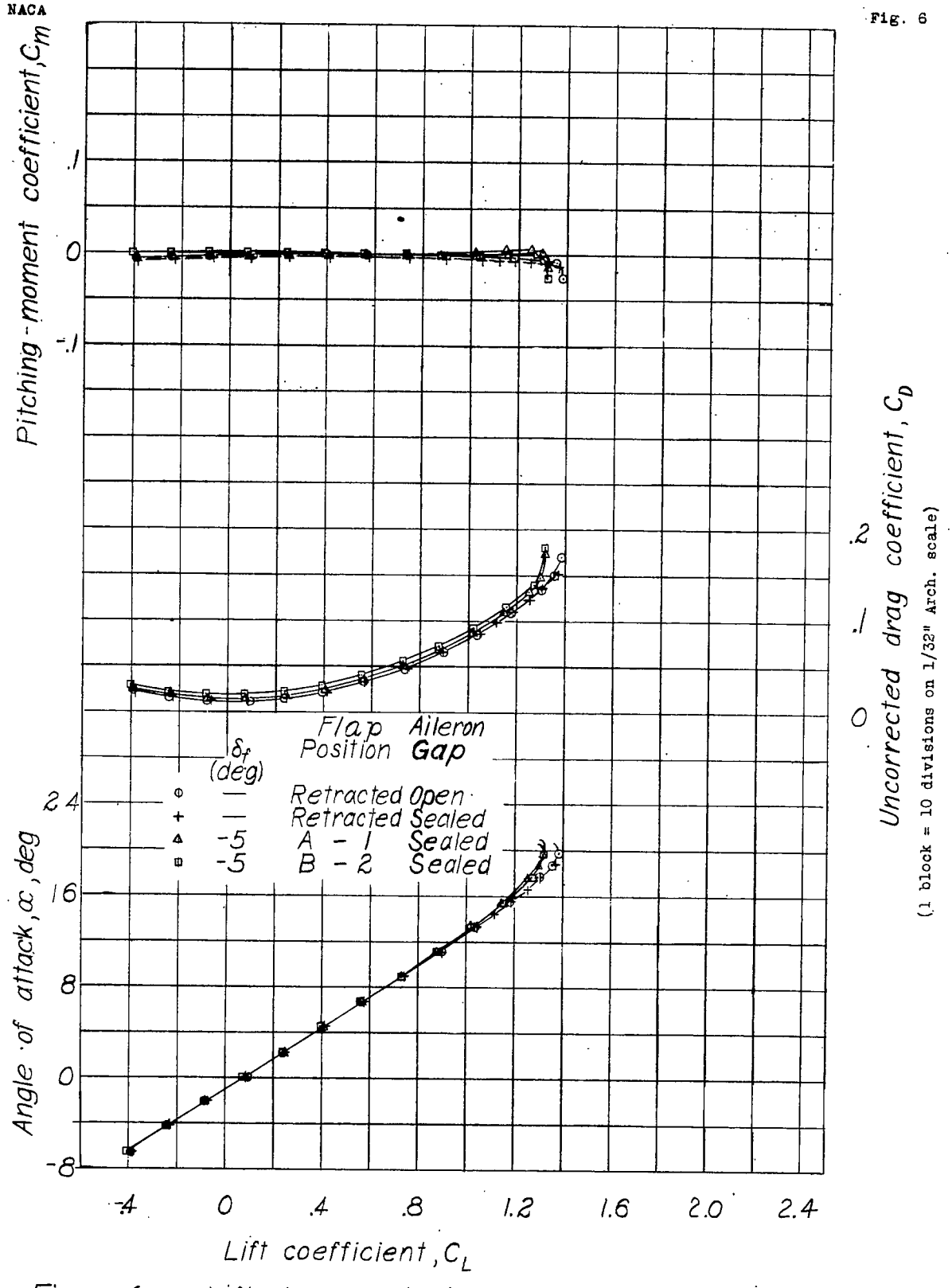

Figure 6.- Lift, drag, and pitching-moment coefficients of the tapered wing model with a full-span flap and full-span aileron. Flap retracted and at chordwise positions A and B; δ_a, 0°.

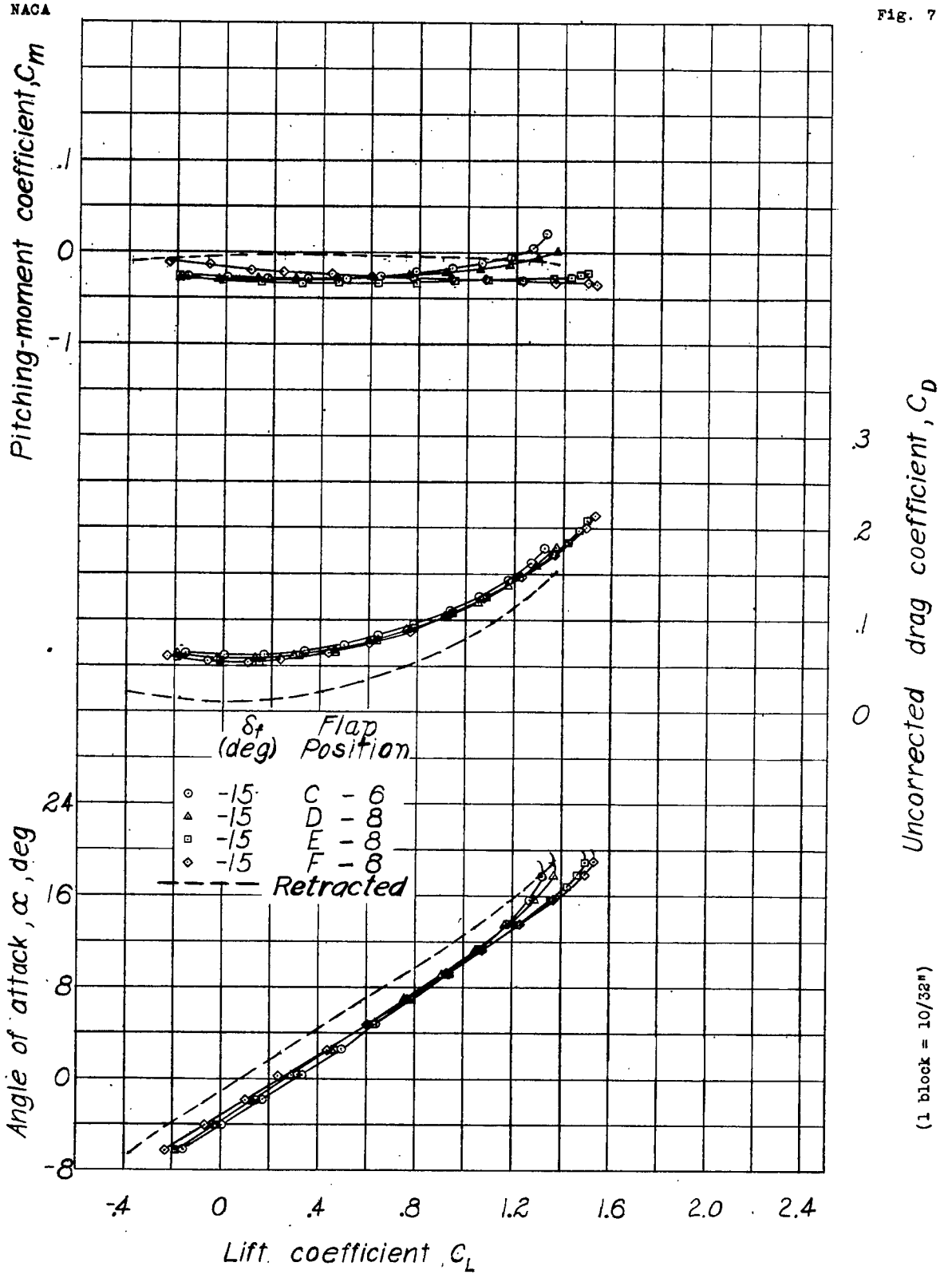

Figure 7.- Lift, drag, and pitching-moment coefficients of the tapered wing model with a full-span flap and a full-span aileron. Flap at chordwise positions C, D, E, and F; δ_a, 0°.

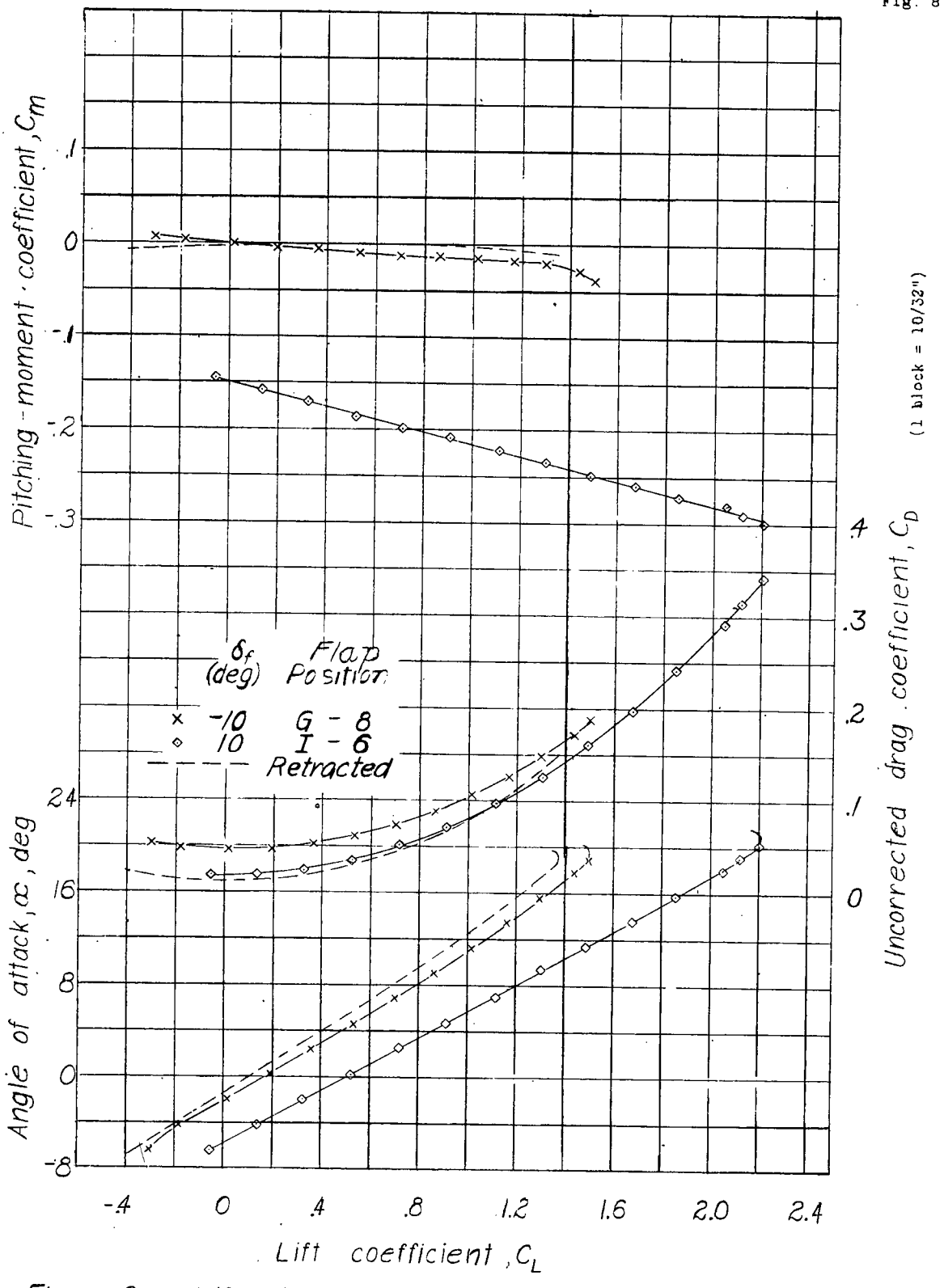

Figure 8 - Lift, drag, and pitching-moment coefficients of the tapered wing model with a full-span flap and a full-span aileron. Flap at chordwise positions G and I; δ_a, 0°

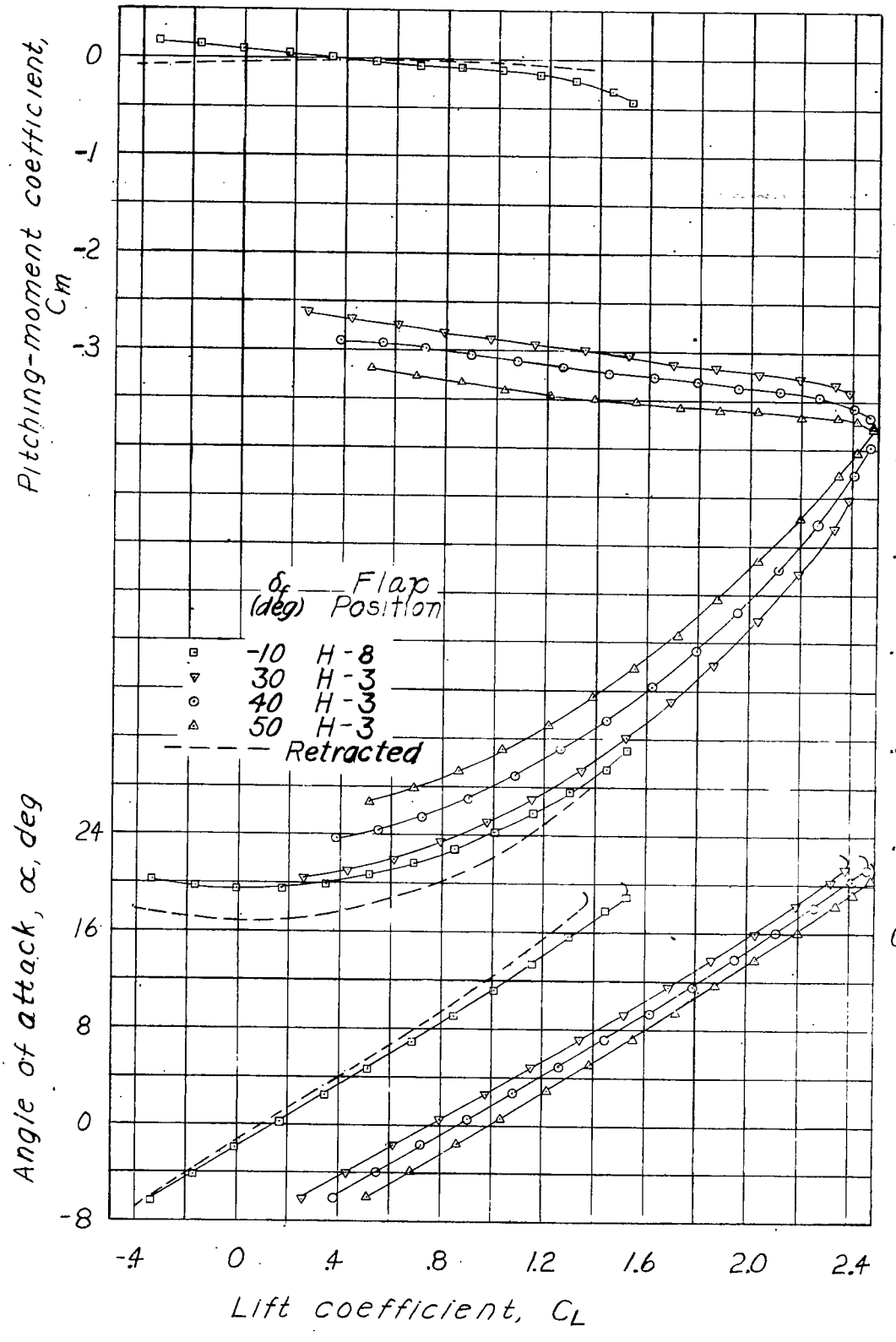

Figure 9.- Lift, drag, and pitching-moment coefficients of the tapered wing model with a full-span flap and a full-span aileron. Flap at chordwise position H; δ_a, 0°.

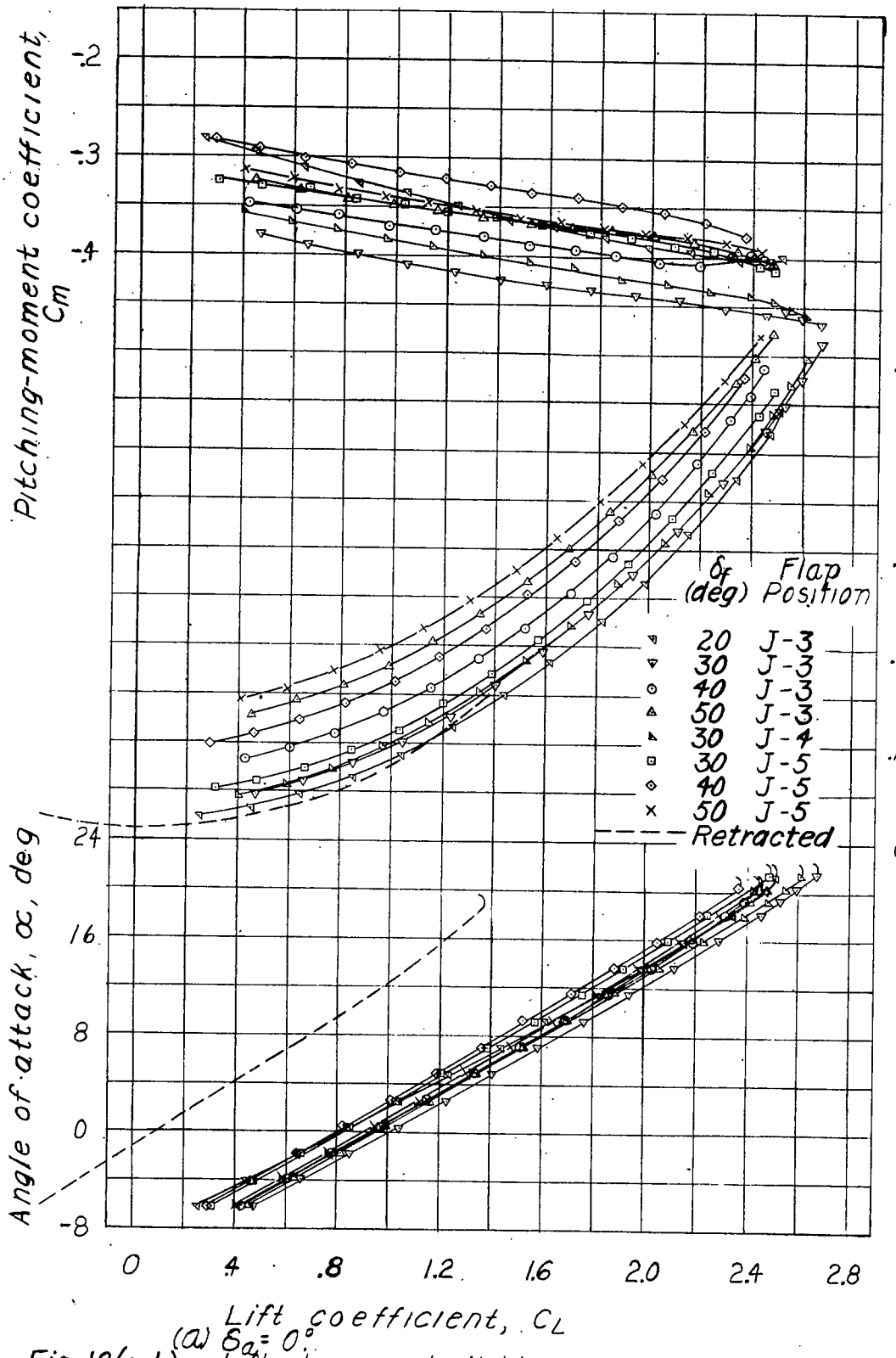

(a) $\delta_a = 0°$.

Fig. 10(a, b) - Lift, drag, and pitching-moment coefficients of the tapered wing model with a full-span flap and a full-span aileron. Flap at chordwise position J.

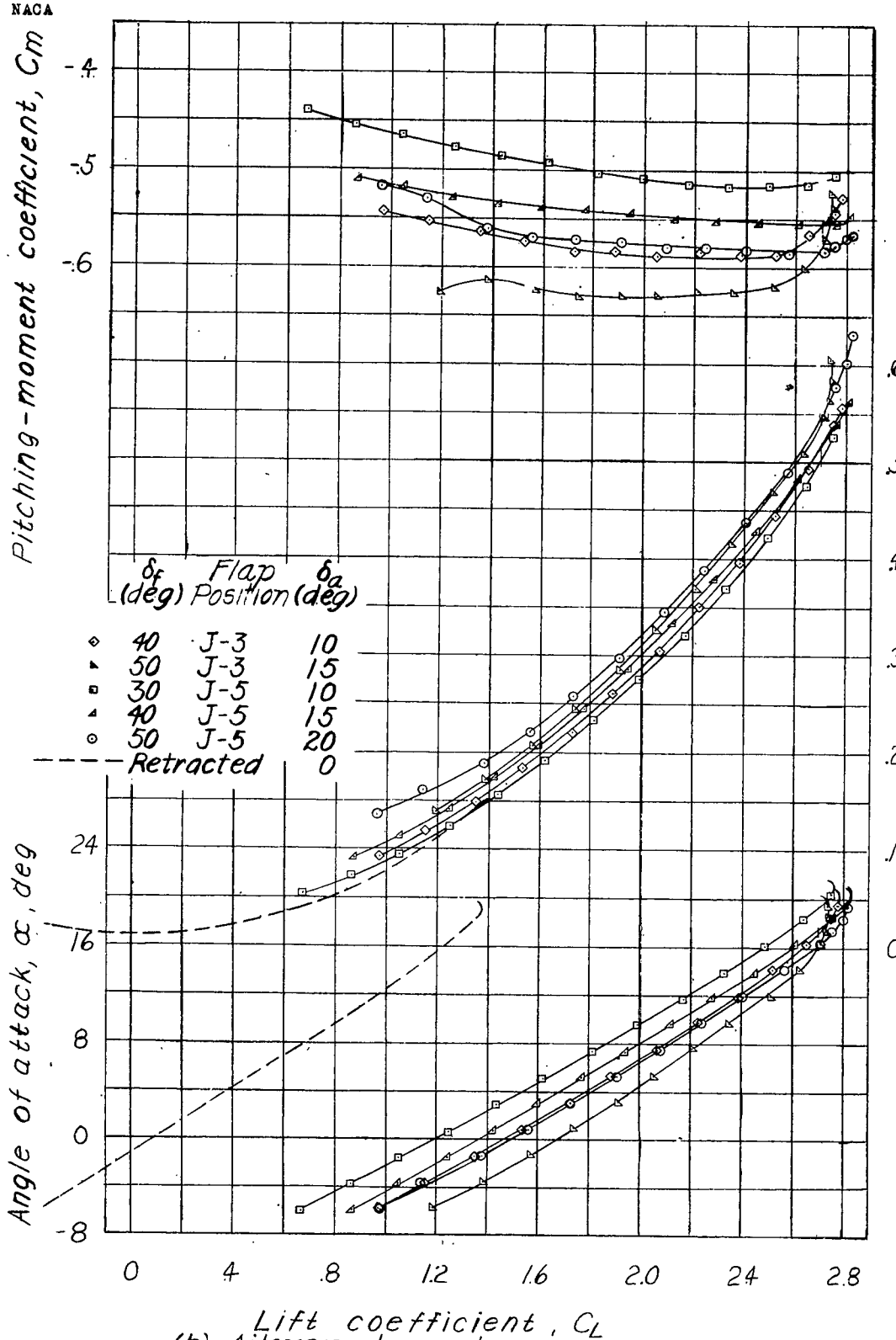

(b) Aileron drooped.

Figure 10.- Concluded.

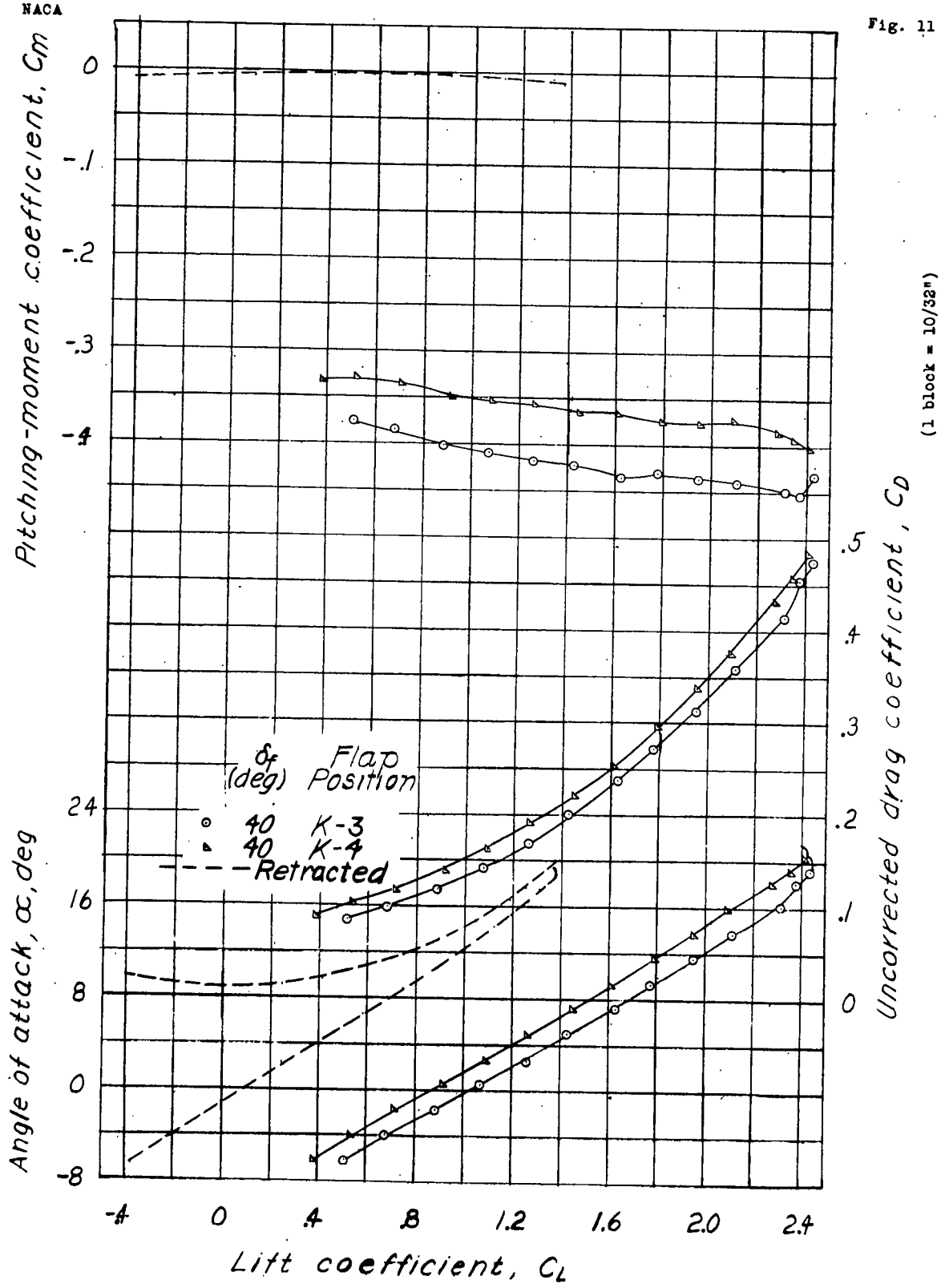

Figure 11.- Lift, drag, and pitching-moment coefficients of the tapered wing model with a full-span flap and a full-span aileron. Flap at chordwise position K; δ_a, 0°.

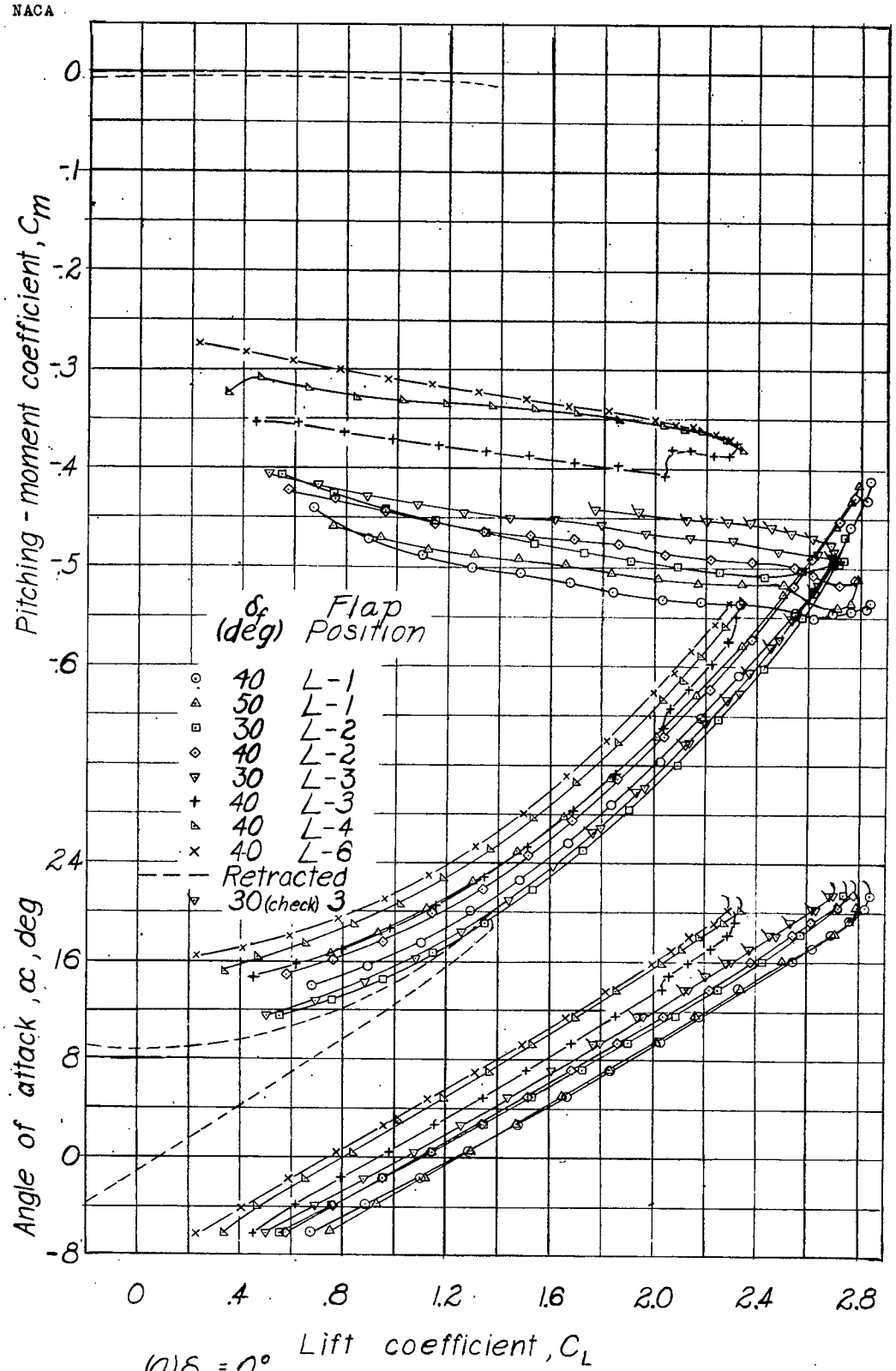

(a) $\delta_a = 0°$.

Fig. 12 (a, b).- Lift, drag, and pitching-moment coefficients of the tapered wing model with a full-span flap and a full-span aileron. Flap at chordwise position L

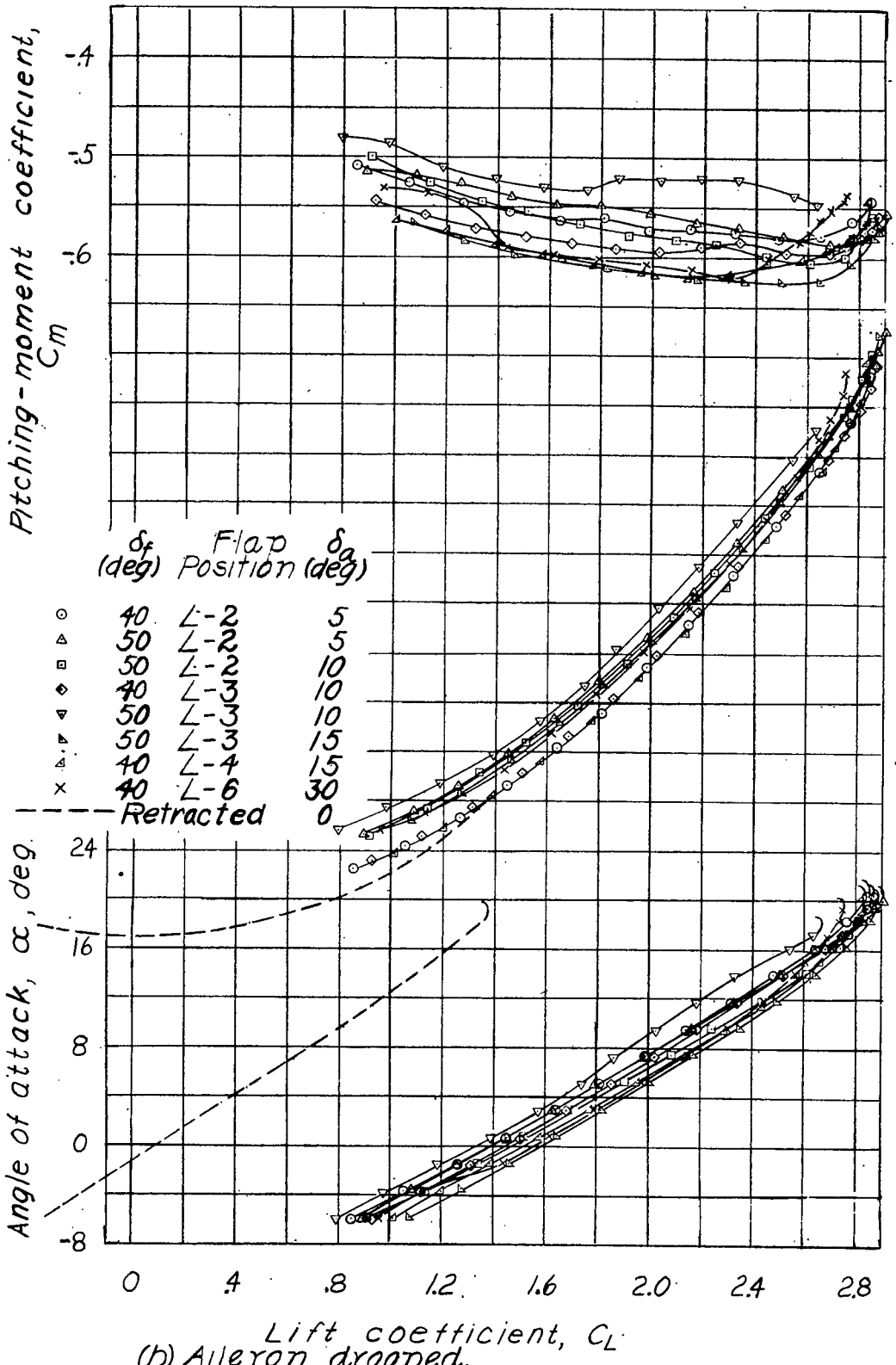

(1 block = 10/32")

(b) Aileron drooped.

Figure 12.- Concluded.

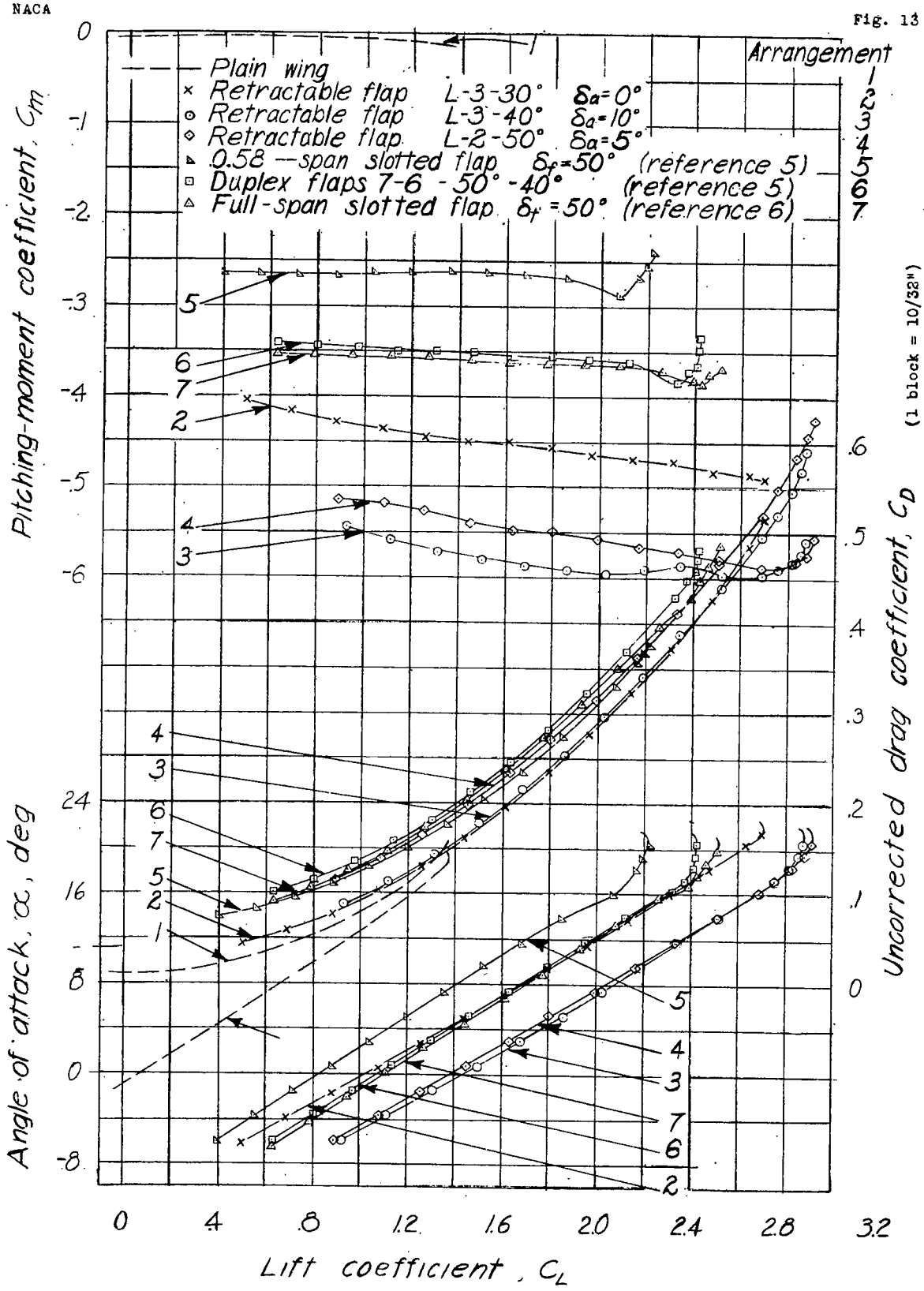

Figure 13.- Comparison of the lift, drag, and pitching-moment coefficients for various arrangements of high-lift and lateral-control devices on a tapered wing model.

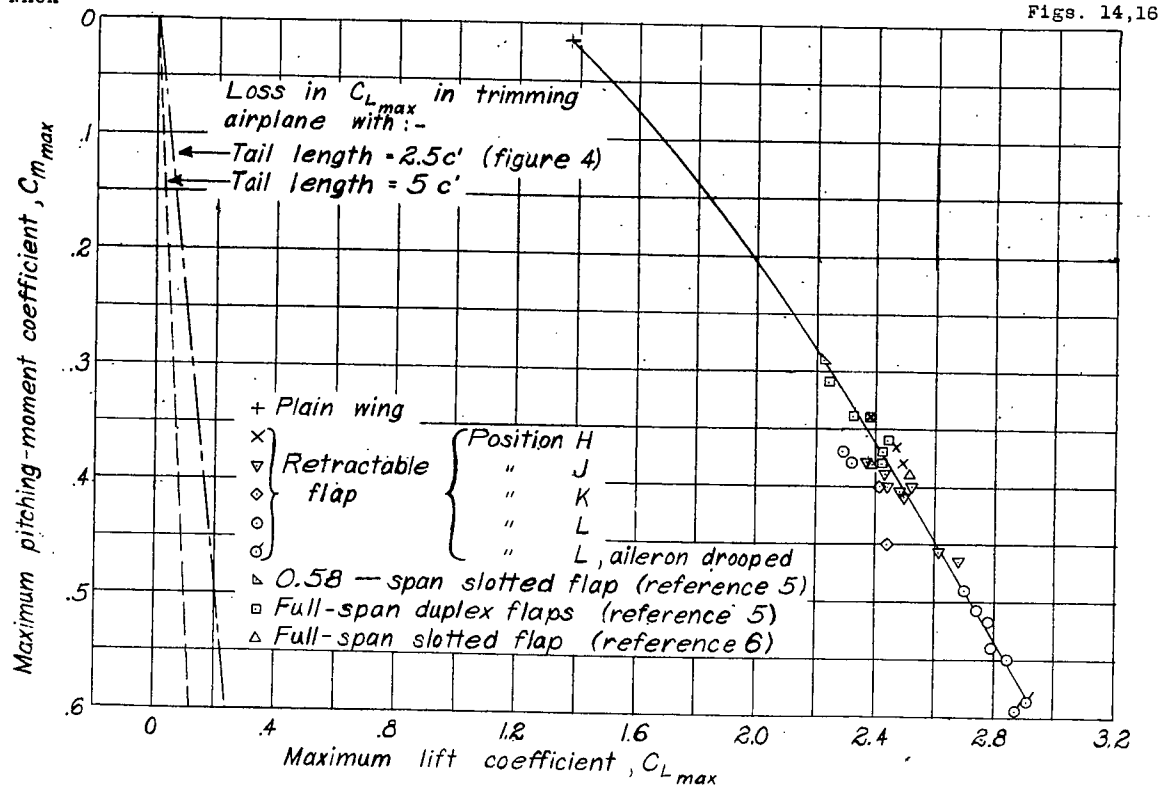

Figure 14.- Variation of the maximum pitching-moment coefficient with maximum lift coefficient for various arrangements of high-lift and lateral-control devices on a tapered wing model.

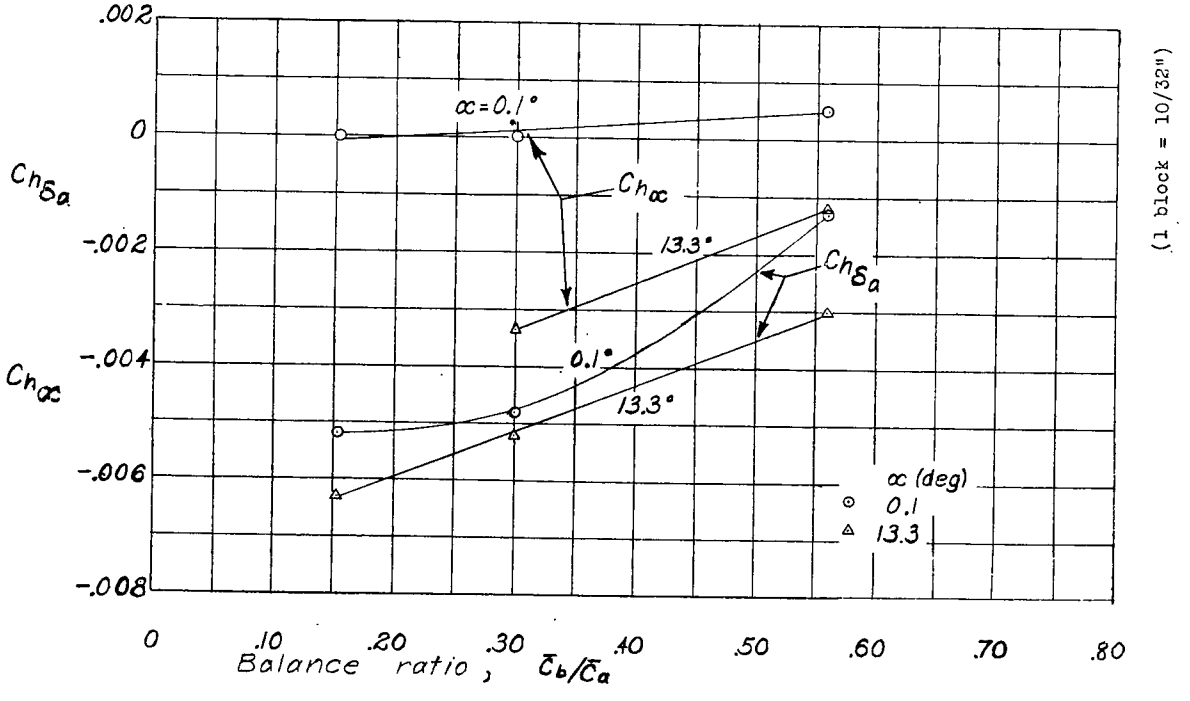

(1 block = 10/32")

Figure 16.- Variation of Ch_α and Ch_{δ_a} with aileron balance, tapered-wing model with full-span flaps retracted.

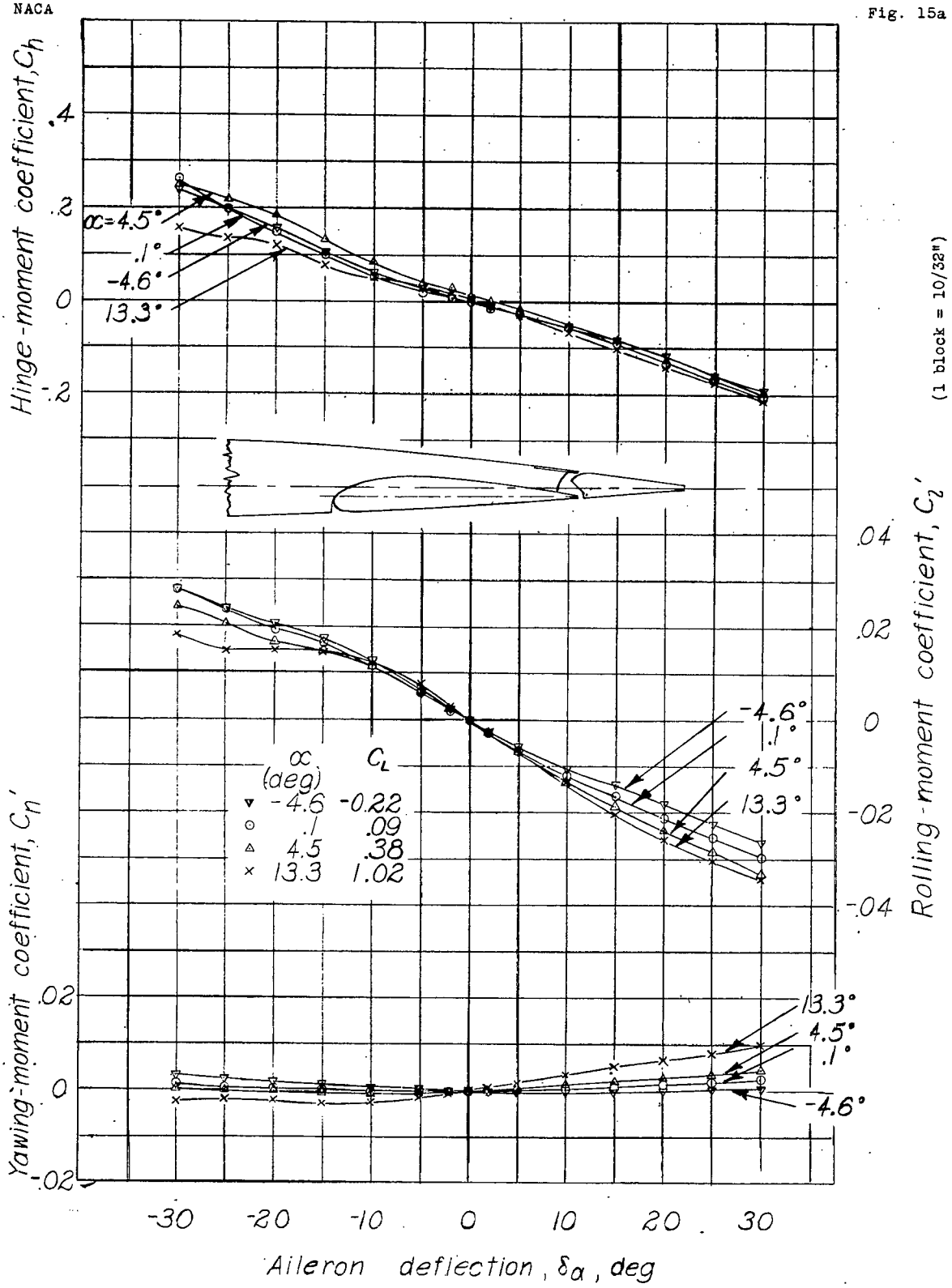

(a) Balance, 0.30$\bar{c}_a$; gap open.

Fig. 15(a to c).-Rolling-, yawing-, and hinge-moment coefficients of the tapered wing model with a full-span flap and a full-span aileron. Flap retracted.

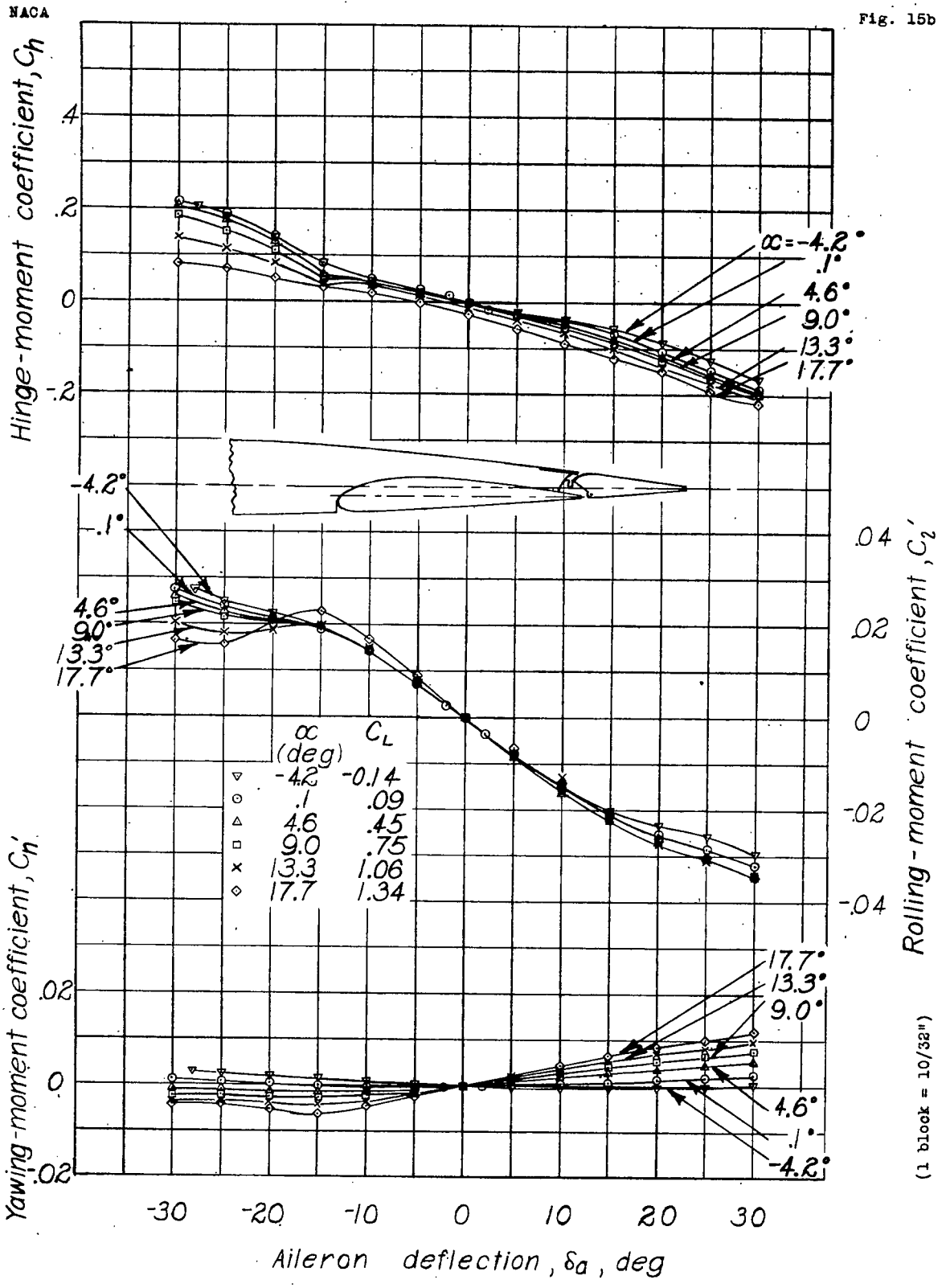

(b) Balance, 0.30 $\bar{c}_a$; gap sealed.

Figure 15 - Continued.

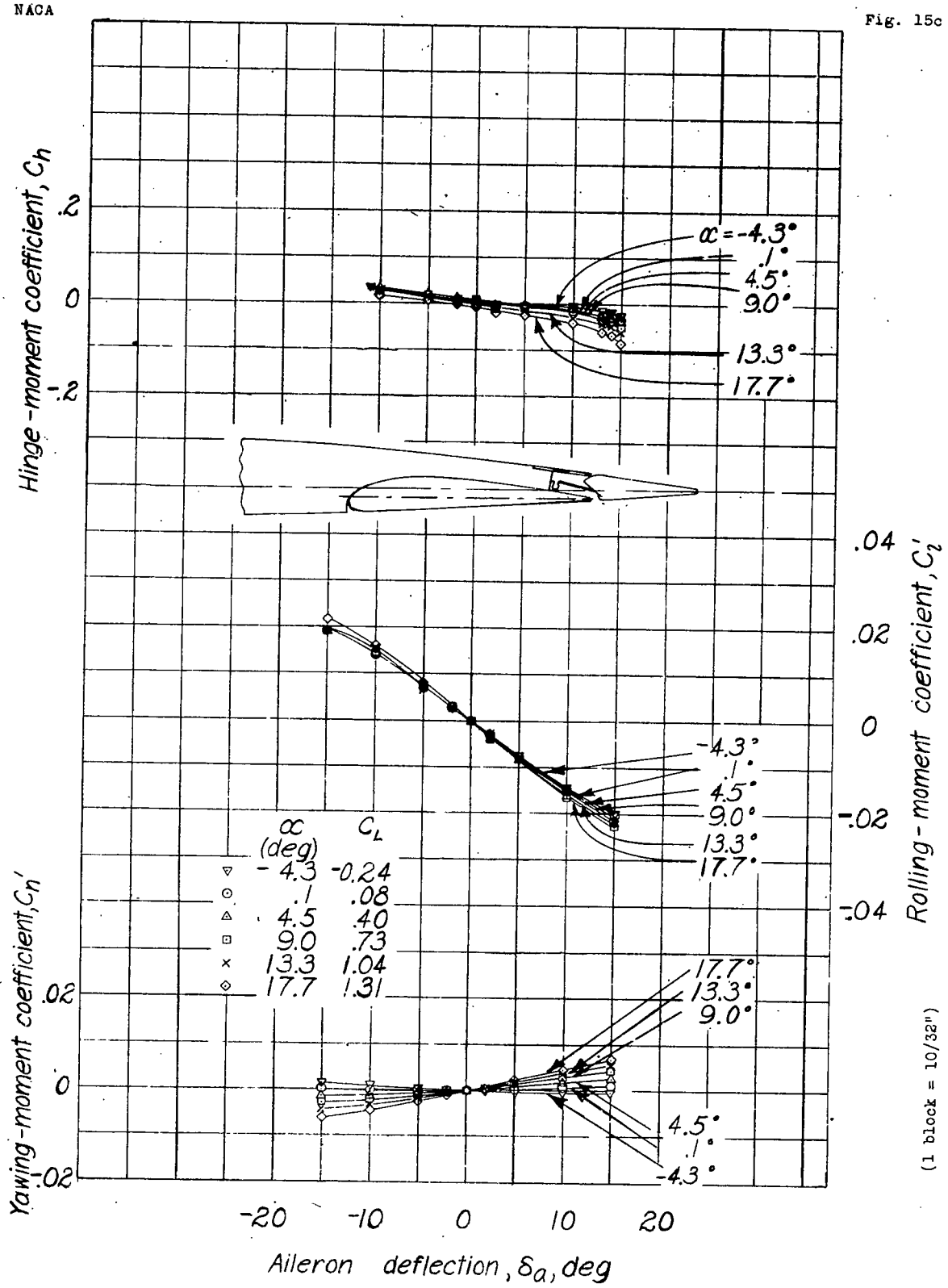

(c) Balance, 0.56 $\bar{c}_a$; gap sealed.

Figure 15.- Concluded.

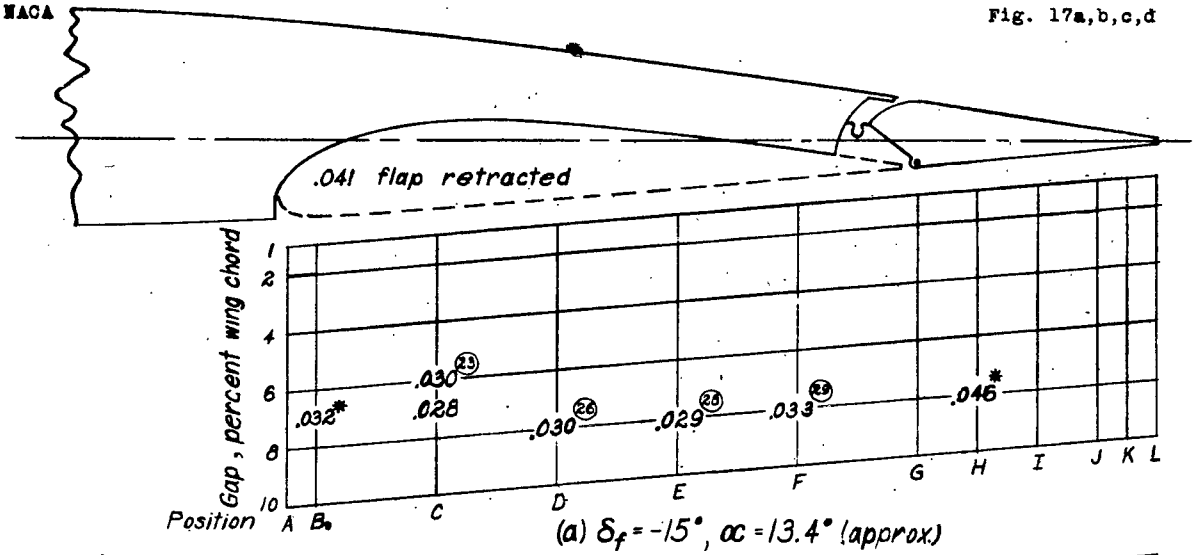

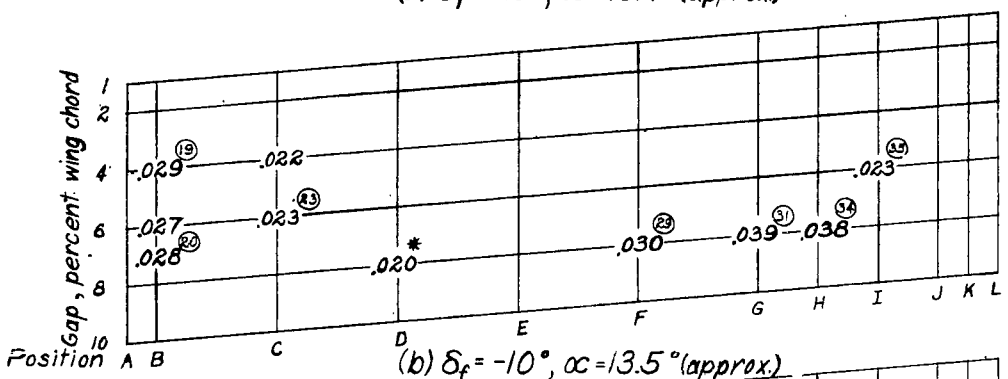

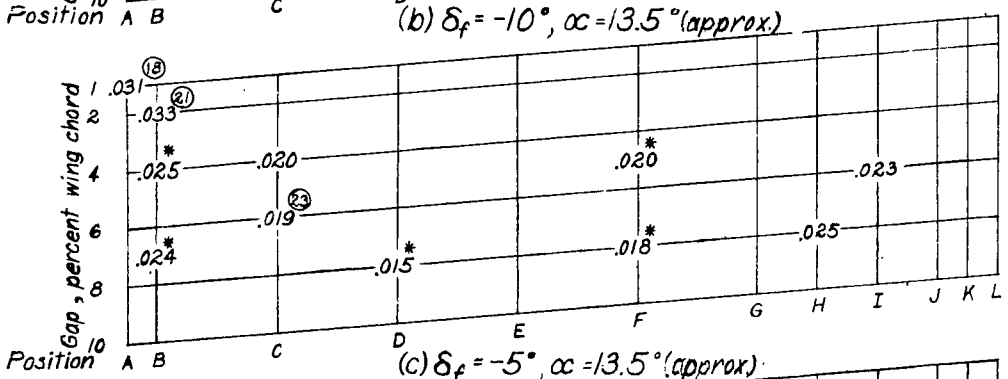

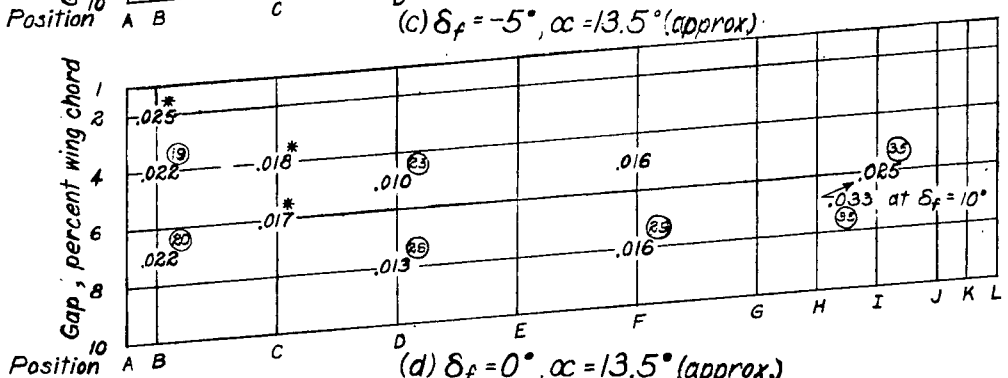

○ Indicates figure in which complete data appear

* Indicates values obtained from cross-plots.

Fig. 17(a to h).- Values of rolling-moment coefficient due to aileron deflections of ±15° at various flap positions and deflections. Tapered wing model with a full-span flap, aileron-gap sealed.

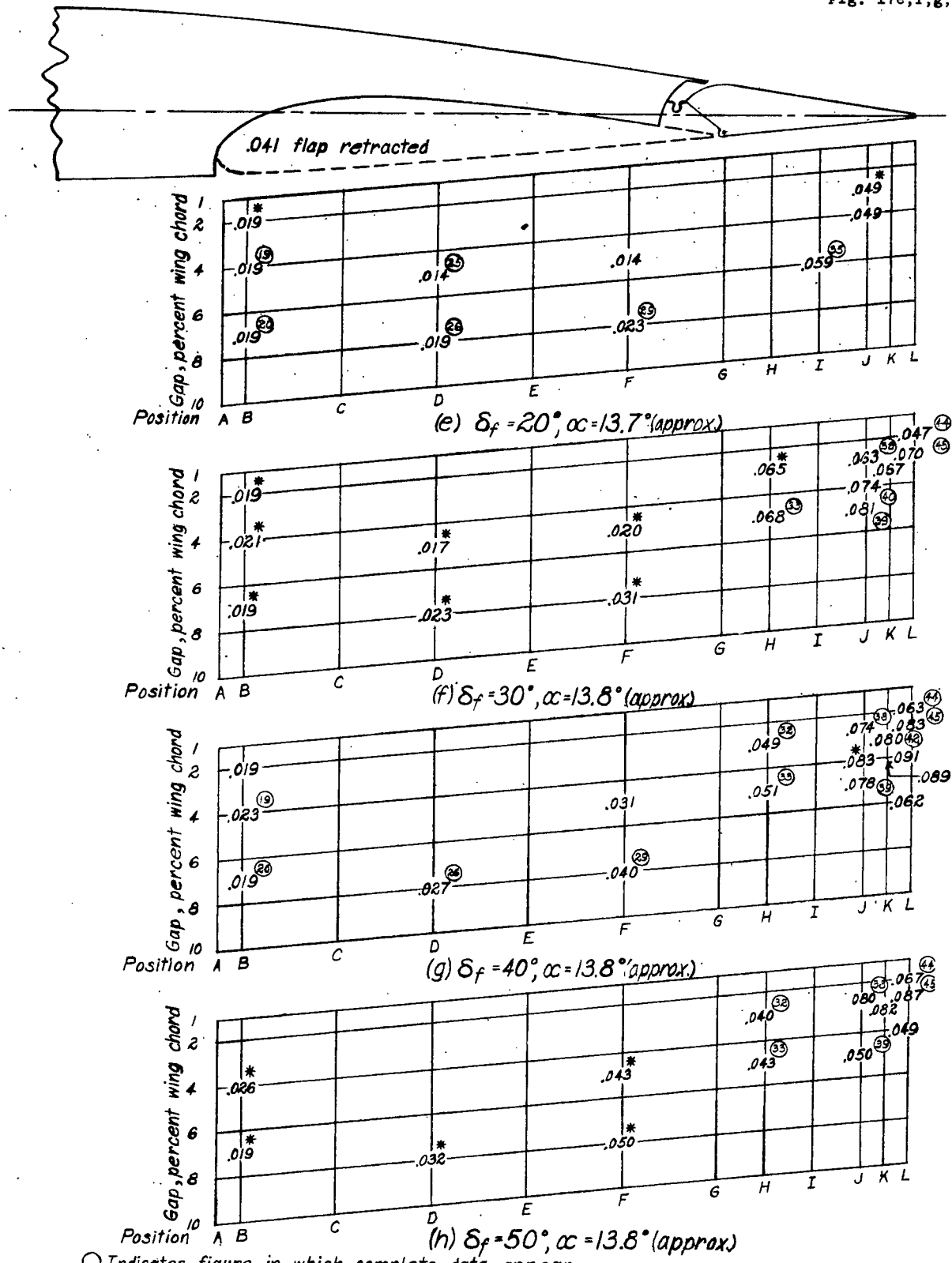

○ Indicates figure in which complete data appear
* Indicates values obtained from cross-plots.

Figure 17. - Concluded.

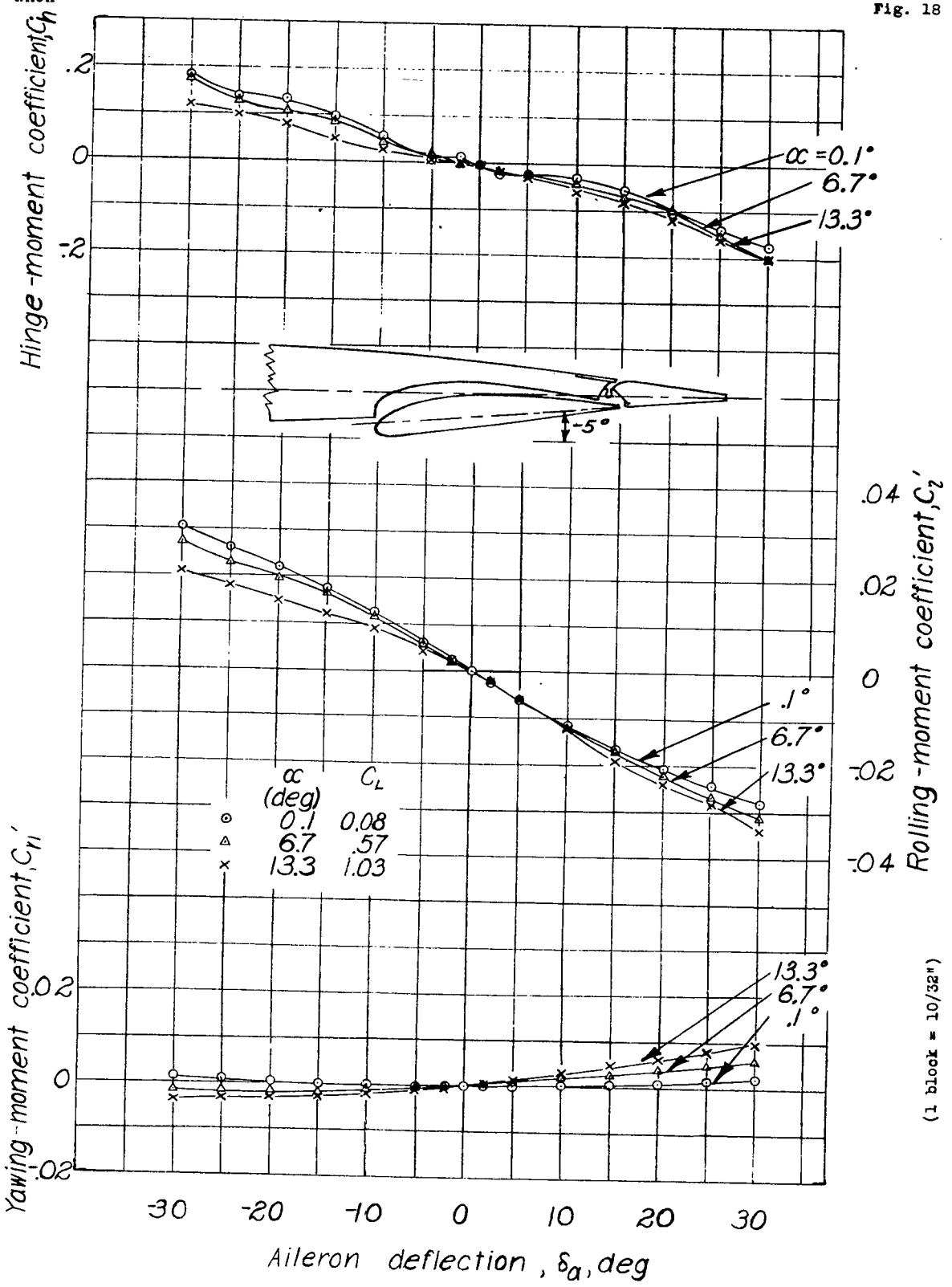

Figure 18. - Rolling-, yawing-, and hinge-moment coefficients of the tapered wing model with a full-span flap and a full-span sealed aileron. Flap position, A-1; balance, 0.30 $\bar{c}_a$: δ_f, -5°

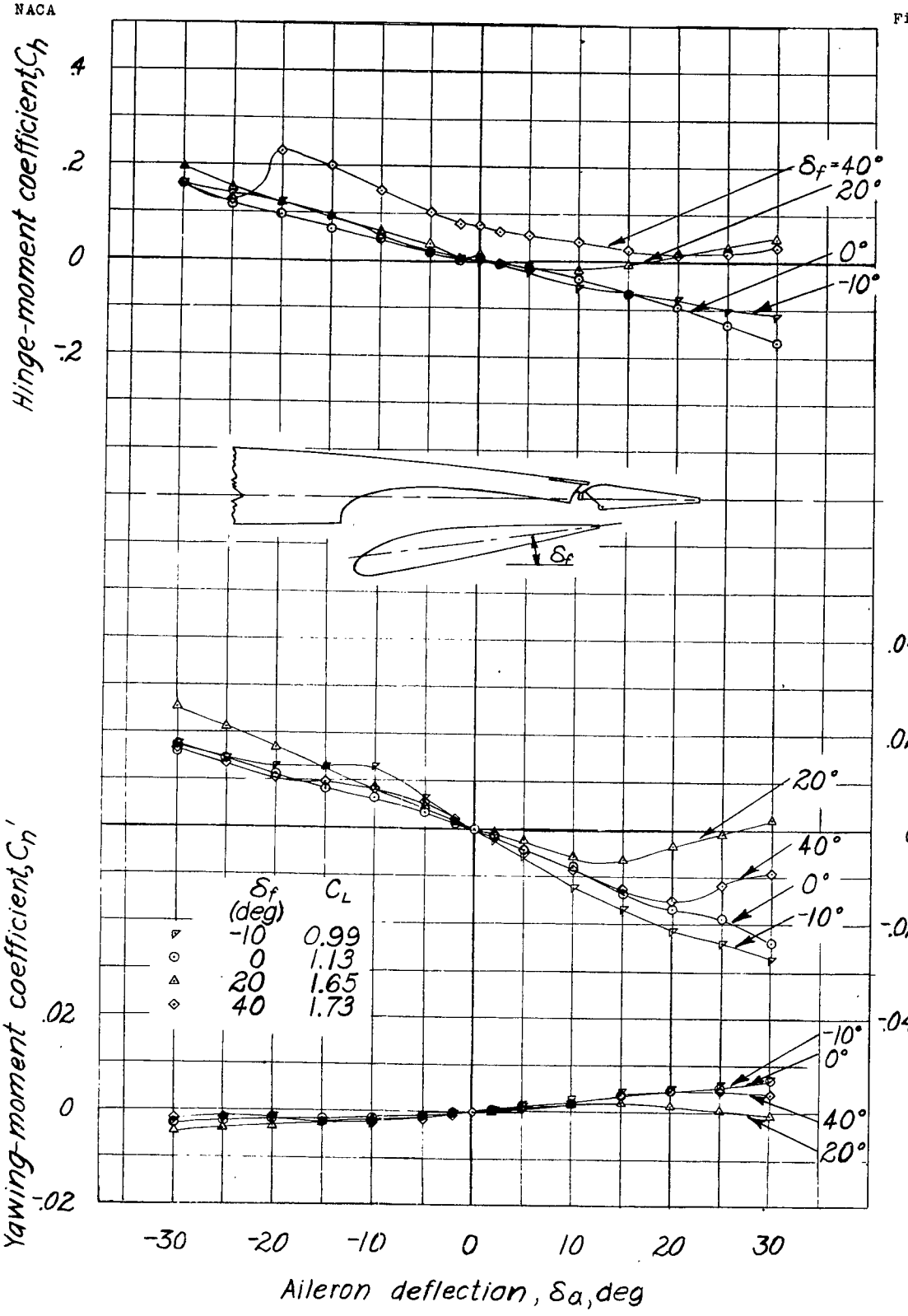

Figure 19.- Rolling-, yawing-, and hinge-moment coefficients of the tapered wing model with a full-span flap and a full-span sealed aileron. Flap position, B-4; balance, $0.30\bar{c}_a$; α, 13.6° (approx.).

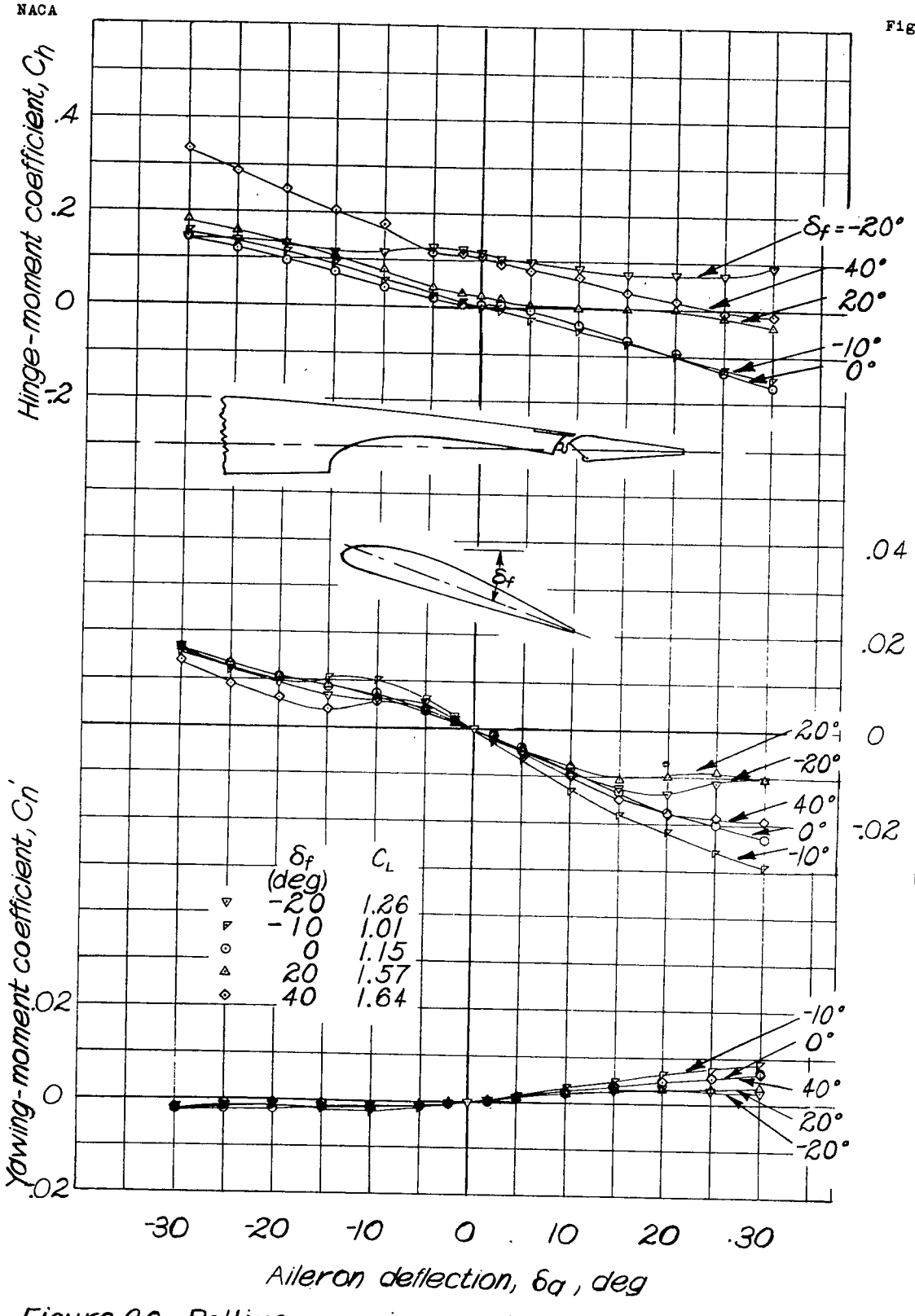

Figure 20.–Rolling-, yawing-, and hinge-moment coefficients of the tapered wing model with a full-span flap and a full-span sealed aileron. Flap position, B-7; balance, 0.30 $\bar{c}_a$; α, 13.6° (approx)

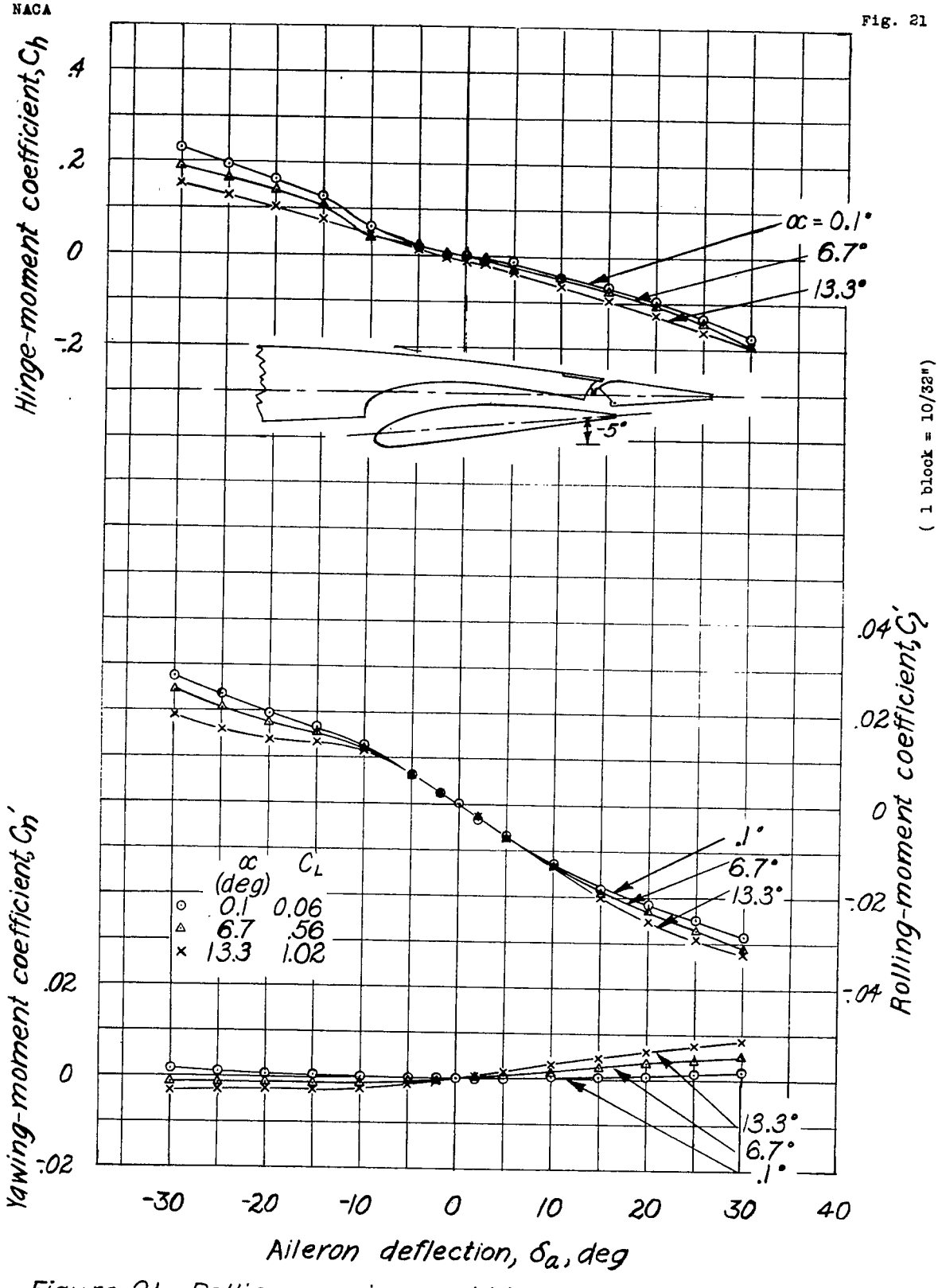

Figure 21.- Rolling-, yawing-, and hinge-moment coefficients of the tapered wing model with a full-span flap and a full-span sealed aileron. Flap position, B-2; balance, 0.30 $\bar{c}_a$; δ_f, -5°.

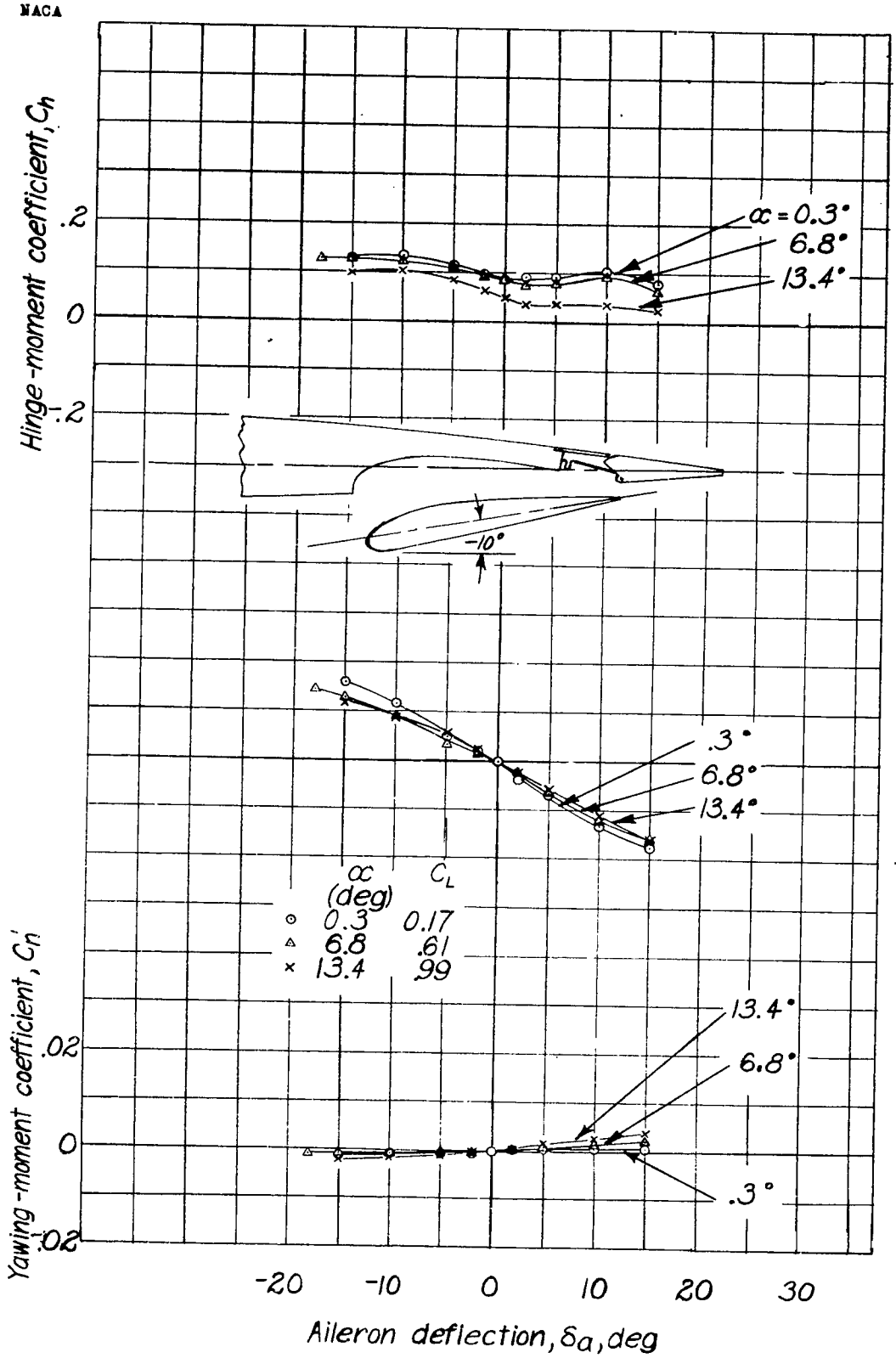

Figure 22.- Rolling-, yawing-, and hinge-moment coefficients of the tapered wing model with a full-span flap and a full-span sealed aileron. Flap position, B-4; balance, 0.56$\bar{c}_a$; δ_a, -10°.

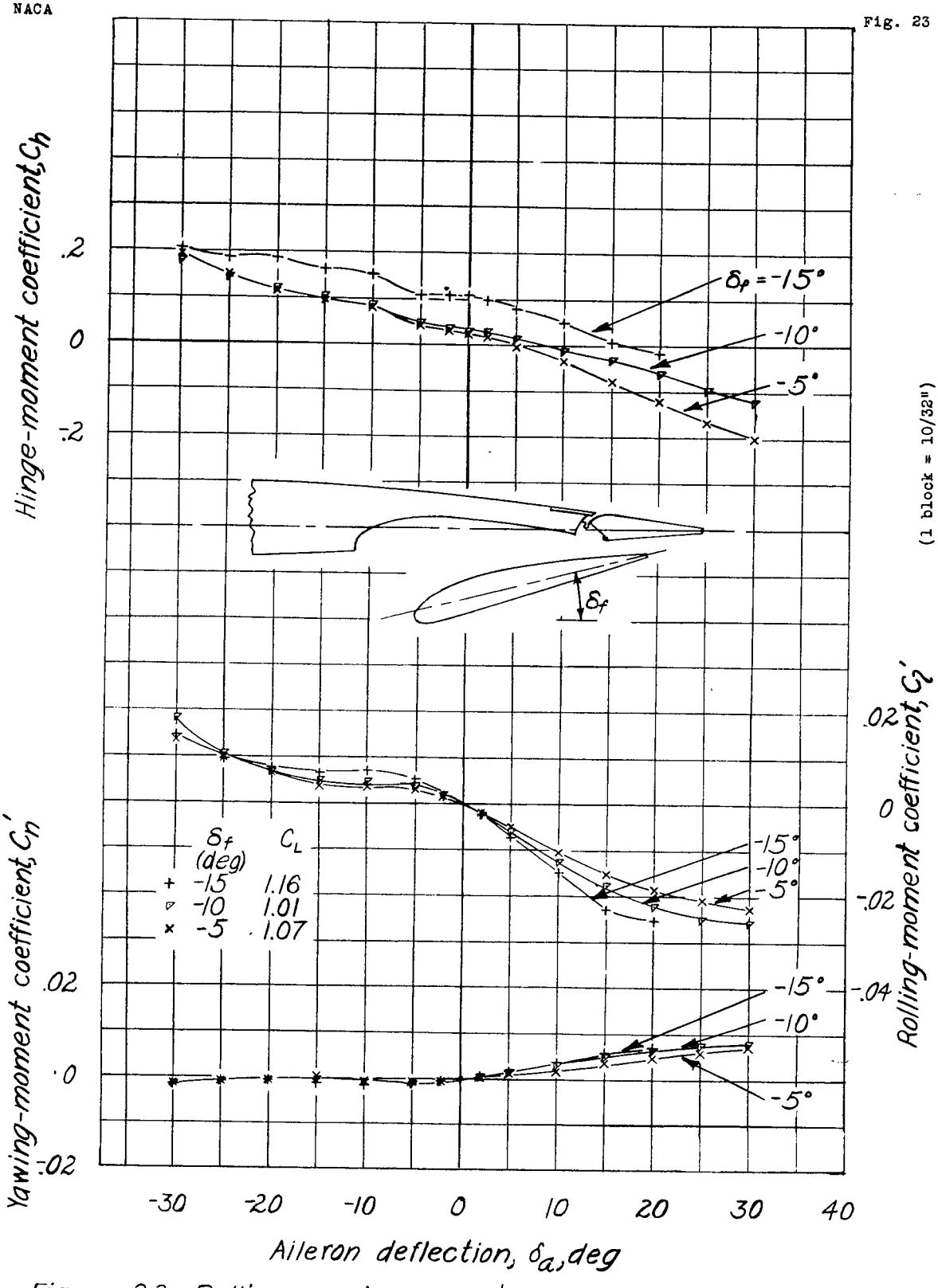

Figure 23.- Rolling-, yawing-, and hinge-moment coefficients of the tapered wing model with a full-span flap and a full-span sealed aileron. Flap position, C-6; balance, 0.30$\bar{c}_a$; α, 13.5° (approx.).

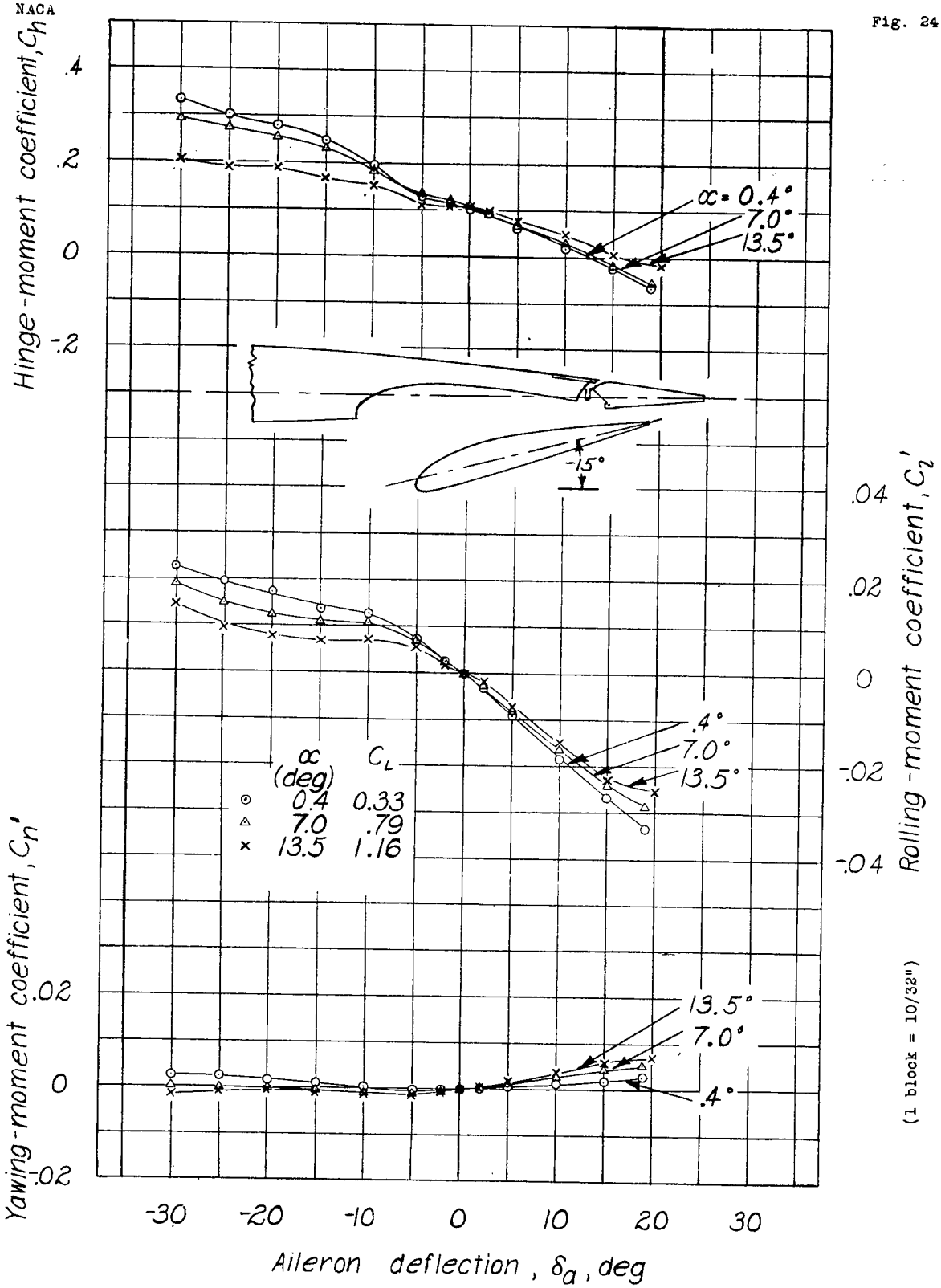

Figure 24.- Rolling-, yawing-, and hinge-moment coefficients of the tapered wing model with a full-span flap and a full-span sealed aileron. Flap position, C-6; balance, 0.30 c_a; δ_f, -15°.

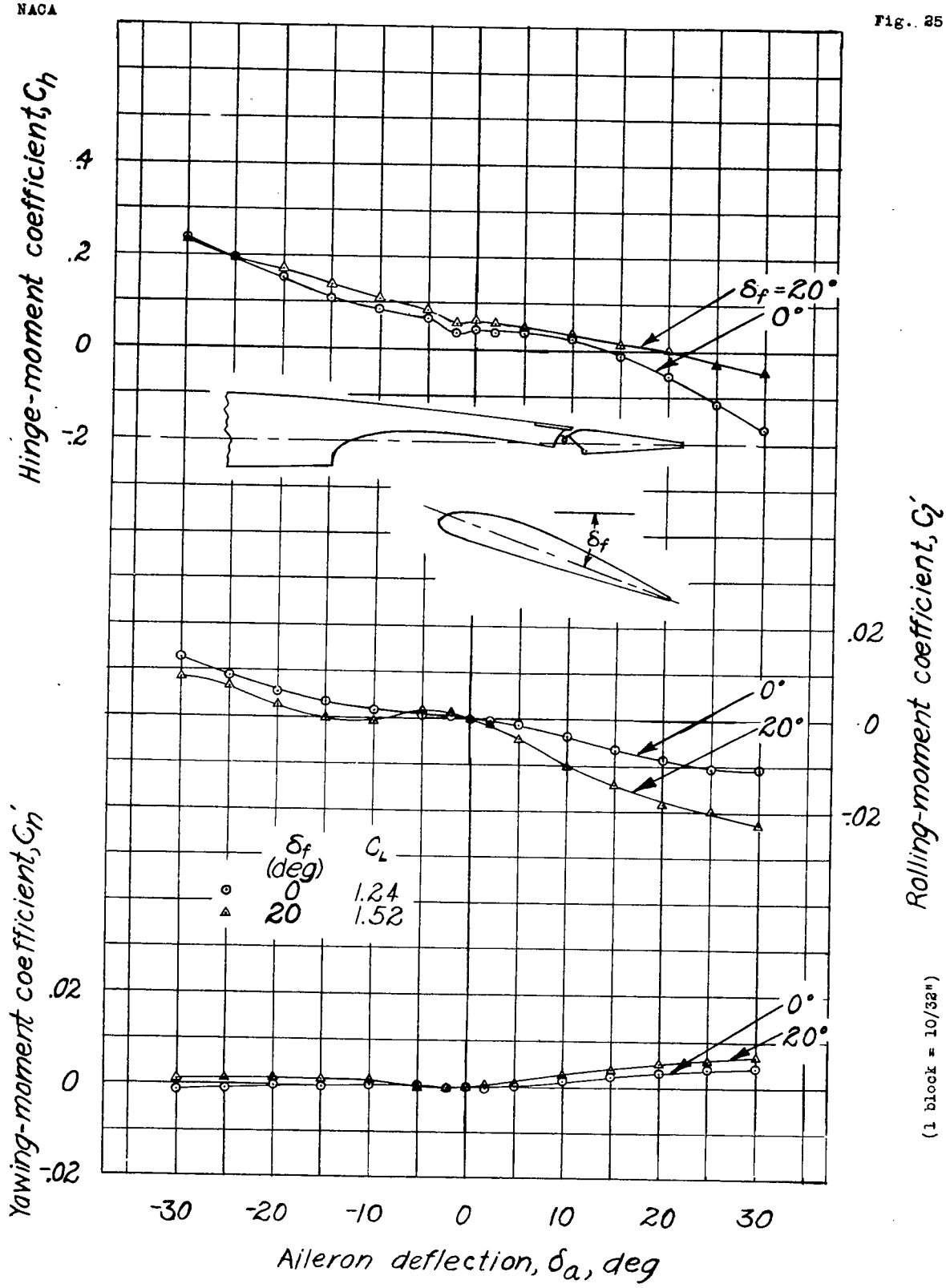

Figure 25.- Rolling-, yawing-, and hinge-moment coefficients of the tapered wing model with a full-span flap and a full-span sealed aileron. Flap position, D-5; balance, 0.30c_a; α, 13.6° (approx.).

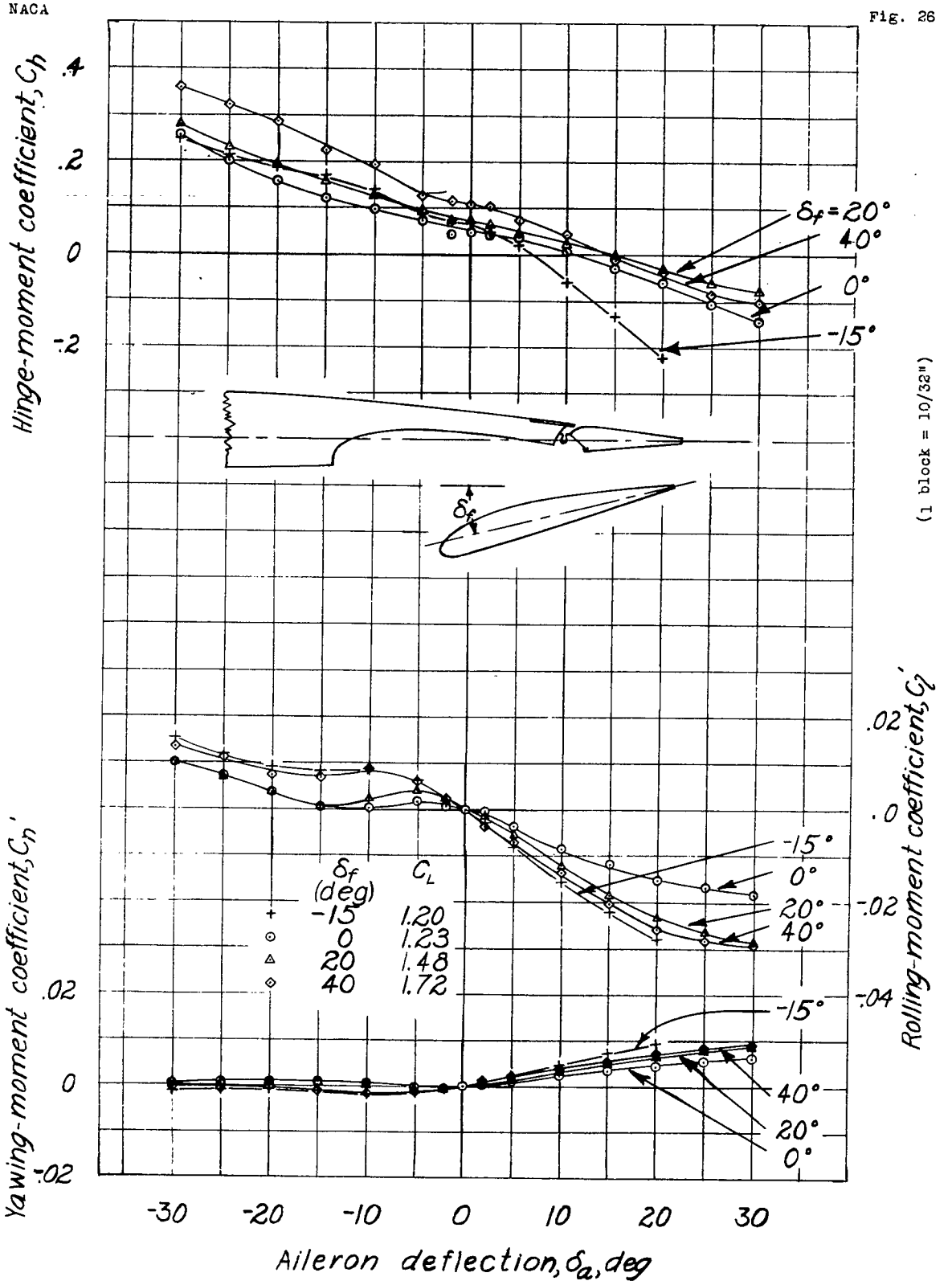

Figure 26.- Rolling-, yawing-, and hinge-moment coefficients of the tapered wing model with a full-span flap and a full-span sealed aileron. Flap position, D-8; balance, $0.30\bar{c}_a$; α, 13.6° (approx.).

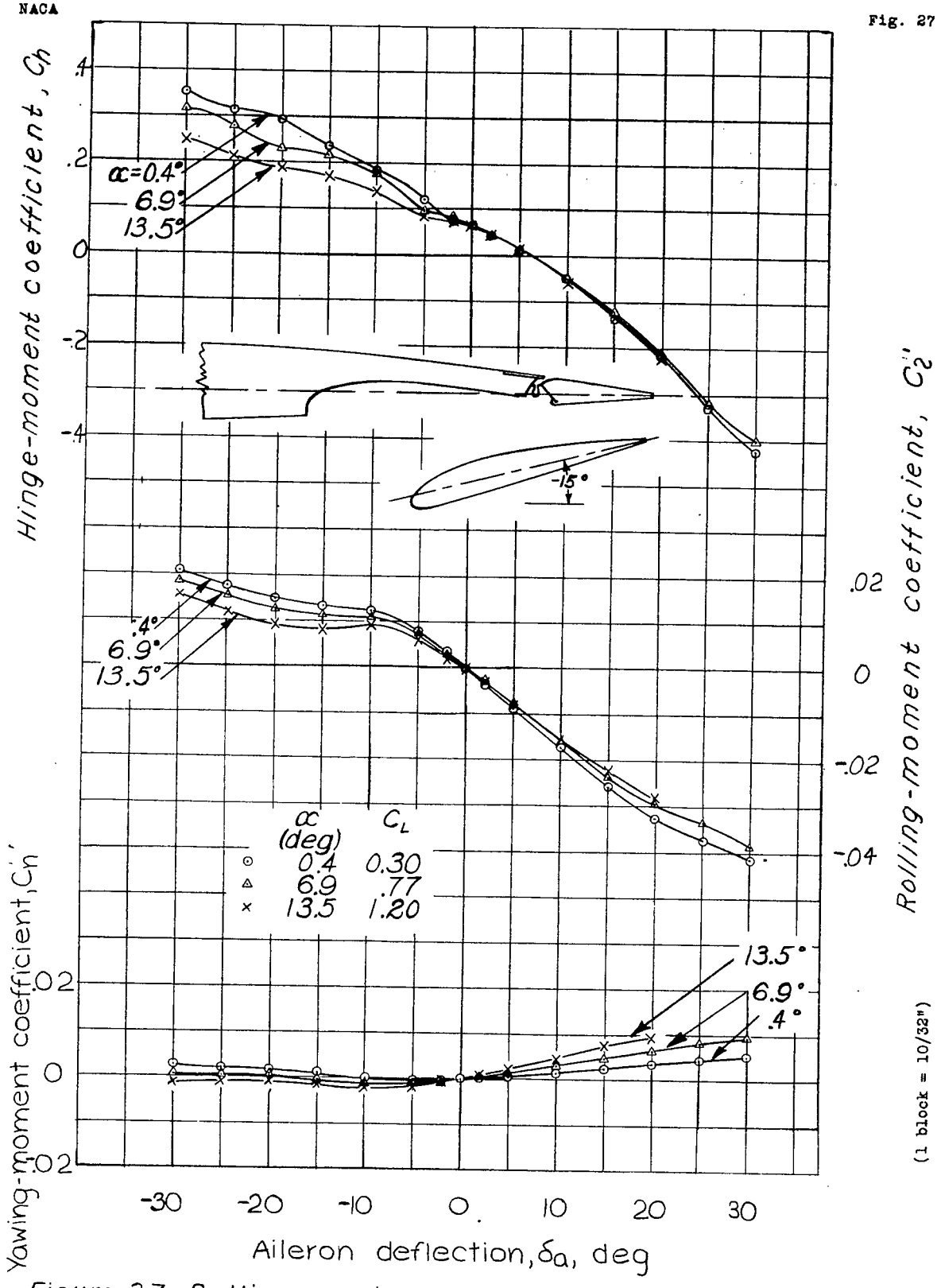

Figure 27.- Rolling-, yawing-, and hinge-moment coefficients of the tapered wing model with a full-span flap and a full-span sealed aileron. Flap position, D-8; balance, 0.30$\bar{c}_a$; δ_f,-15°.

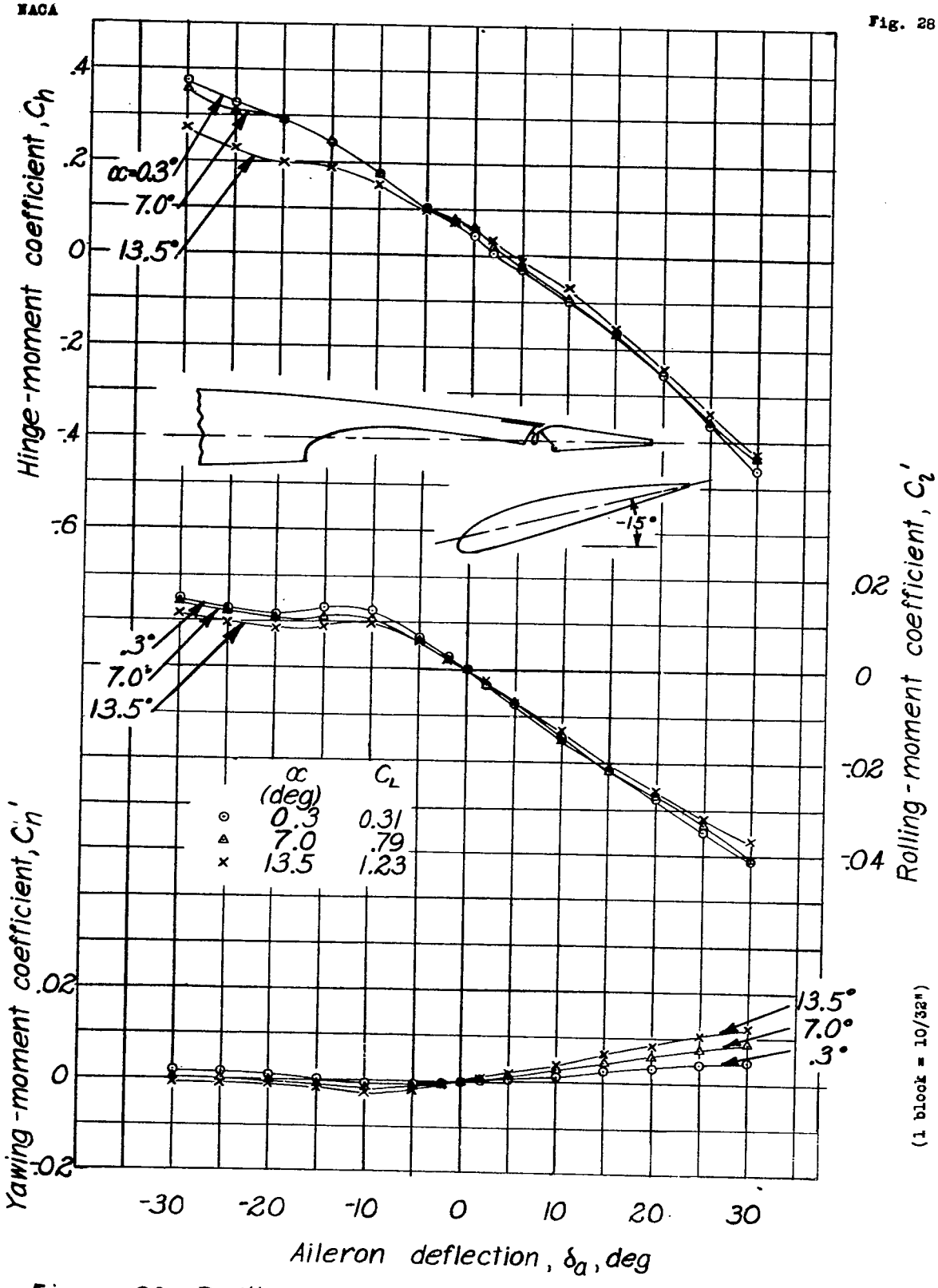

Figure 28.- Rolling-, yawing-, and hinge-moment coefficients of the tapered wing model with a full-span flap and a full-span sealed aileron. Flap position, E-8; balance, 0.30$\bar{c}_a$; δ_f, -15°.

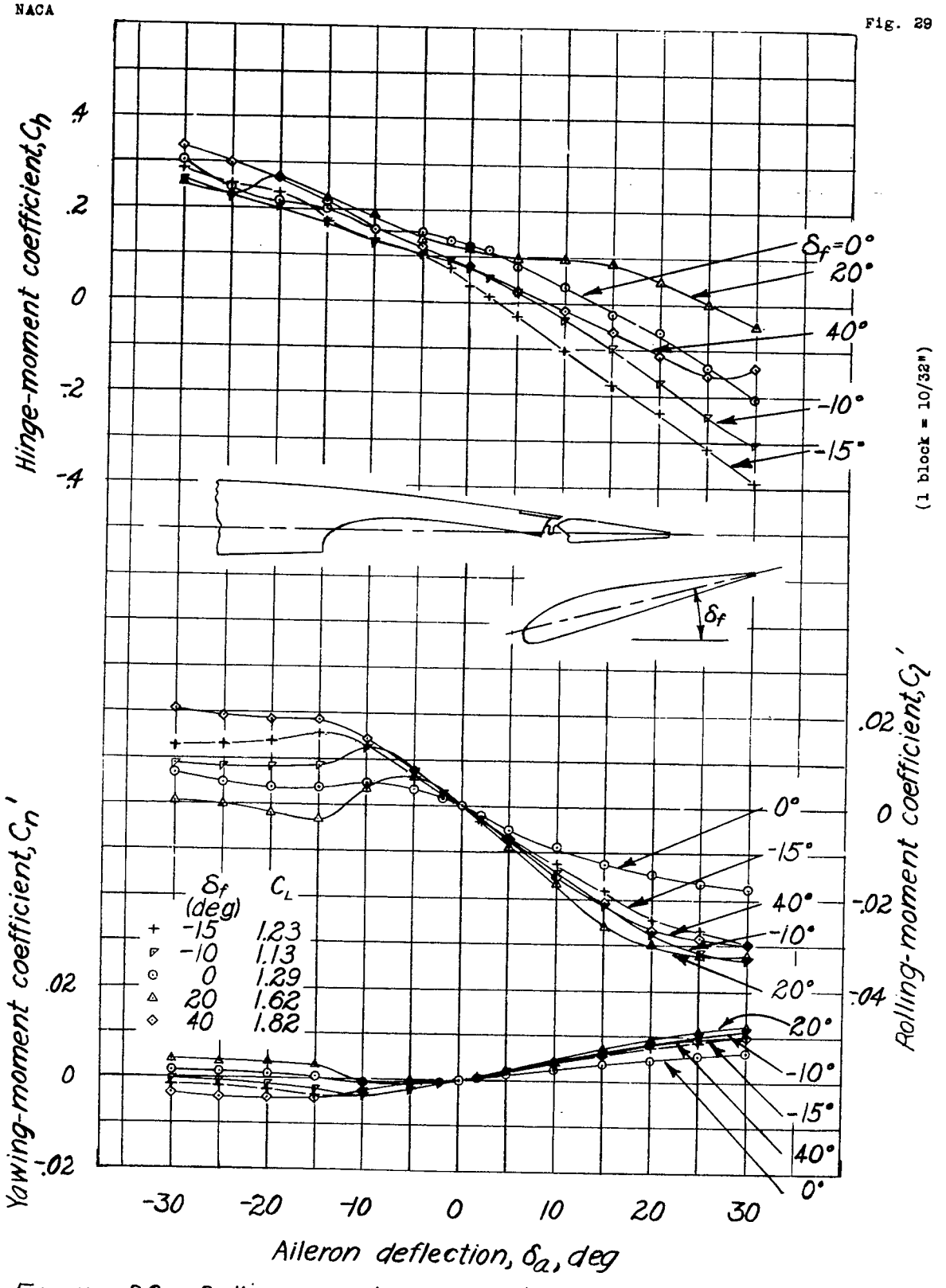

(1 block = 10/32")

Figure 29.- Rolling-, yawing-, and hinge-moment coefficients of the tapered wing model with a full-span flap and a full-span sealed aileron. Flap position, F-8; balance 0.30$\bar{c}_a$; α, 13.6° (approx.).

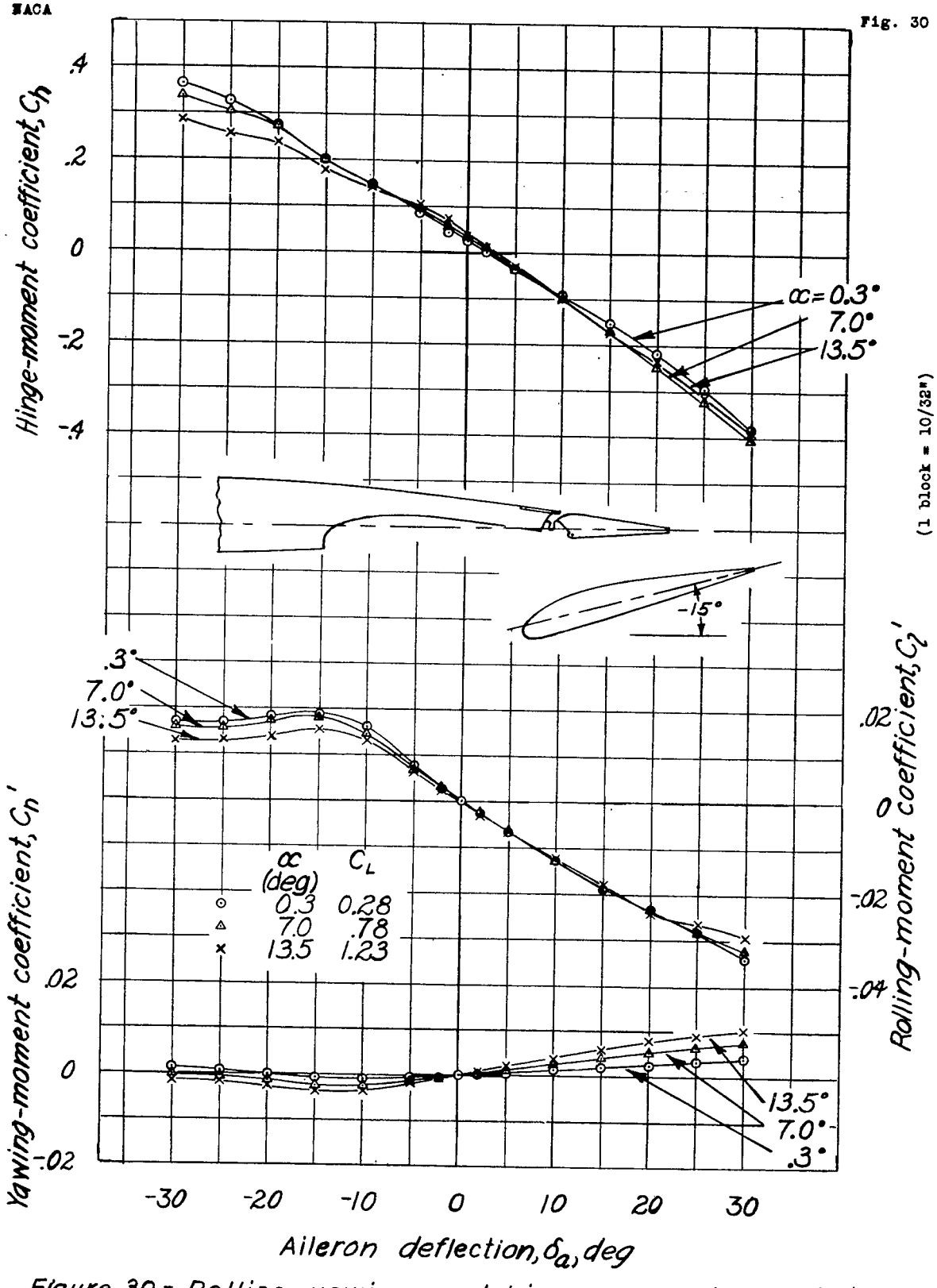

Figure 30.- Rolling-, yawing-, and hinge-moment coefficients of the tapered wing model with a full-span flap and a full-span sealed aileron. Flap position, F-8; balance, 0.30$\bar{c}_a$; δ_f, -15°.

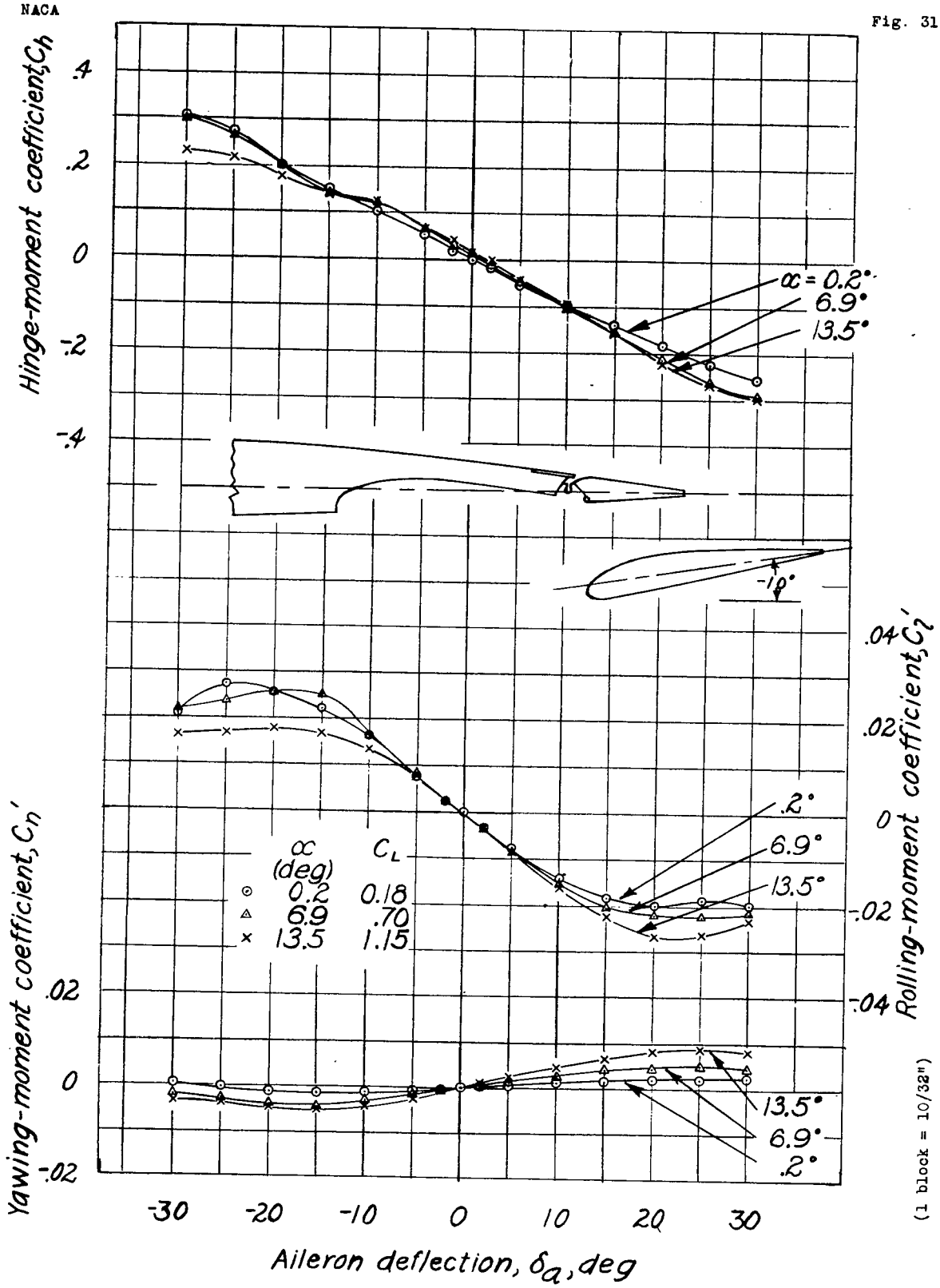

Figure 31.- Rolling-, yawing-, and hinge-moment coefficients of the tapered wing model with a full-span flap and a full-span sealed aileron. Flap position, G-8; balance, 0.30 c_a; δ_f, -10°.

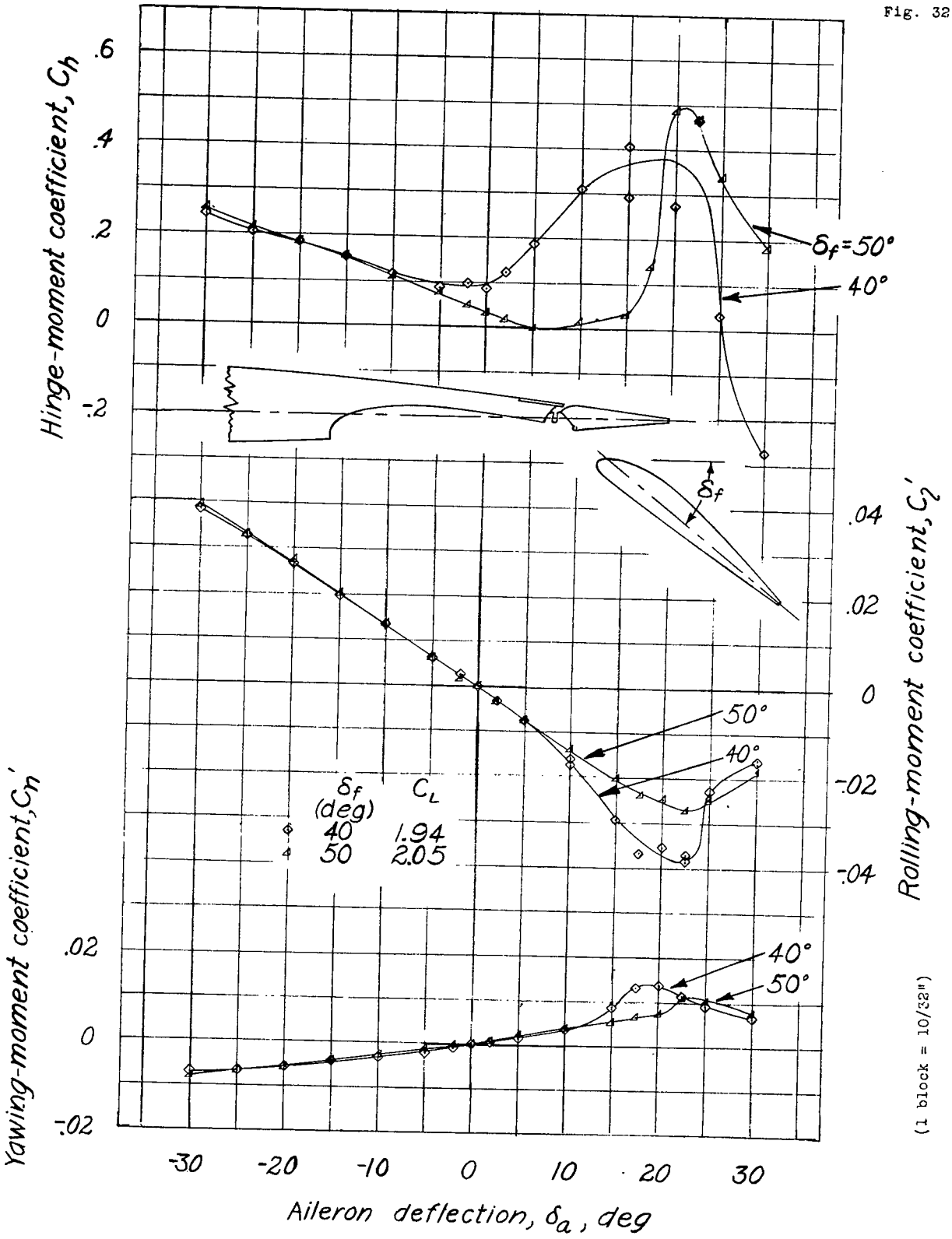

Figure 32.- Rolling-, yawing-, and hinge-moment coefficients of the tapered wing model with a full-span flap and a full-span sealed aileron. Flap position, H-3; balance, 0.30 $\bar{c}_a$; α, 13.8°

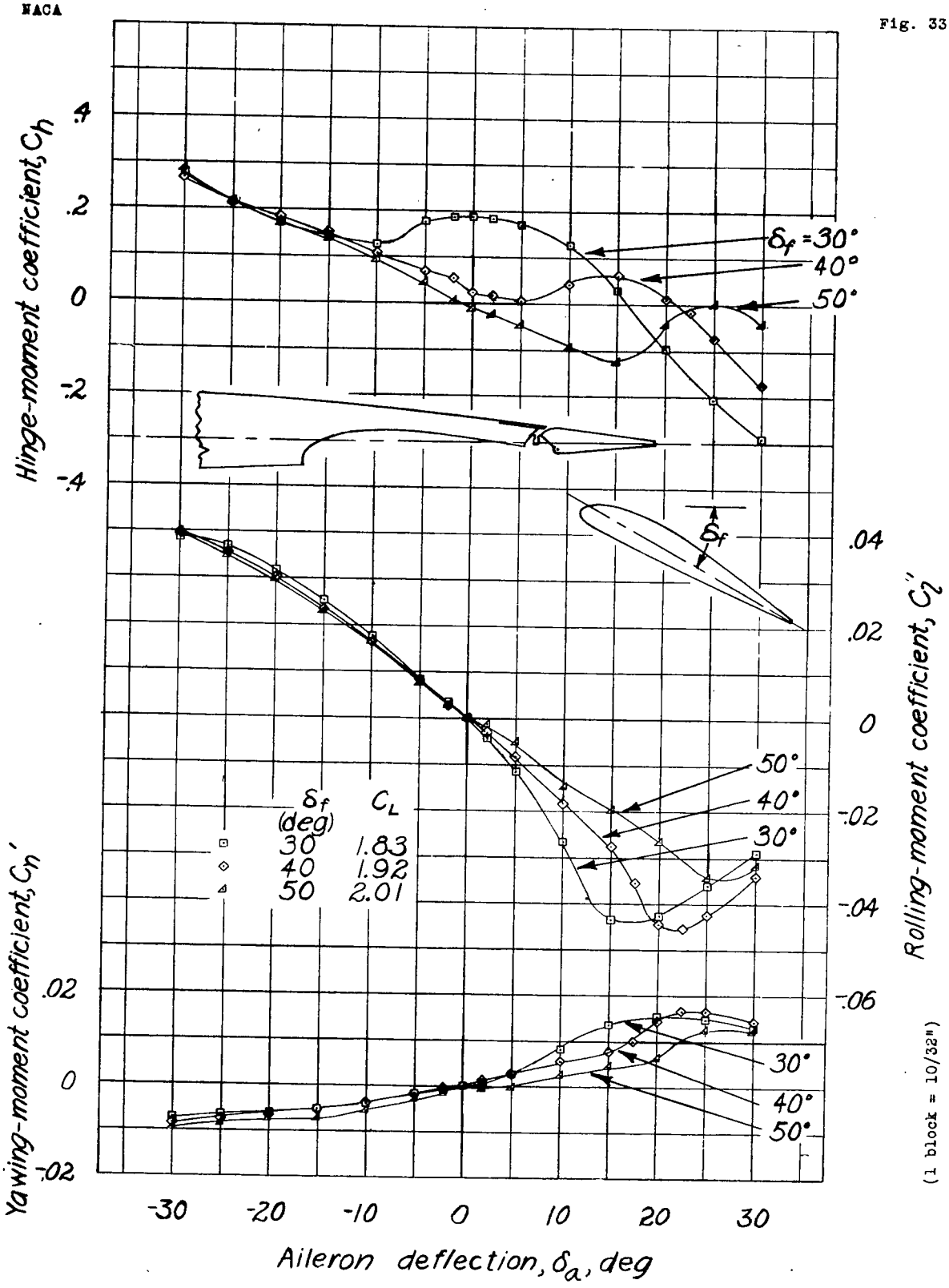

Figure 33 - Rolling-, yawing-, and hinge-moment coefficients of the tapered wing model with a full-span flap and a full-span sealed aileron. Flap position, H-5; balance, 0.30 $\bar{c}_a$; α, 13.8°.

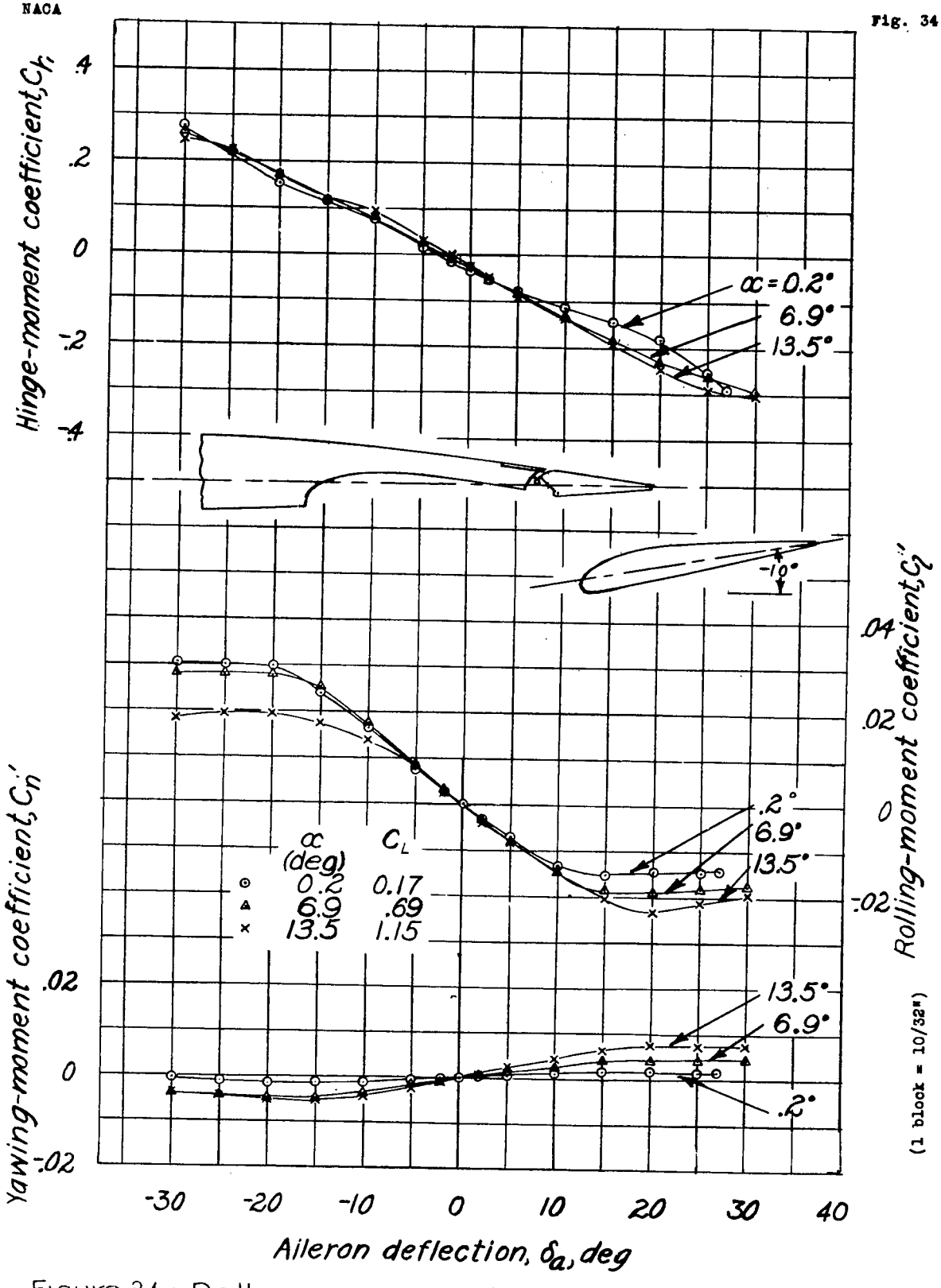

Figure 34.- Rolling-, yawing-, and hinge-moment coefficients of the tapered wing model with a full-span flap and a full-span sealed aileron. Flap position, H-8; balance, 0.30 c_a; δ_f, -10°.

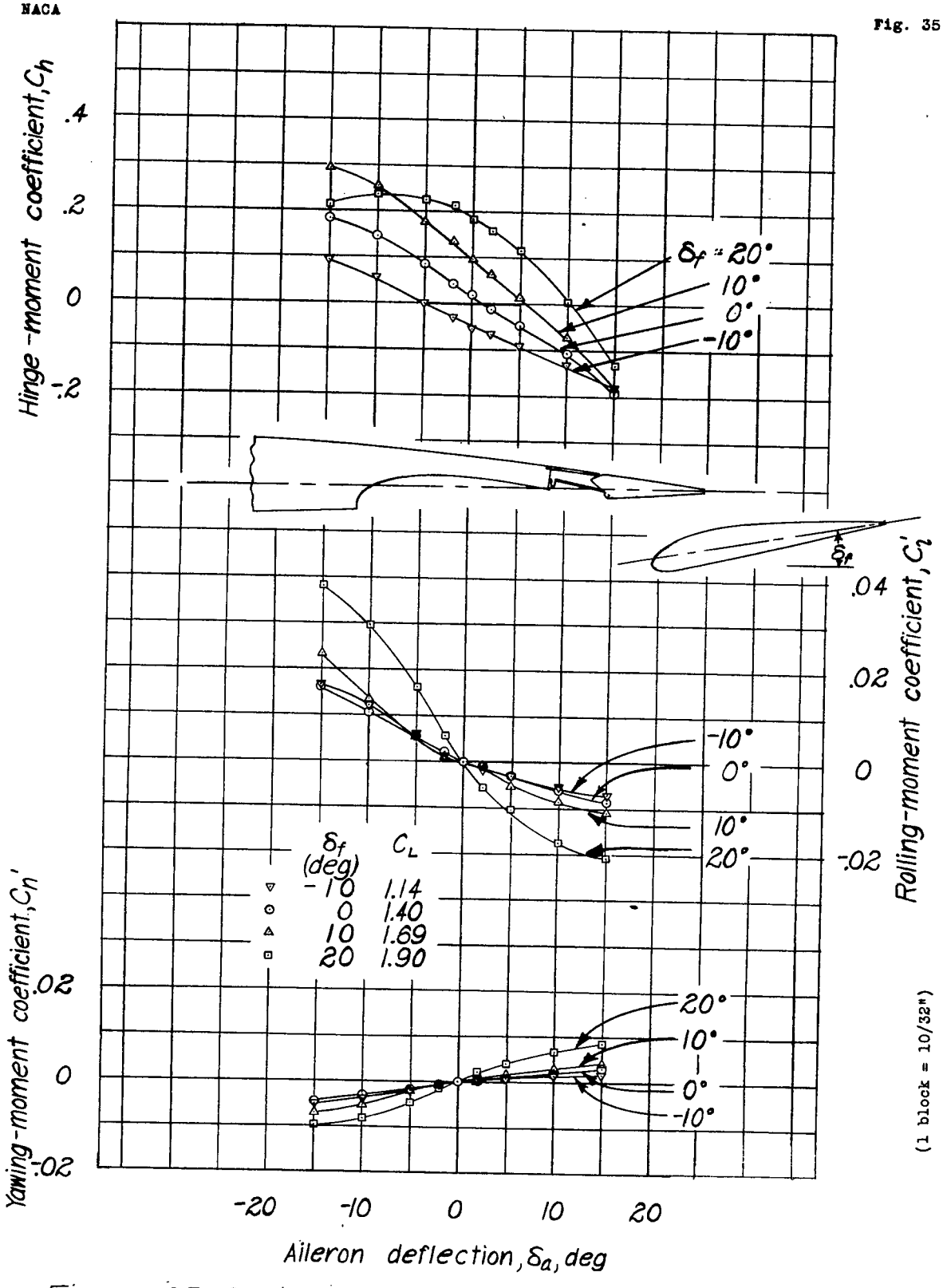

Figure 35.- Rolling-, yawing-, and hinge-moment coefficients of the tapered wing model with a full-span flap and a full-span sealed aileron. Flap position, I-6; balance, 0.56 c_a; α, 13.6° (approx).

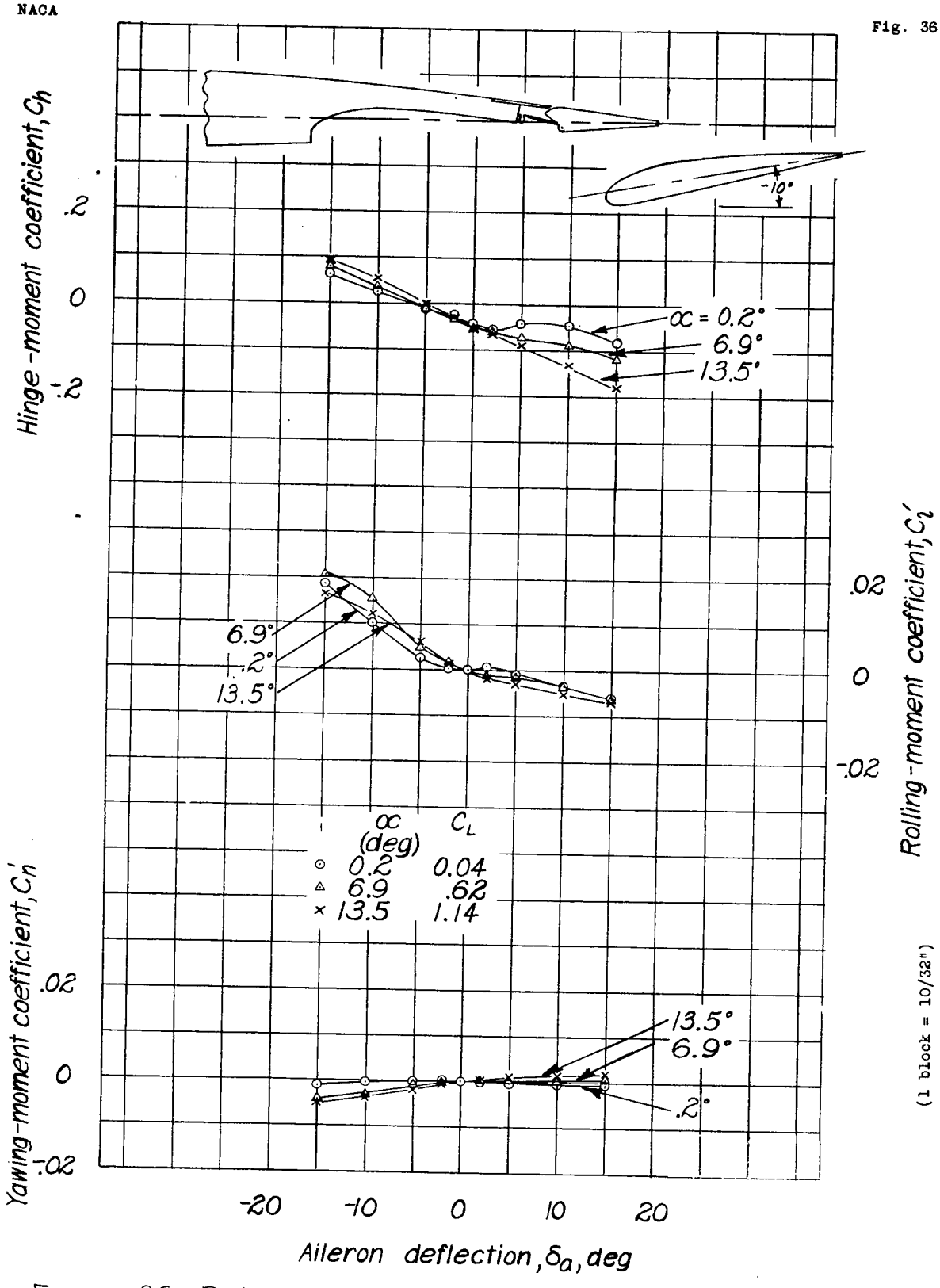

Figure 36.- Rolling-, yawing-, and hinge-moment coefficients of the tapered wing model with a full-span flap and a full-span sealed aileron. Flap position, I-6; balance, 0.56 $\bar{c}_a$; δ_f, -10°

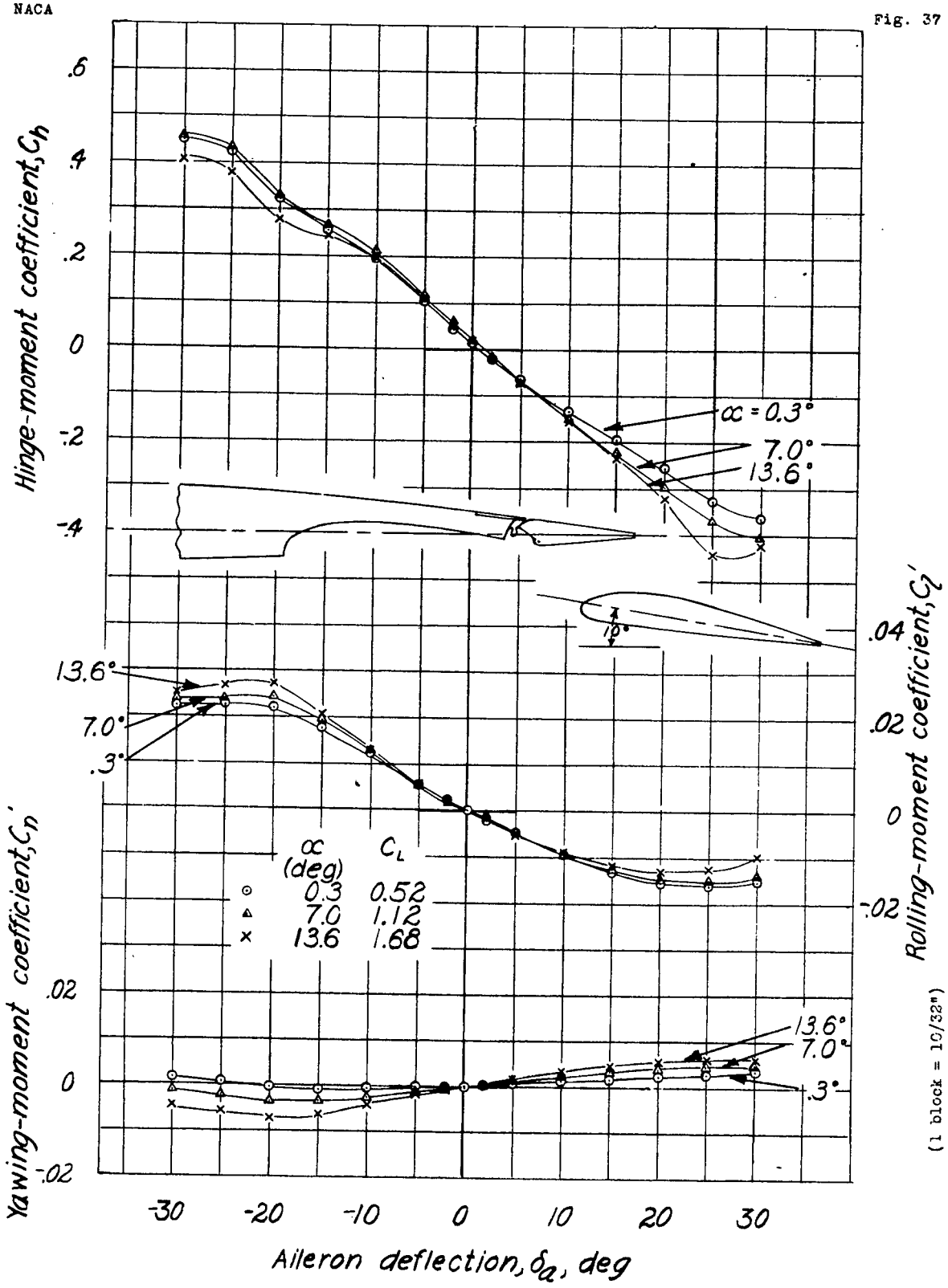

Figure 37.- Rolling-, yawing-, and hinge-moment coefficients of the tapered wing model with a full-span flap and a full-span sealed aileron. Flap position, I-6; balance, 0.30 $\bar{c}_a$; δ_f, 10°.

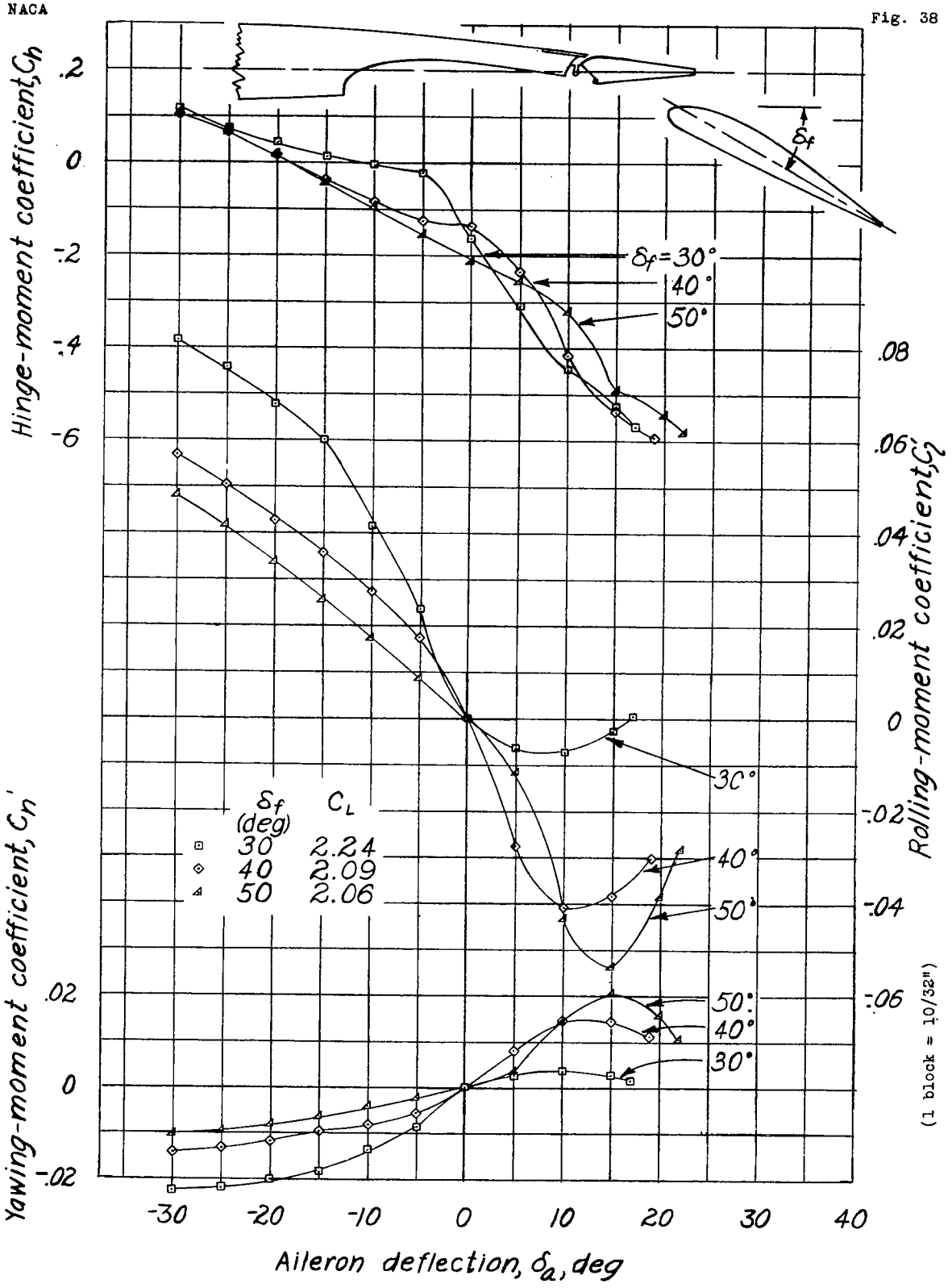

Figure 38.- Rolling-, yawing-, and hinge-moment coefficients of the tapered wing model with a full-span flap and a full-span sealed aileron. Flap position, J-3; balance 0.30 $\bar{c}_a$; α, 13.8°.

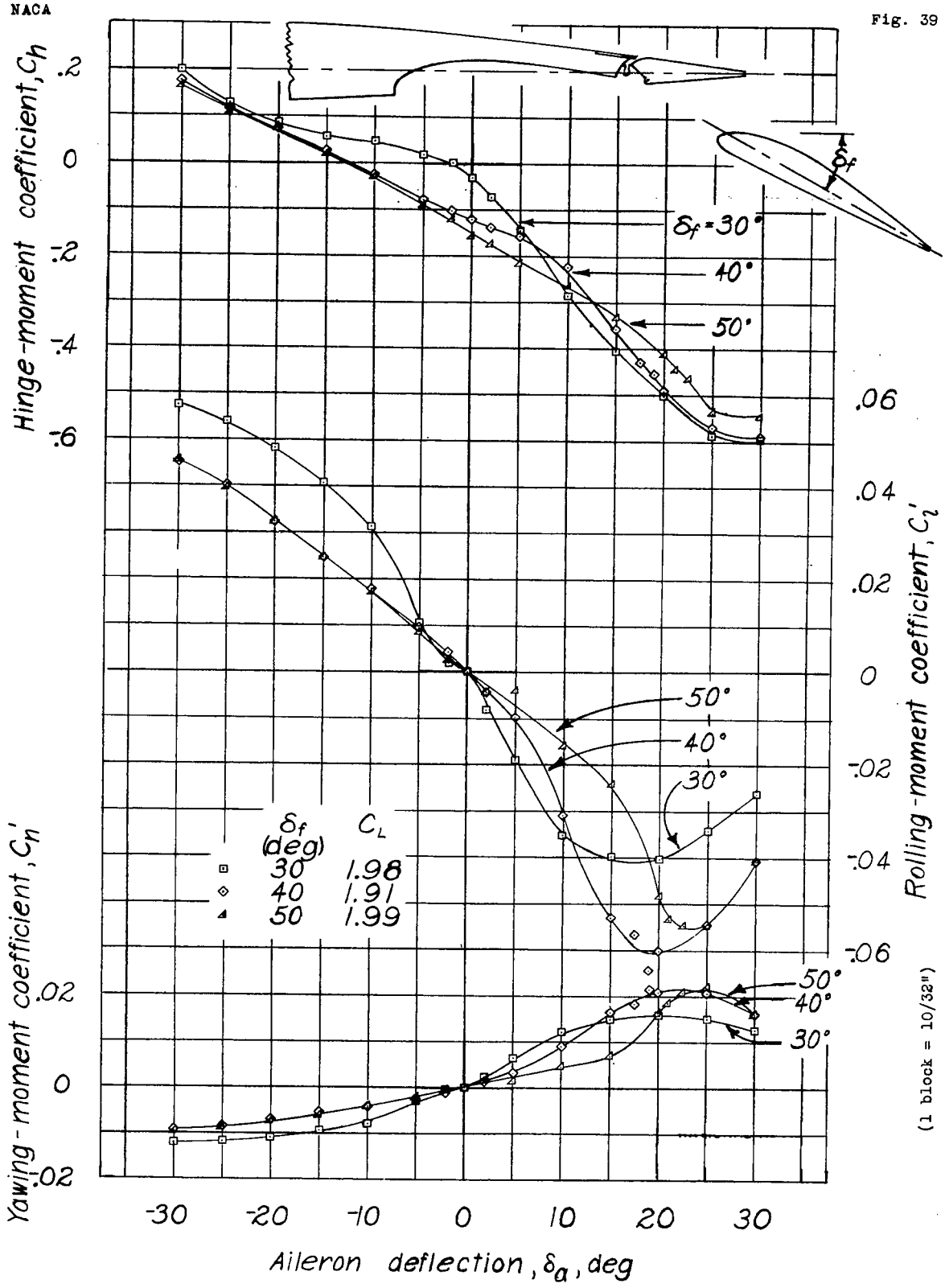

Figure 39.- Rolling-, yawing-, and hinge-moment coefficients of the tapered wing model with a full-span flap and a full-span sealed aileron. Flap position, J-5; balance, 0.30 $\bar{c}_a$; α, 13.8°.

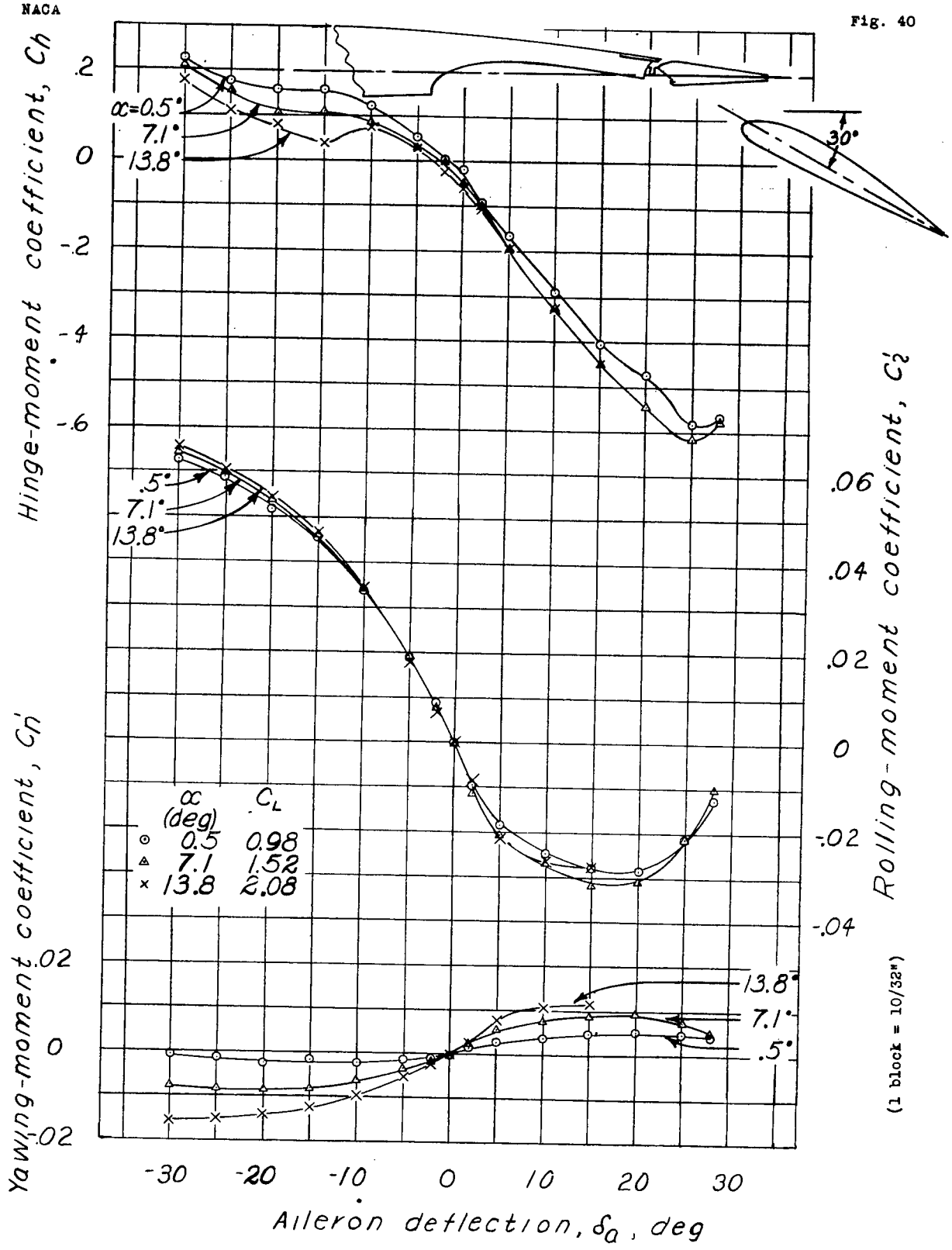

Figure 40.- Rolling-, yawing-, and hinge-moment coefficients of the tapered wing model with a full-span flap and a full-span sealed aileron. Flap position, J-4; balance, 0.30 $\bar{c}_a$; δ_f, 30°.

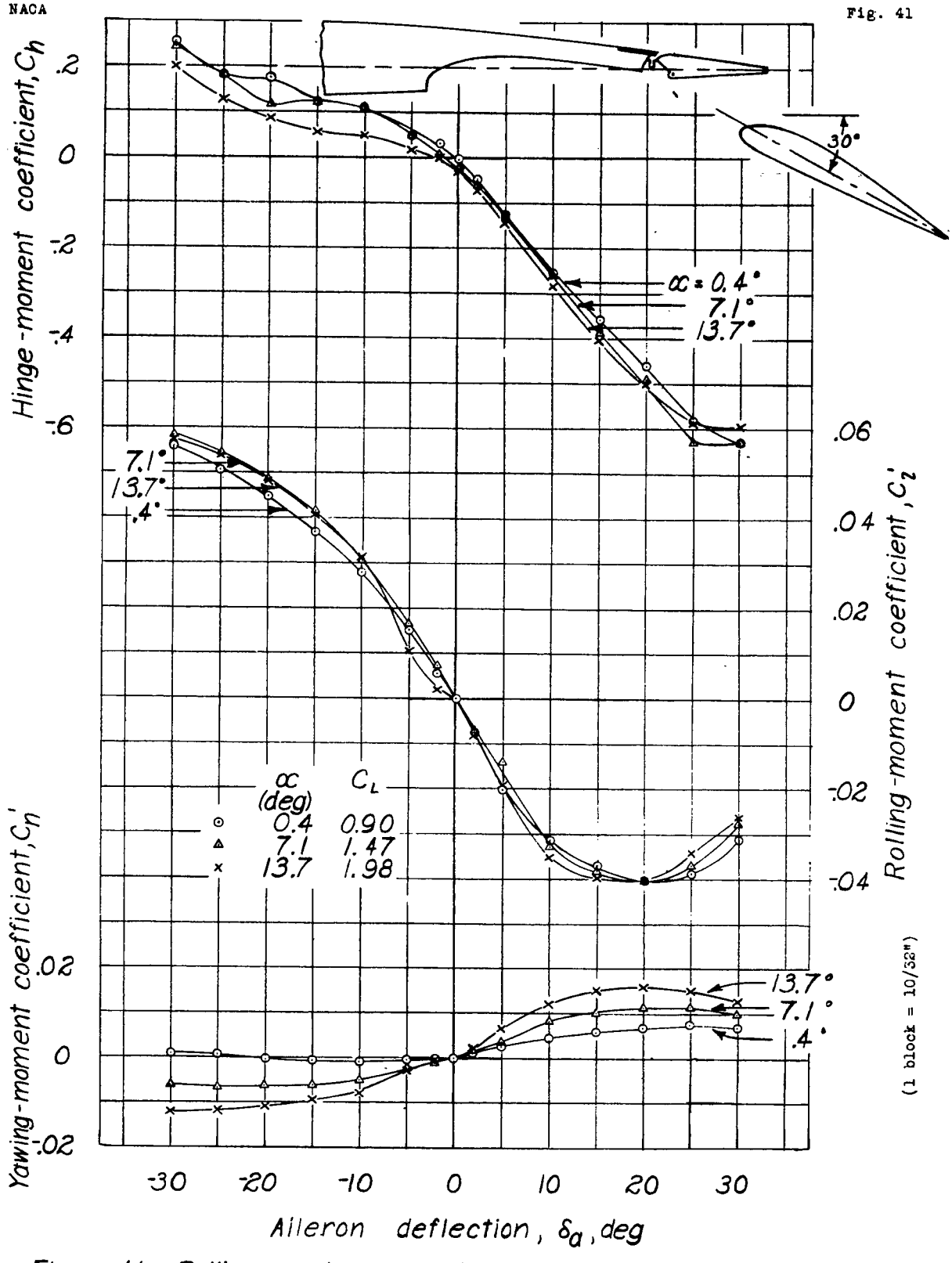

Figure 41.- Rolling-, yawing-, and hinge-moment coefficients of the tapered wing model with a full-span flap and a full-span sealed aileron. Flap position, J-5; balance, 0.30 c_a; δ_f, 30°.

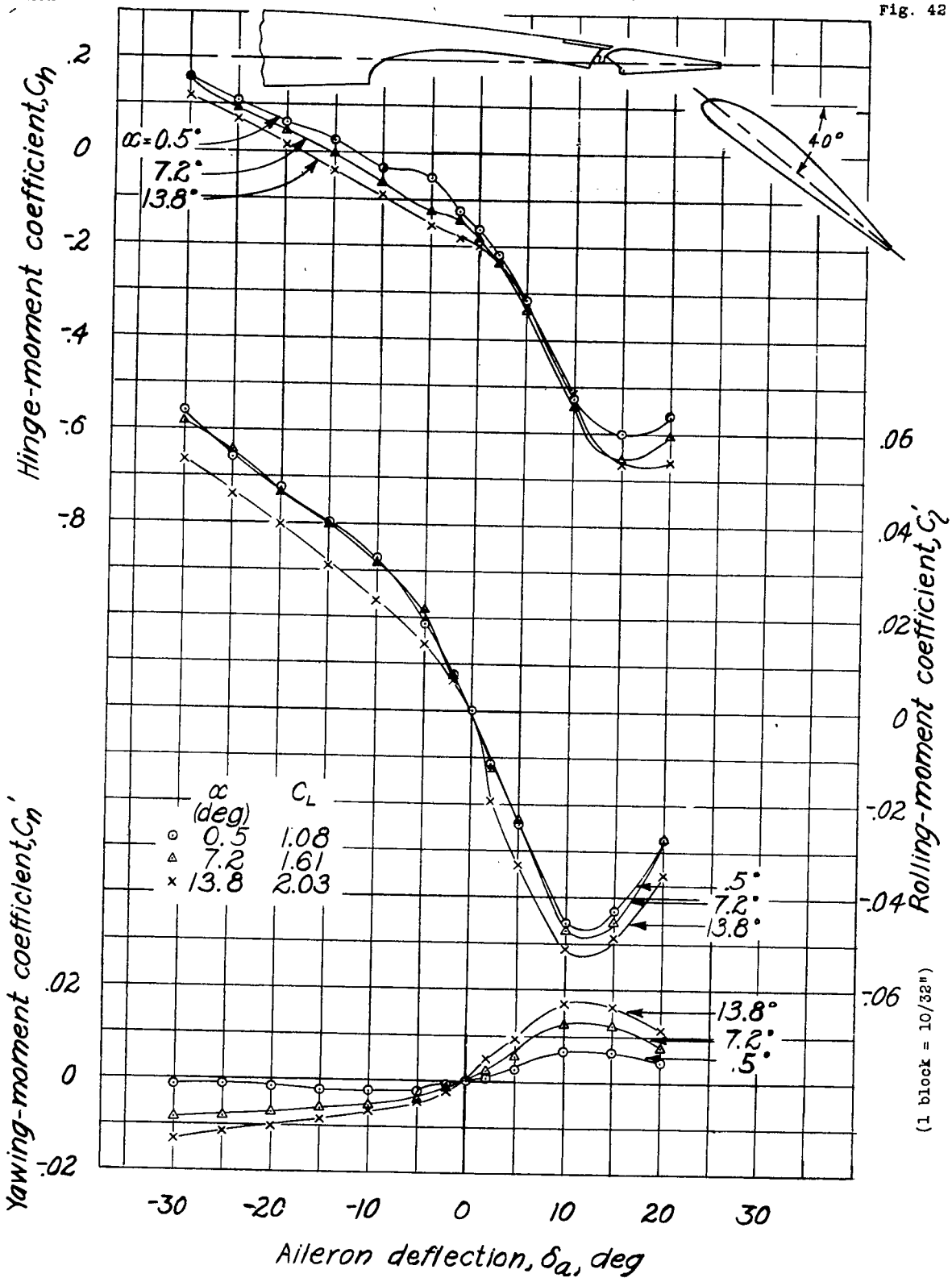

Figure 42.- Rolling-, yawing-, and hinge-moment coefficients of the tapered wing model with a full-span flap and a full-span sealed aileron. Flap position, K-3; balance, 0.30 $\bar{c}_a$; δ_f, 40°.

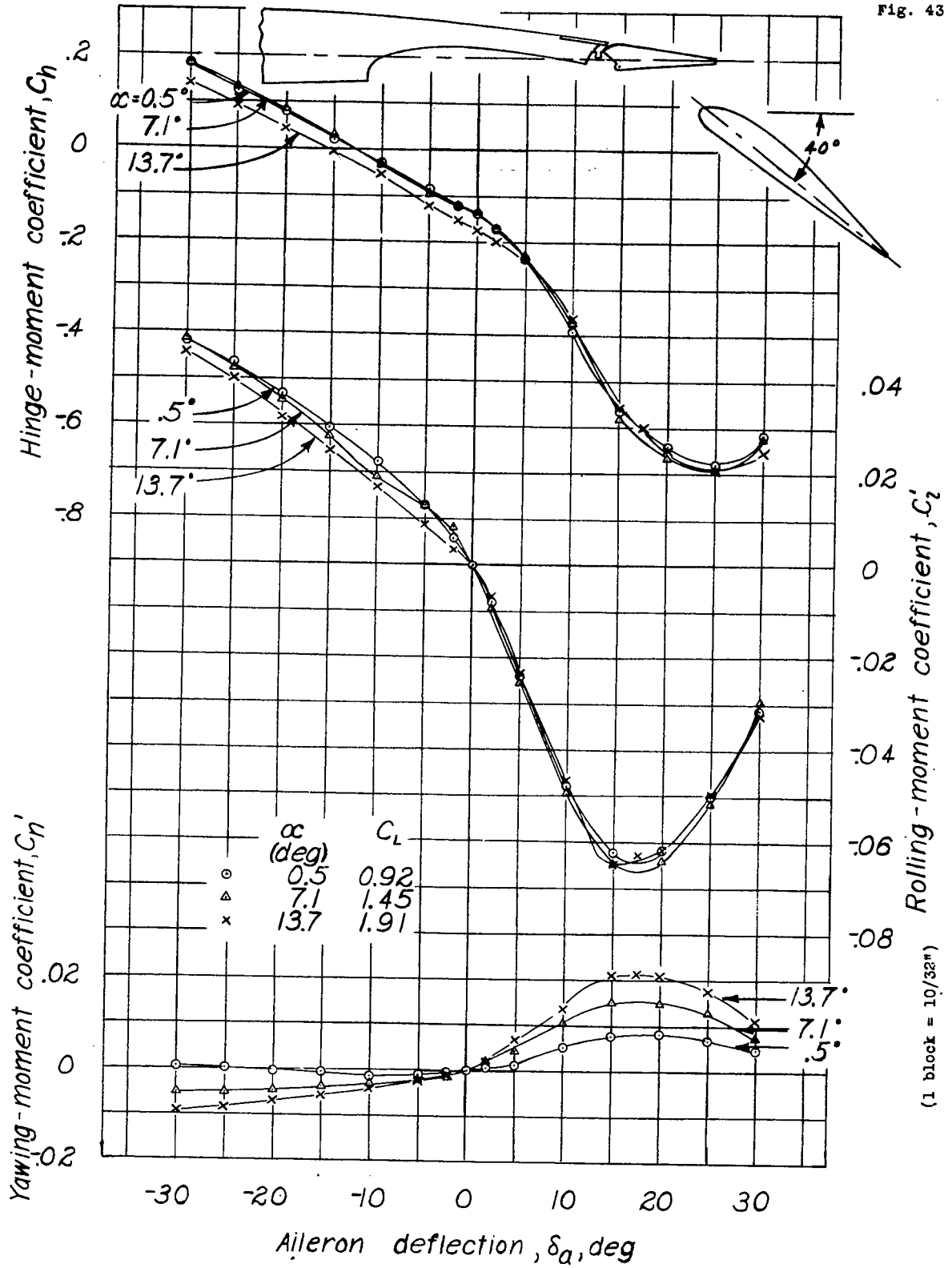

Figure 43.—Rolling-, yawing-, and hinge-moment coefficients of the tapered wing model with a full-span flap and a full-span sealed aileron. Flap position, K-4; balance, 0.30 c_a; δ_f, 40°.

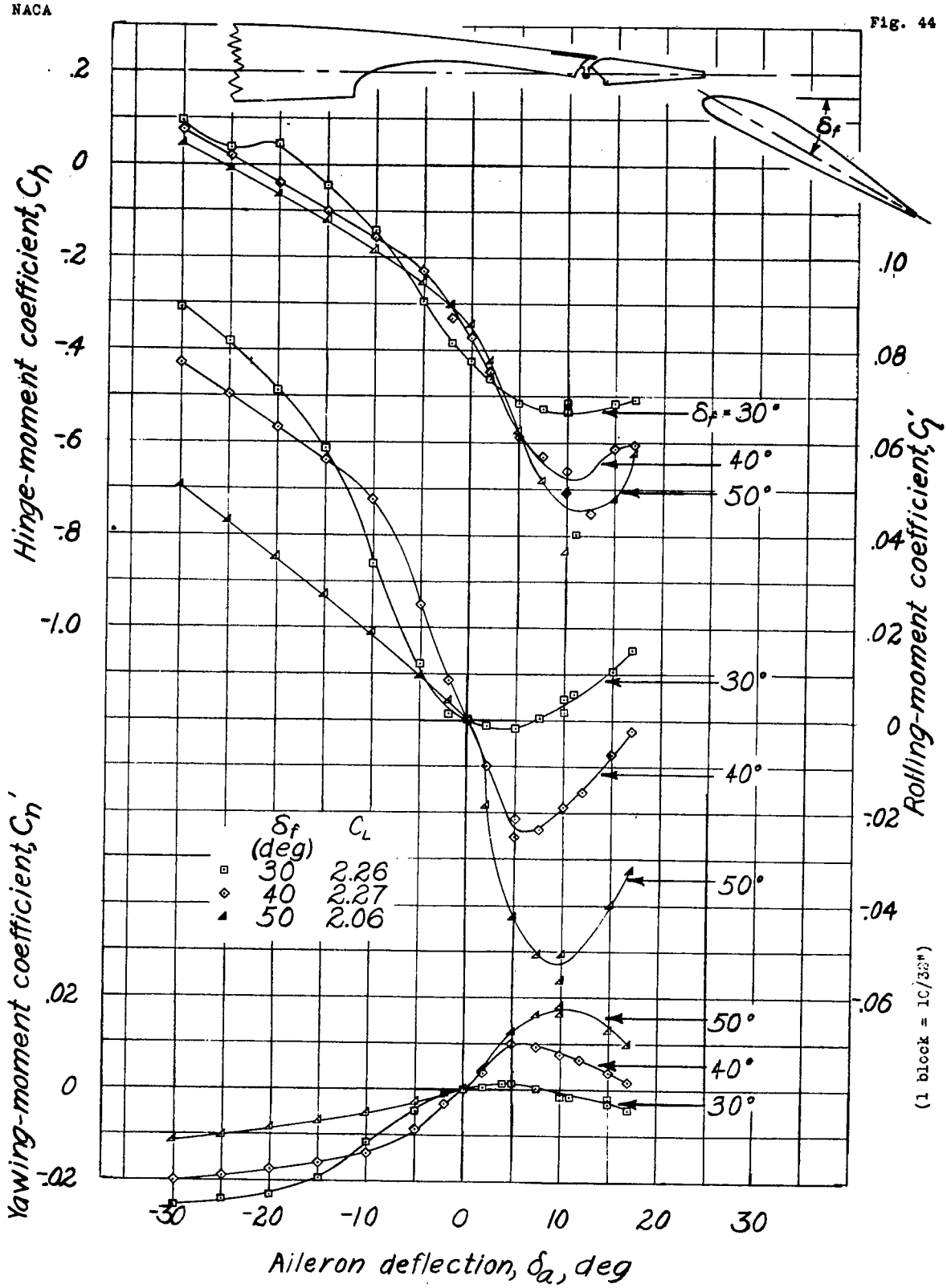

Figure 44.- Rolling-, yawing-, and hinge-moment coefficients of the tapered wing model with a full-span flap and a full-span sealed aileron. Flap position, L-2 ; balance, 0.30 $\bar{c}_a$; α, 13.8° (approx.).

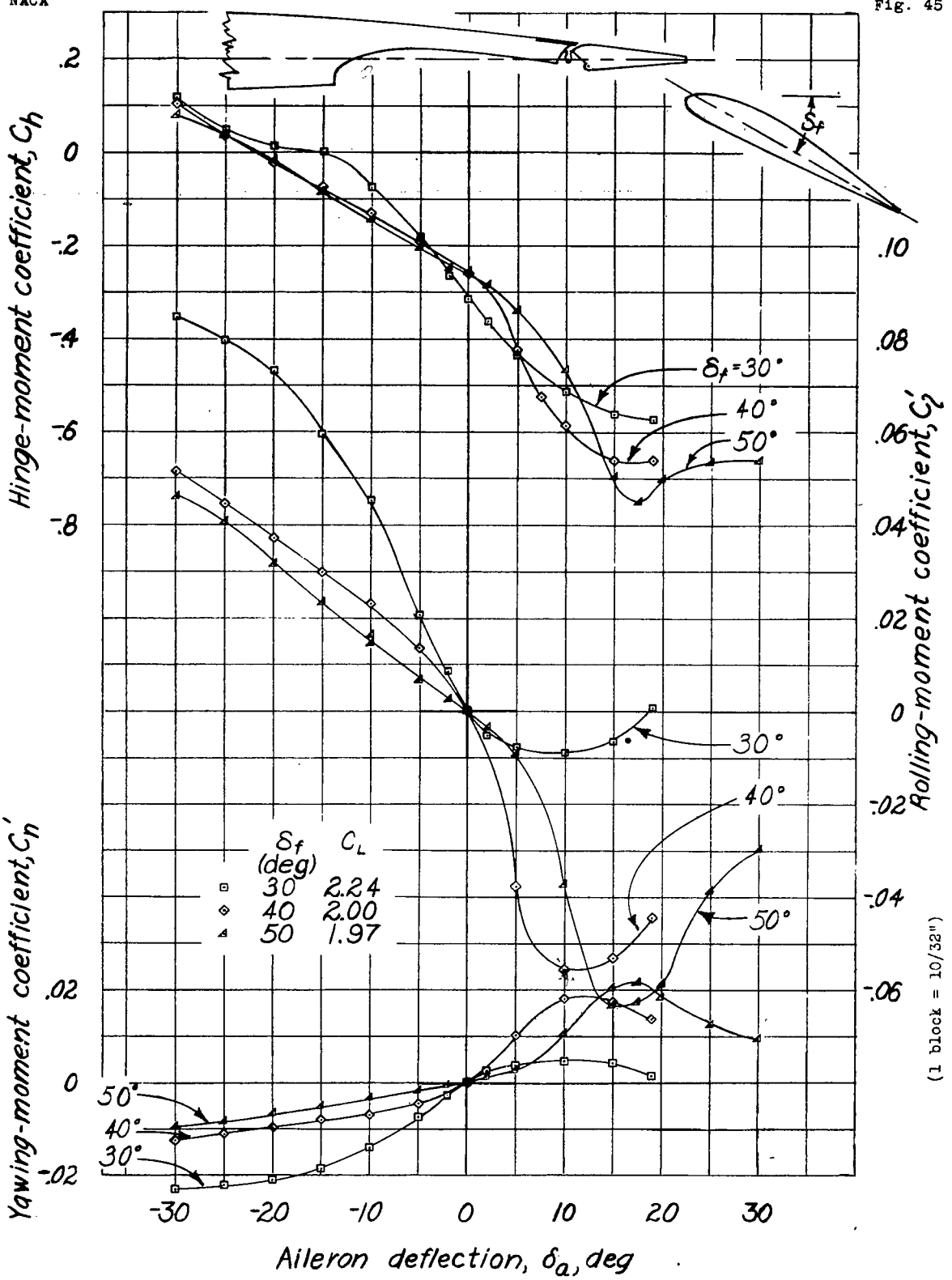

Figure 45.-Rolling-, yawing-, and hinge-moment coefficients of the tapered wing model with a full-span flap and a full-span sealed aileron. Flap position, L-3; balance, 0.30 $\bar{c}_a$; α, 13.8° (approx.).

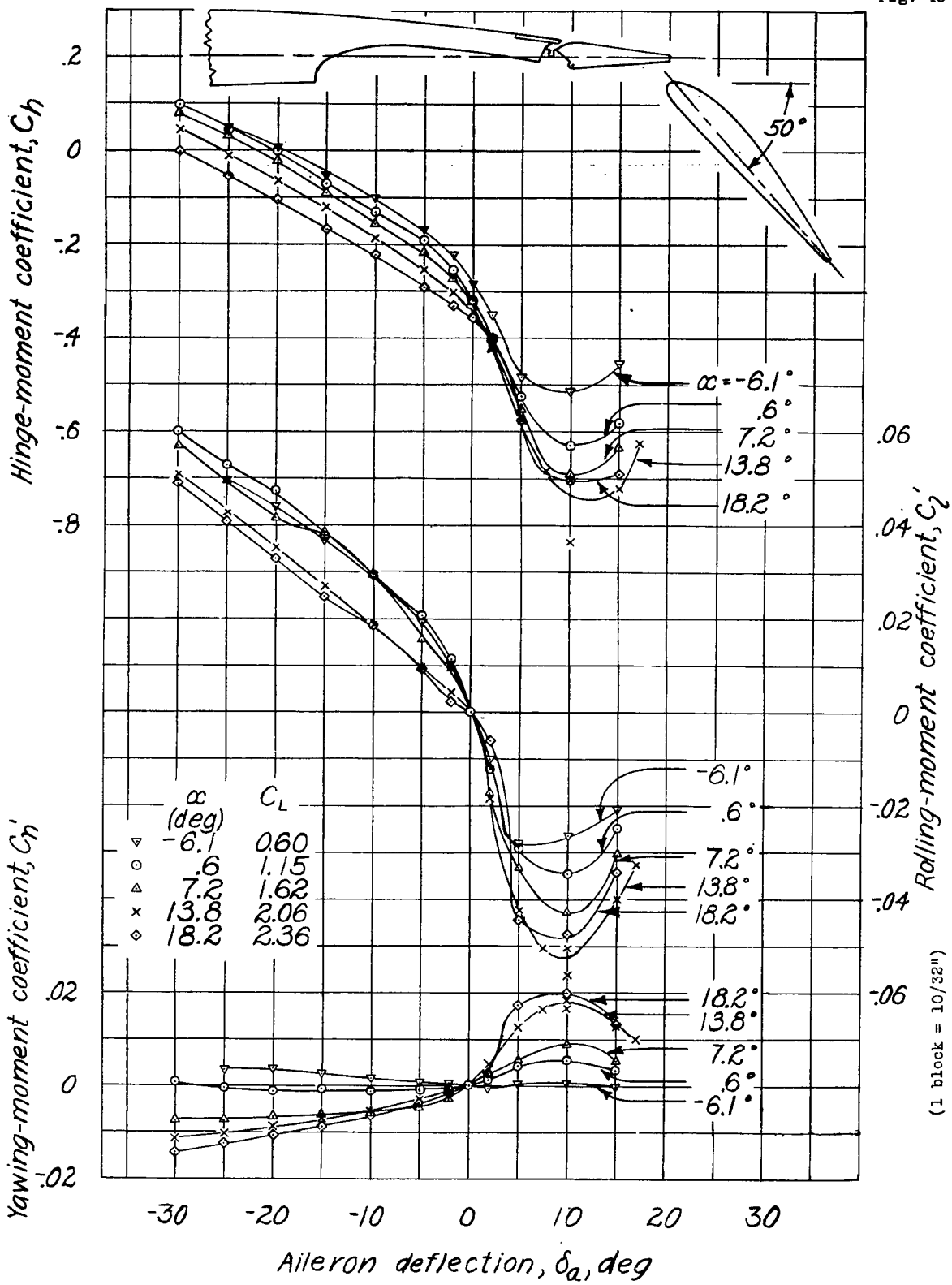

Figure 46.- Rolling-, yawing-, and hinge-moment coefficients of the tapered wing model with a full-span flap and a full-span sealed aileron. Flap position, L-2; balance, 0.30 $\bar{c}_a$; δ_f, 50°.

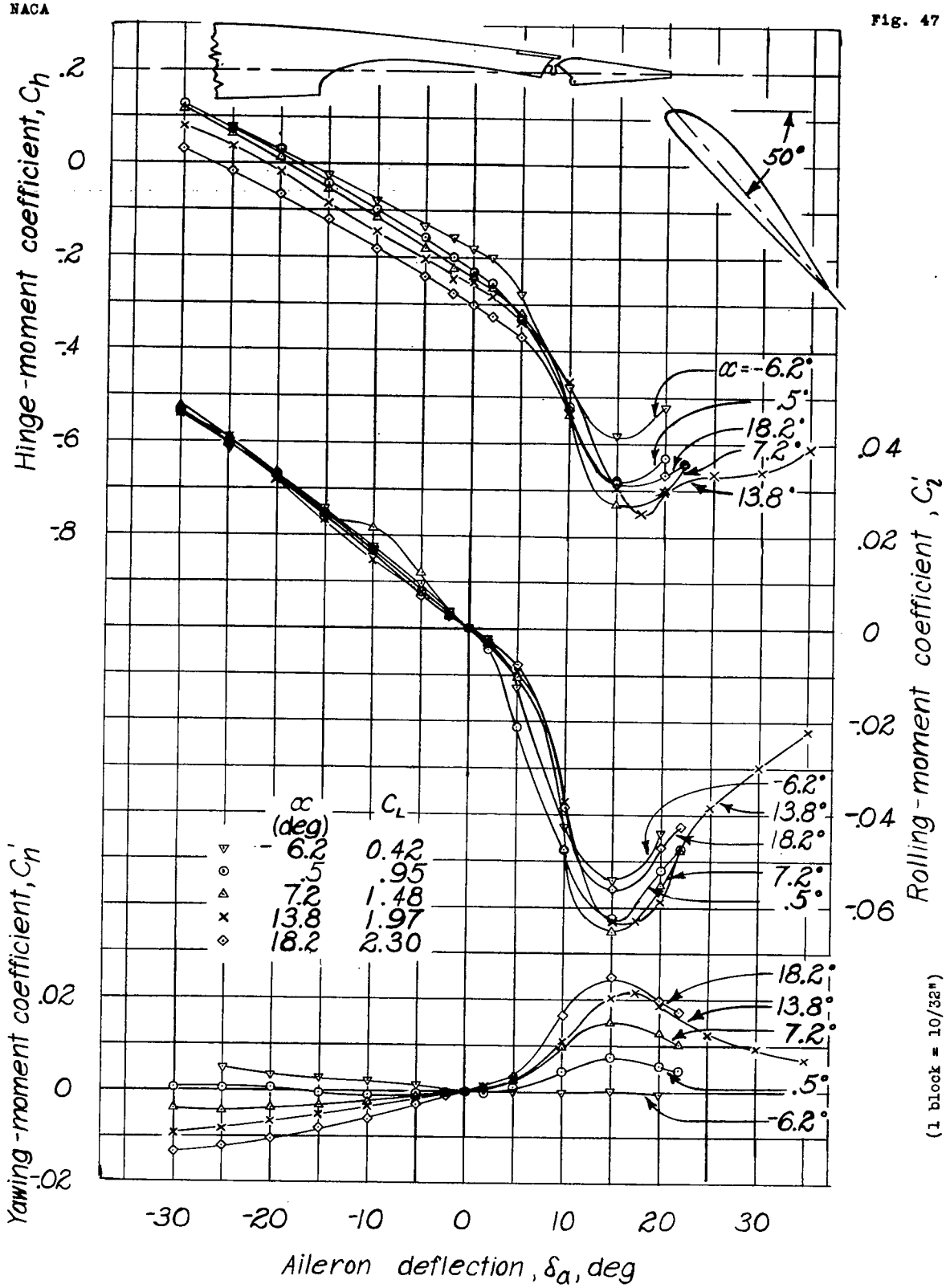

Figure 47. - Rolling-, yawing-, and hinge-moment coefficients of the tapered wing model with a full-span flap and a full-span sealed aileron. Flap position, L-3; balance, 0.30 $\bar{c}_a$; δ_f, 50°.

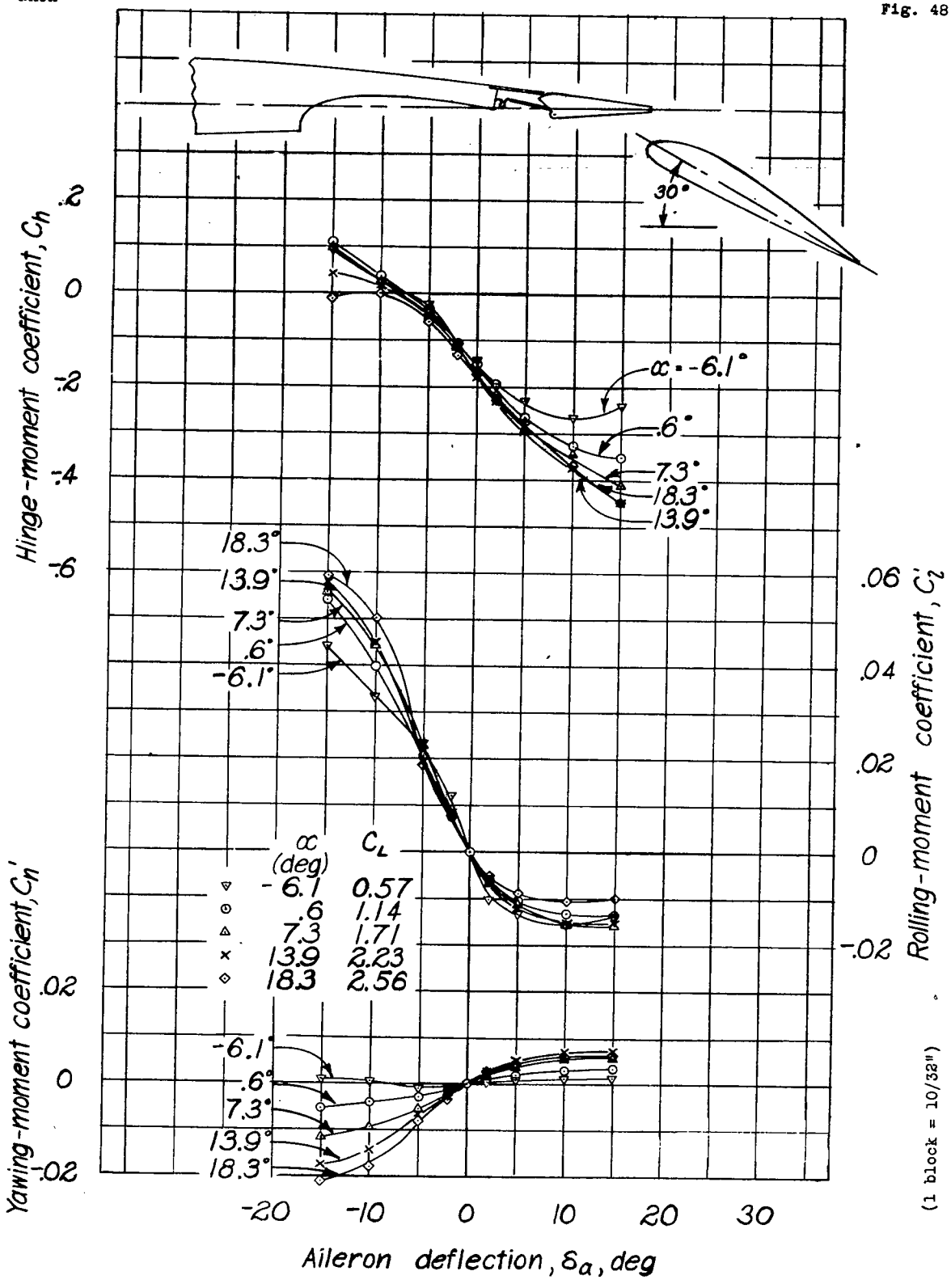

Figure 48.- Rolling-, yawing-, and hinge-moment coefficients of the tapered wing model with a full-span flap and a full-span sealed aileron. Flap position, L-3; balance, 0.56 $\bar{c}_a$; δ_f, 30°

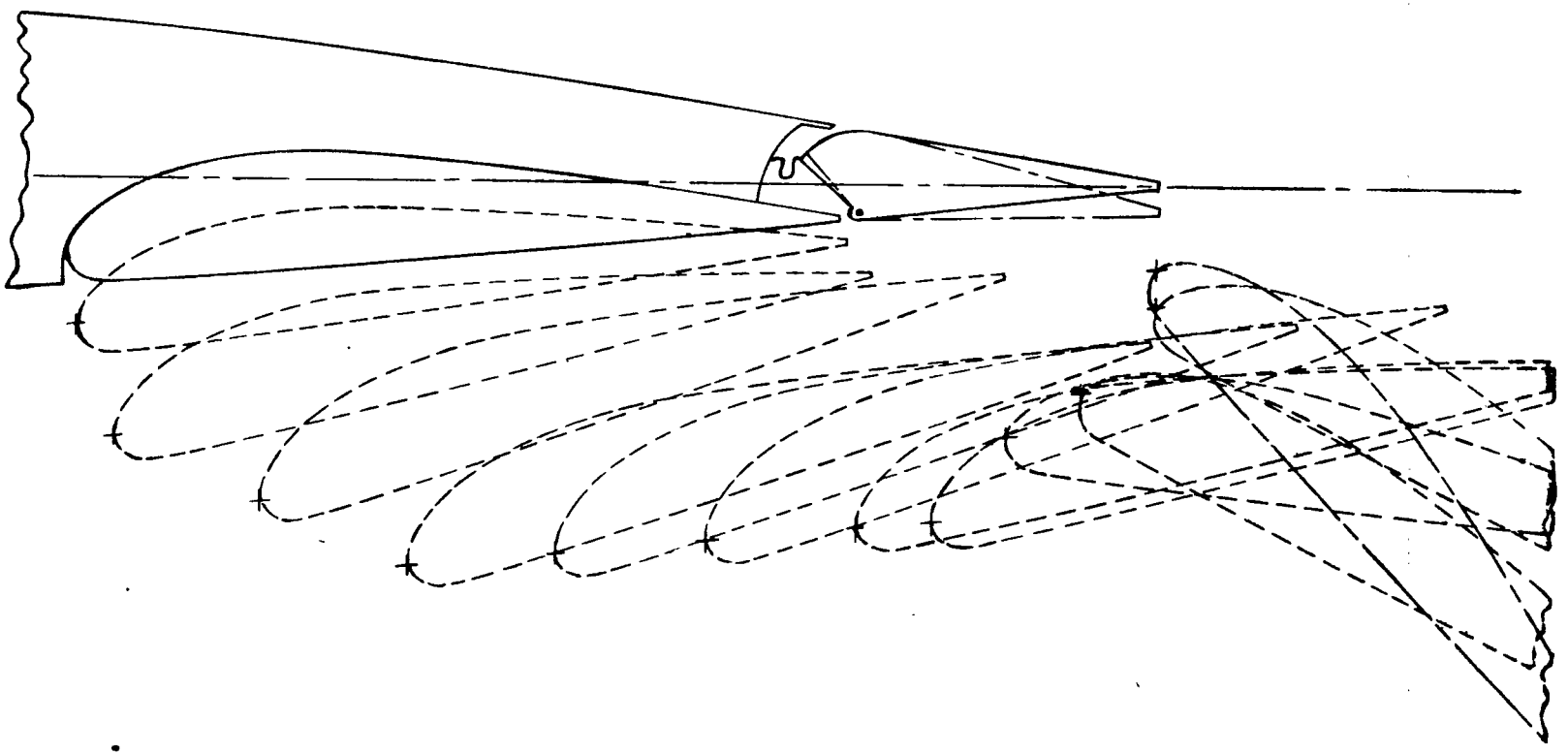

Figure 49. - Schematic diagram of flap position along the selected flap path.

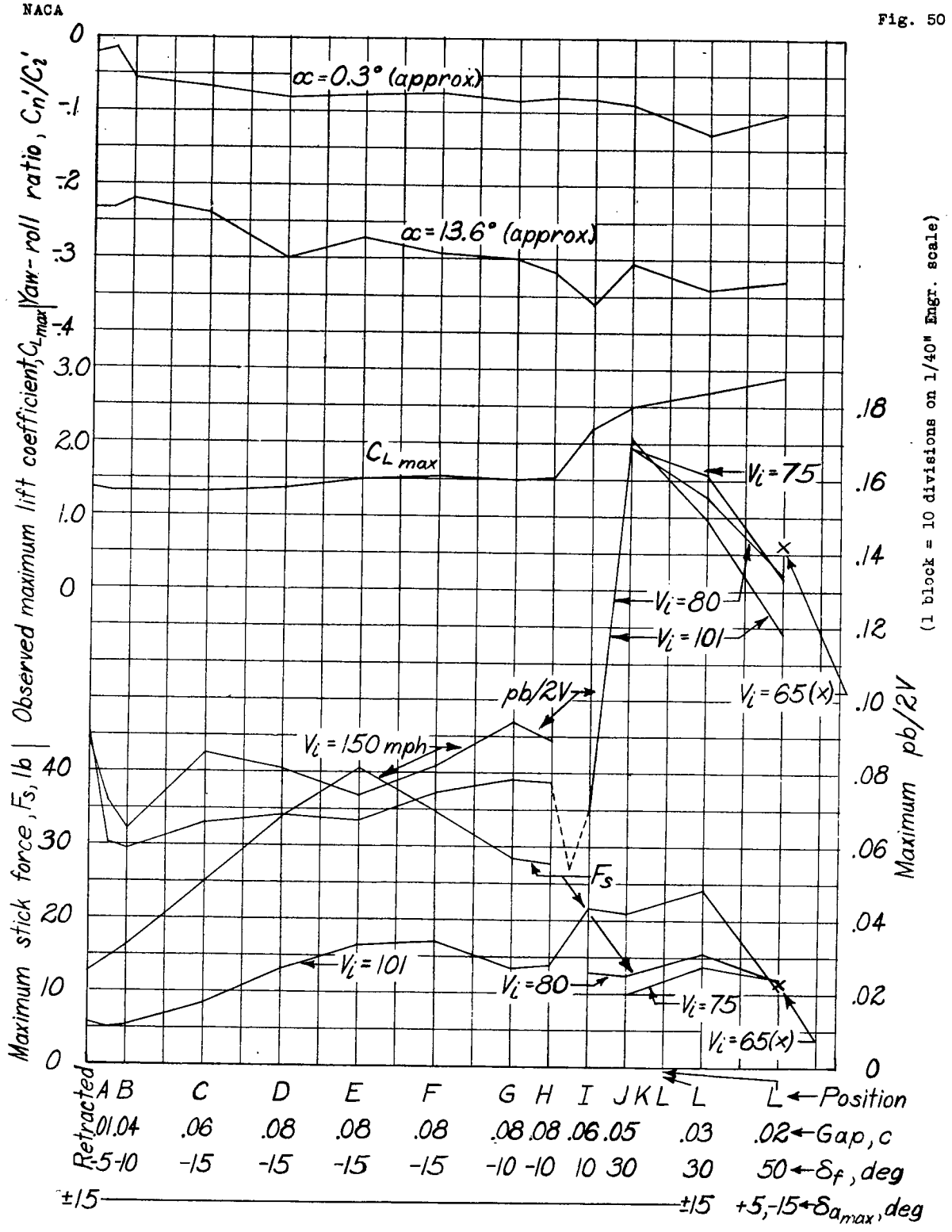

Figure 50.- Estimated aileron-control characteristics of the airplane with tapered wings, full-span flaps, and full-span ailerons. Balance, 0.30 $\bar{c}_a$; gap sealed.

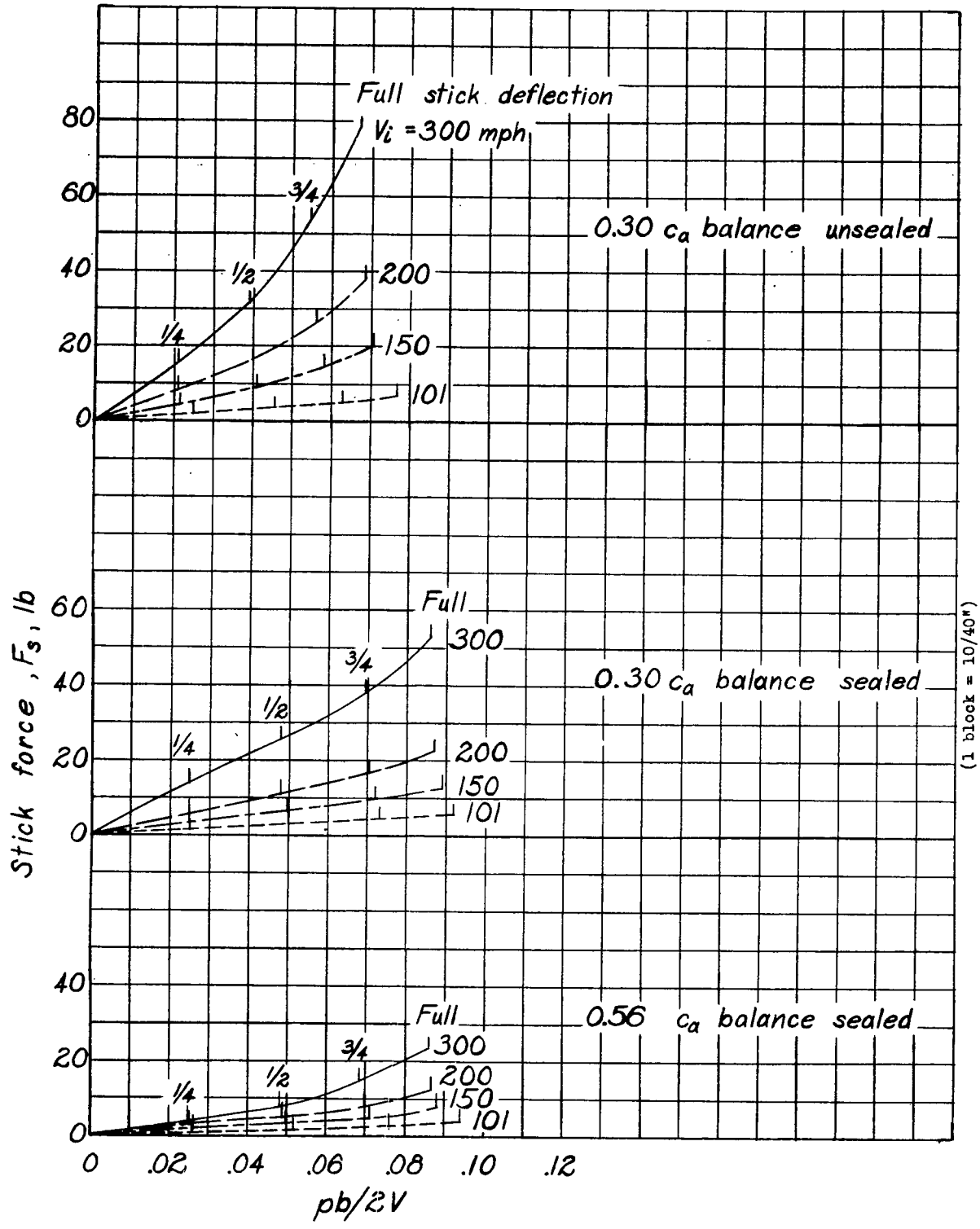

Figure 51. - Estimated aileron-control characteristics of the airplane with tapered wings, full-span flaps retracted, and balanced full-span ailerons linked for a deflection range of ± 15°.

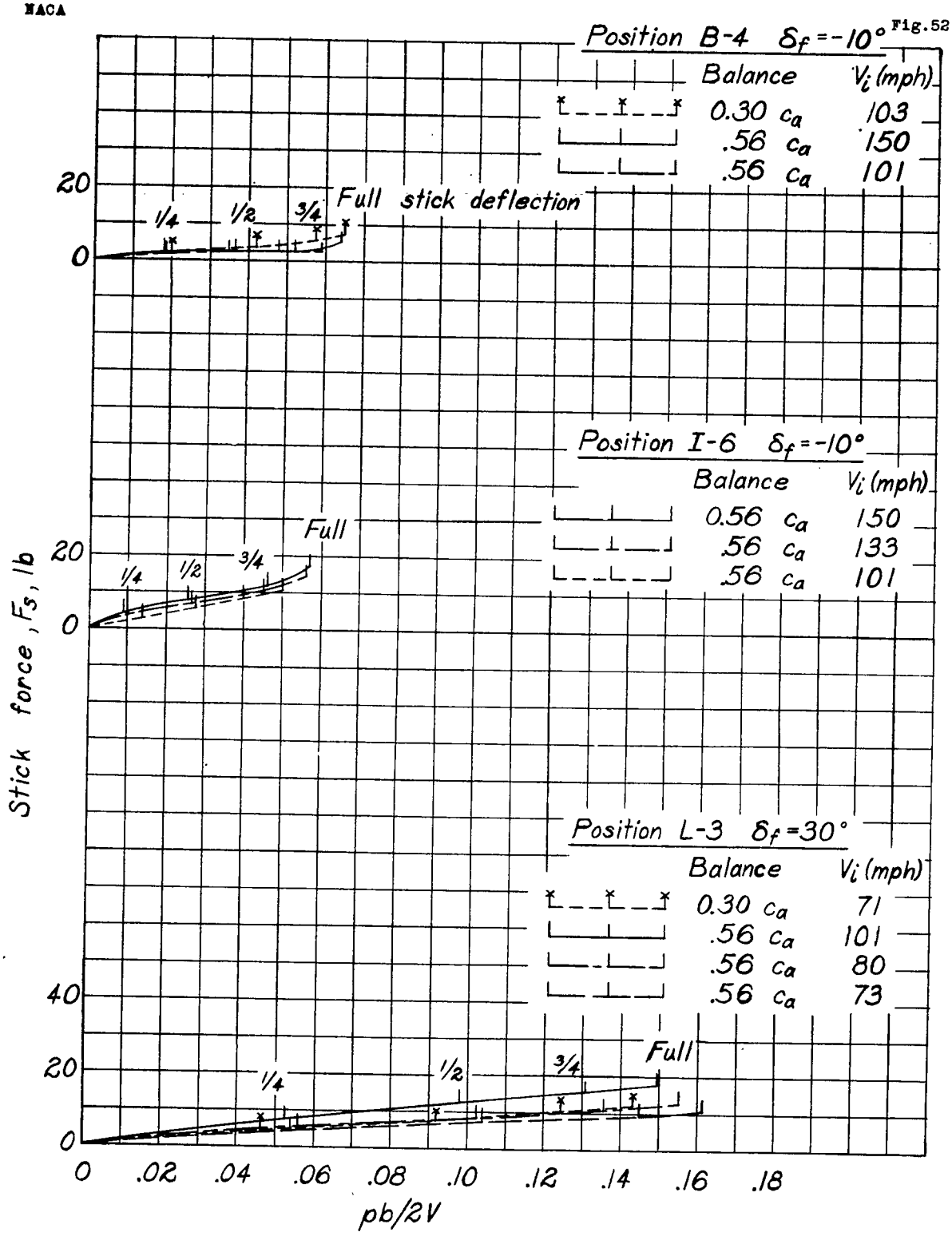

Figure 52.- Estimated aileron-control characteristics of the airplane with tapered wings, full-span retractable flaps, and balanced full-span sealed ailerons linked for deflection range of ±15°.

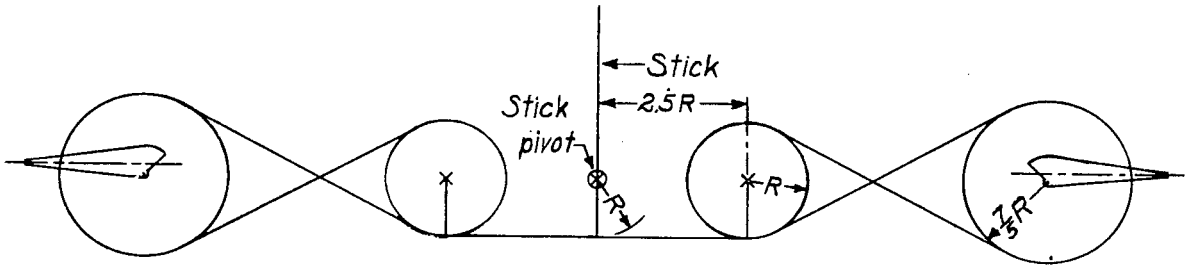

Figure 53.-Schematic diagram of aileron linkage for equal up and down deflections. $\delta_{a_{max}}$, ±15°.

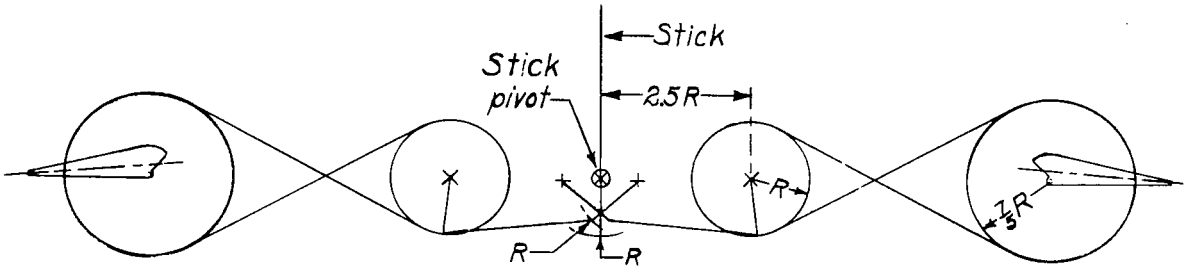

Figure 54.-Schematic diagram of 3:1 differential aileron linkage with a 5° aileron droop. $\delta_{a_{max}}$, +5°, -15°

Differential	$\delta_{a_{max}}$	Location of pivot ②	
		x ±+	y ±+
3-1	+5°,-15°	-0.625R	-0.055 R
2-1	+5°,-10°	-.463 R	.183 R

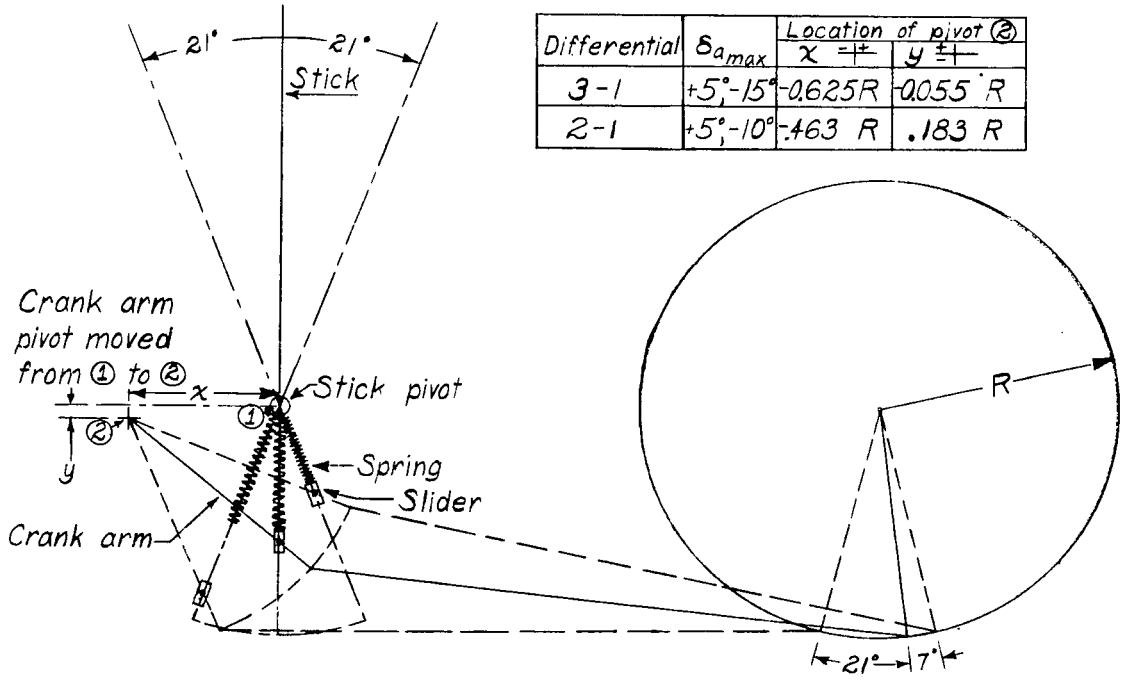

Figure 55.-Detail diagram of the differential linkage.

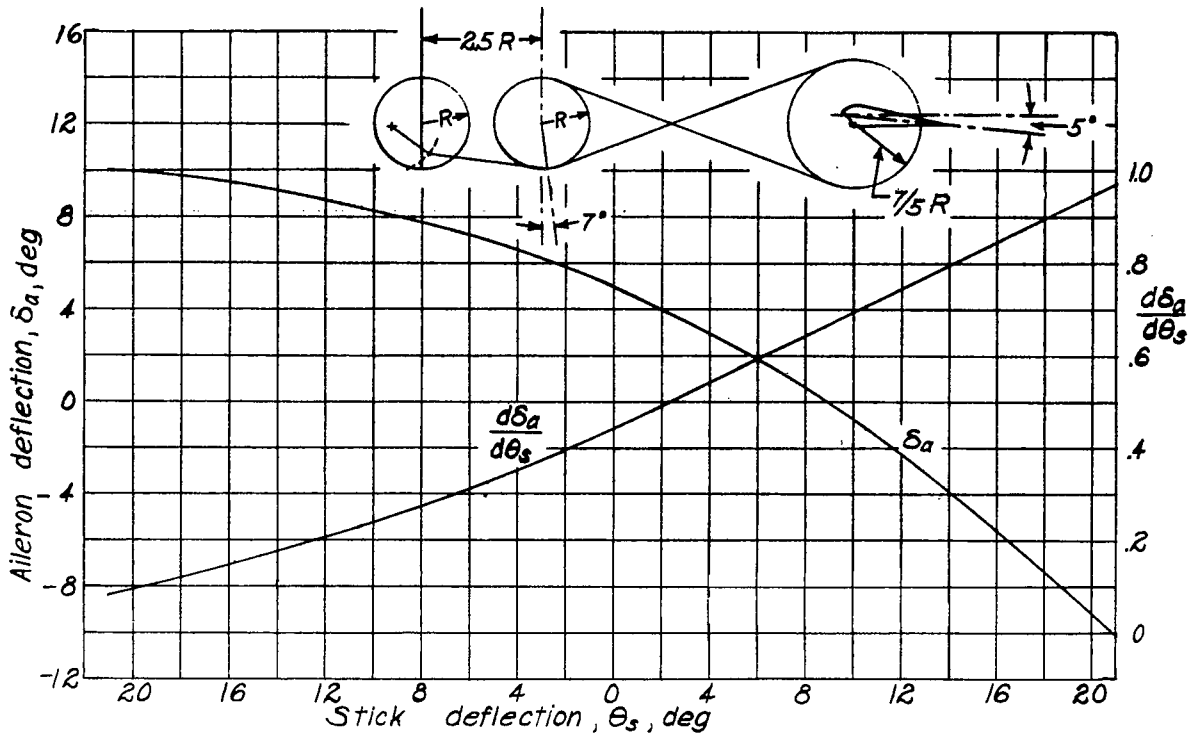

Figure 56.- Variation of aileron angle and mechanical advantage with stick deflection. Aileron drooped 5° with a 3:1 differential; $\delta_{a\,max}$ = +5°,-15°.

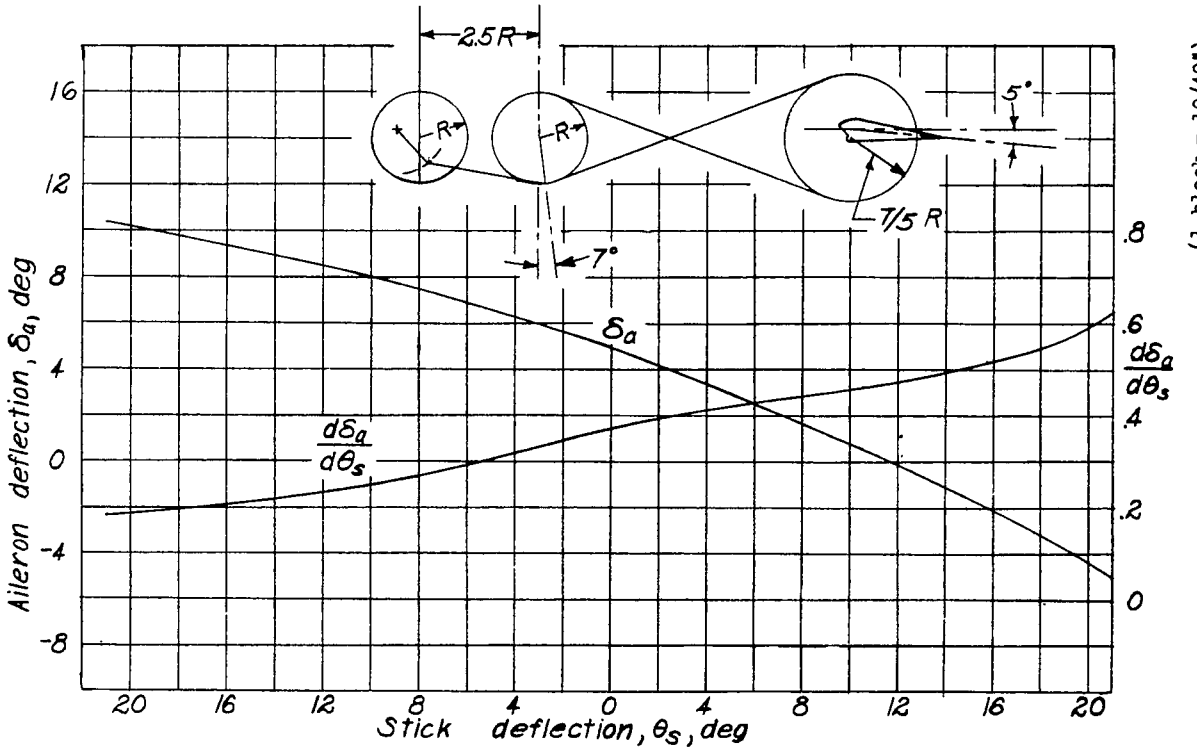

Figure 57. -Variation of aileron angle and mechanical advantage with stick deflection. Aileron drooped 5° with a 2:1 differential; $\delta_{a\,max}$ = +5°,-10°.

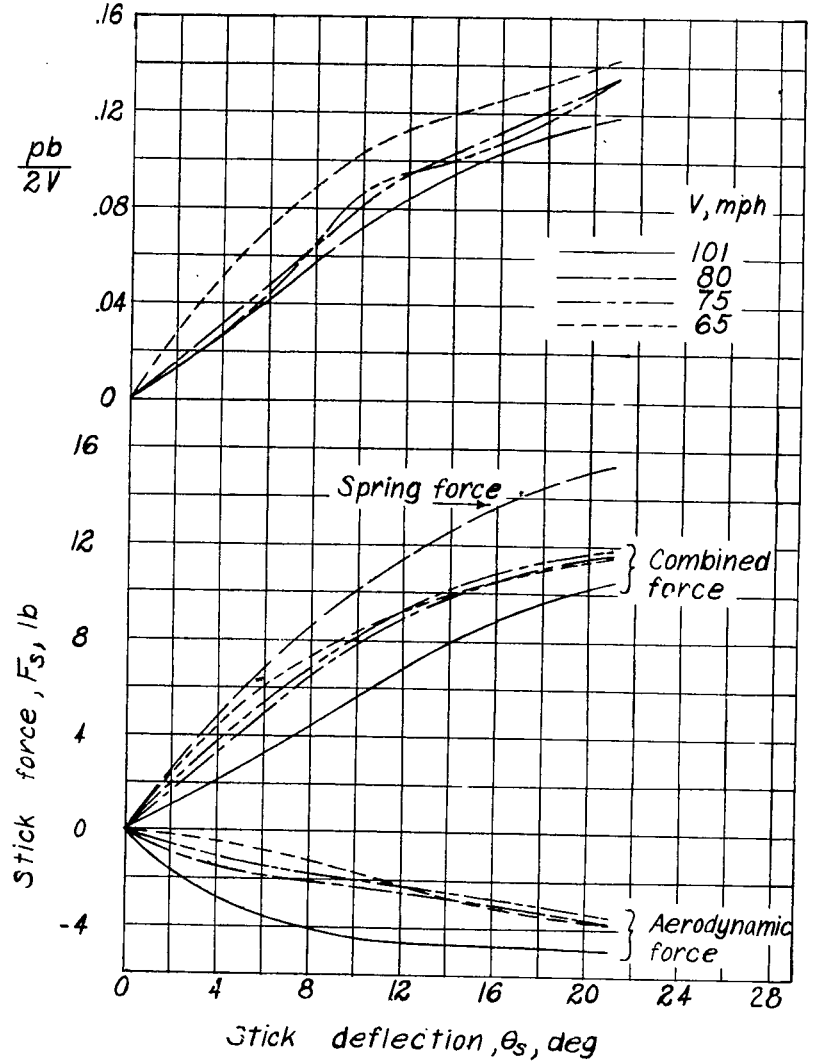

Figure 58.- Variation of stick force and pb/2V with stick deflection. Flap position, L-2, $\delta_f = 50°$, $\delta_a = 5°$; 3:1 differential with $\delta_{a\,max} =$ +5°, -15°.

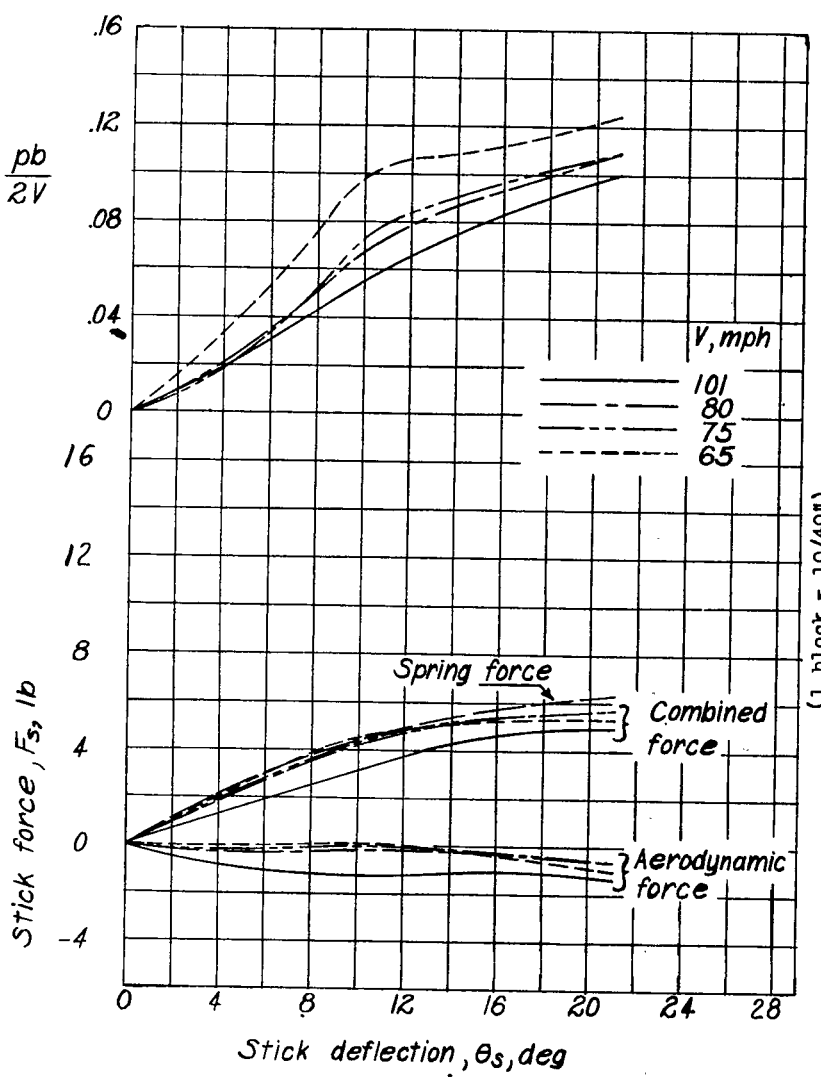

Fig 59.- Variation of stick force and pb/2V with stick deflection. Flap position, L-2, $\delta_f = 50°$, $\delta_a = 5°$; 2:1 differential with $\delta_{a\,max} = +5°, -10°$.

NACA

Fig. 60a

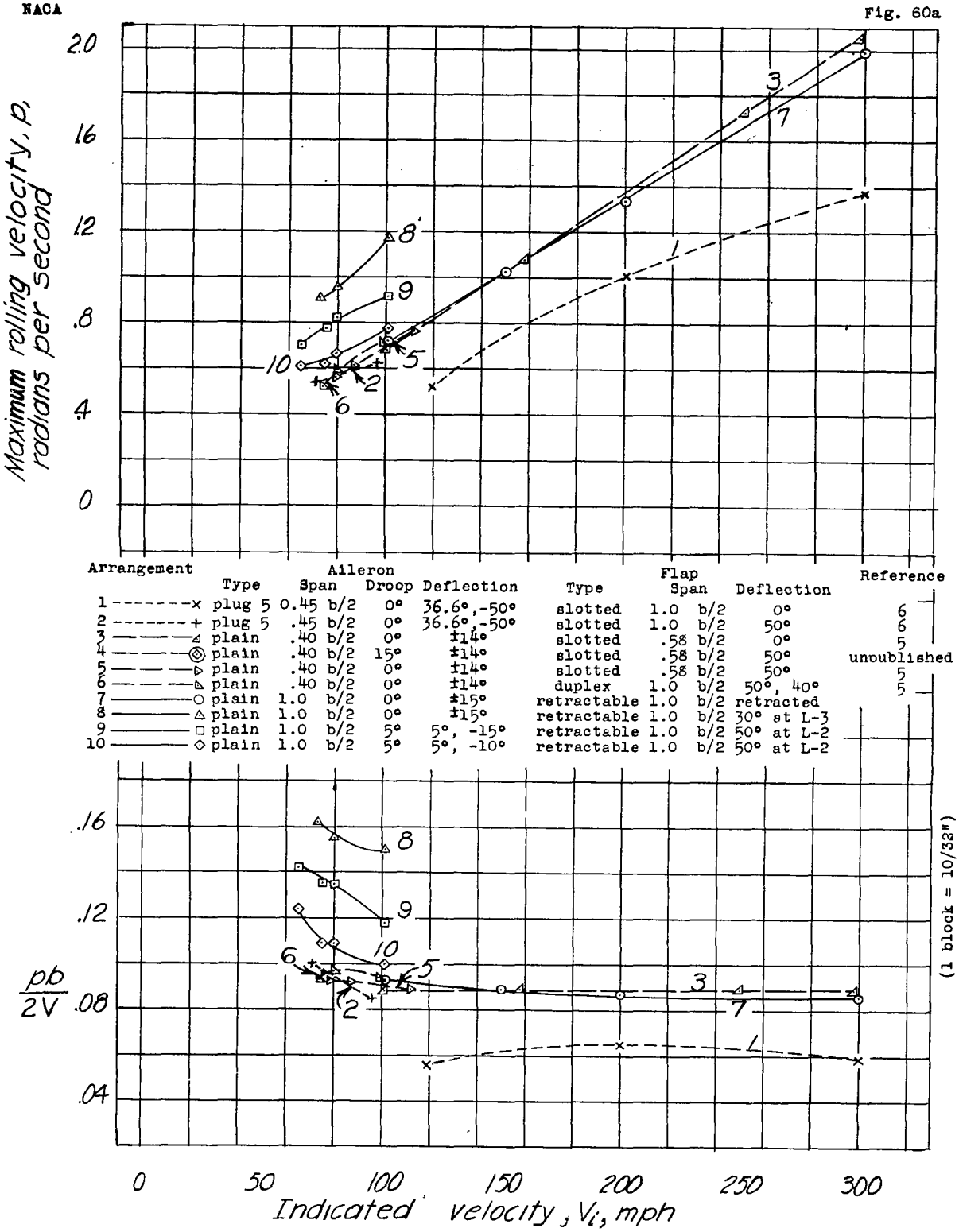

(a) Variation of rolling effectiveness with velocity.

Fig. 60(a,b).- Comparison of the effect of aileron deflection on estimated airplane characteristics for several high-lift and lateral-control arrangements on a tapered wing model.

Arrangement	Aileron Type	Span	Droop	Deflection	Flap Type	Span	Deflection	Reference
1 ------ ×	plug 5	0.45 b/2	0°	36.6°,-50°	slotted	1.0 b/2	0°	6
2 ------ +	plug 5	.45 b/2	0°	36.6°,-50°	slotted	1.0 b/2	50°	6
3 ———	plain	.40 b/2	0°	±14°	slotted	.58 b/2	0°	5
4 ———	plain	.40 b/2	15°	±14°	slotted	.58 b/2	50°	unpublished
5 ———	plain	.40 b/2	0°	±14°	slotted	.58 b/2	50°	5
6 ———	plain	.40 b/2	0°	±14°	duplex	1.0 b/2	50°,40°	5
7 ———	plain	1.0 b/2	0°	±15°	retractable	1.0 b/2	retracted	
8 ———	plain	1.0 b/2	0°	±15°	retractable	1.0 b/2	30° at L-3	
9 ———	plain	1.0 b/2	5°	5°, -15°	retractable	1.0 b/2	50° at L-2	
10 ———	plain	1.0 b/2	5°	5°, -10°	retractable	1.0 b/2	50° at L-2	

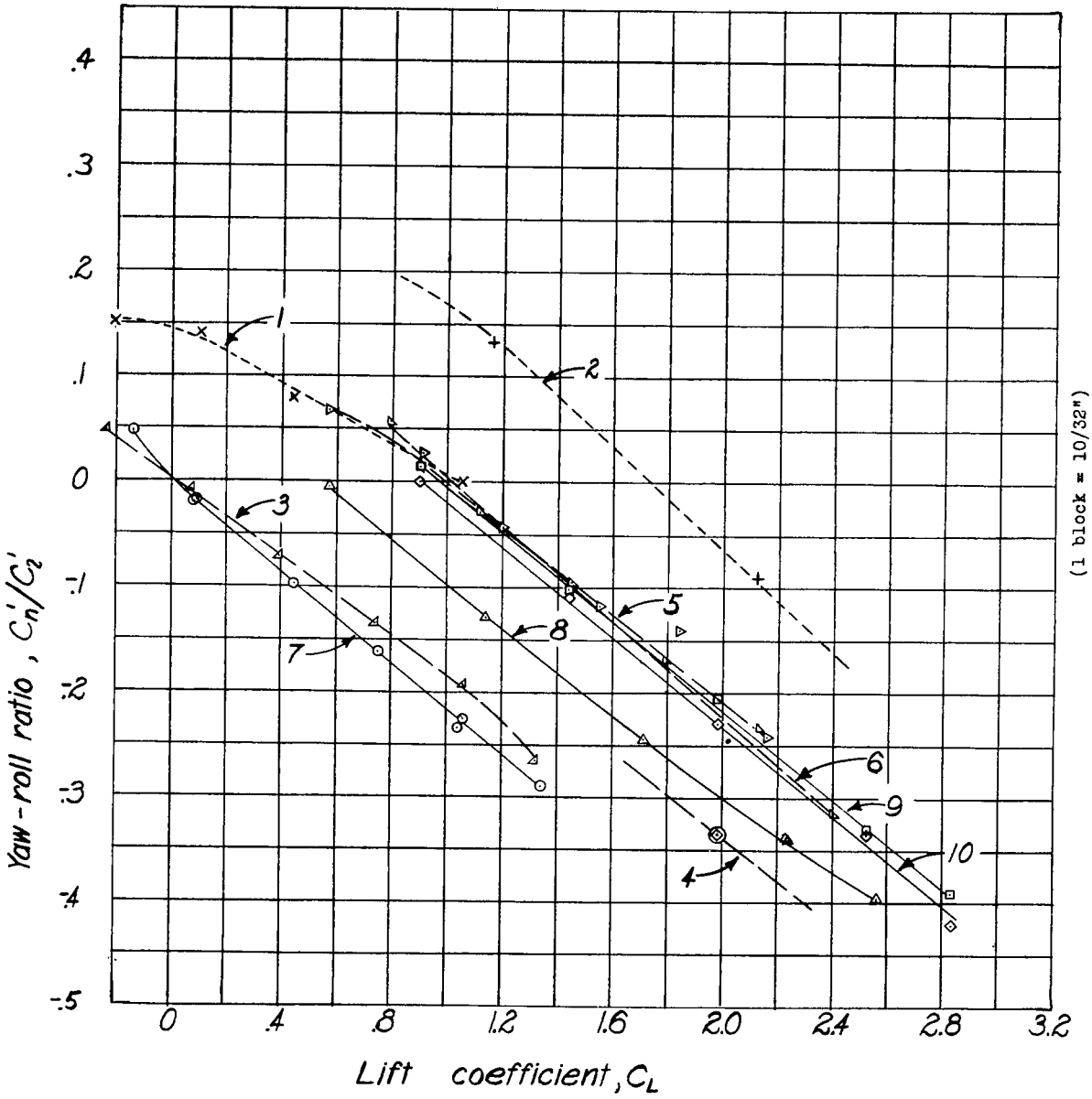

(b). Variation of C_n'/C_l' with C_L.

Figure 60.- Concluded.